A COMPARATIVE STUDY OF THE ANTI-BREAST CANCER AND IMMUNOMODULATORY EFFECTS OF [6]-, [8]-, AND [10]-GINGEROL

by

Megan M. Bernard

Submitted in partial fulfilment of the requirements
for the degree of Master of Science

at

Dalhousie University
Halifax, Nova Scotia
July 2013

Table of Contents

List of Tables

List of Figures

Abstract

[6]-Gingerol, [8]-gingerol, and [10]-gingerol are phytochemical extracts from ginger that are thought to contribute to its health-benefitting properties. The objectives of this investigation were to explore and compare the *in vitro* anti-proliferative and cytotoxic effects of [6]-, [8]-, and [10]-gingerol on human and mouse mammary carcinoma cells, as well as their ability to inhibit T cell proliferation. [8]-Gingerol and [10]-gingerol induced mammary carcinoma cell death that did not require ROS production or caspase activation. All three gingerols inhibited the proliferation of mammary carcinoma cells and T cells, and the production of IFN-γ by T cells. The production of IL-2 and the expression of early T cell activation markers, CD25 and CD69, were significantly decreased by [8]- and [10]-gingerol. The results demonstrated that [10]-gingerol was the most potent, followed by [8]-gingerol, then [6]-gingerol. Consequently, [8]- and [10]-gingerol warrant further investigation for the treatment of breast cancer and the control of inflammation.

List of Abbreviations and Symbols Used

$5\text{-}HT_3$	5-Hydroxytryptamine
α	Alpha
n	Alkyl side chain length
α-	Anti-
ANOVA	Analysis of variance
APC	Antigen presenting cell
AP-1	Activator protein-1
β	Beta
Bcl-2	B cell lymphoma-2
BMDC	Bone marrow-derived dendritic cells
BSA	Bovine serum albumin
C	Cytokinesis checkpoint
°C	Degrees Celsius
$CaCl_2$	Calcium chloride
Caspase	Cysteine aspartate-specific protease
CD	Cluster of Differentiation
Cdk	Cyclin-dependent kinases
cDMEM	Complete Dulbecco's Modified Eagle's Medium
cRPMI	Complete Roswell Park Memorial Medium 1640
CO_2	Carbon Dioxide
ConA	Concanavalin A
COX	Cyclooxygenase

cpm	Counts per minute
CTL	Cytotoxic T lymphocyte
δ	Delta
DC	Dendritic cell
DCIS	Ductal carcinoma in situ
ddH_20	Double distilled water
DiOC6	3,3'-dihexyloxacarbocyanine iodide
DMEM	Dulbecco's Modified Eagle's Medium
DMSO	Dimethylsulphoxide
DNA	Deoxyribonucleic acid
DNase	Deoxyribonuclease
EDTA	Ethylene diamine tetraacetic acid
ER	Endoplasmic Reticulum
ER+	Estrogen receptor positive
ERK	Extracellular signal-related kinases
FBS	Fetal bovine serum
FGM	Fibroblast growth medium
FL	Fluorescence label
FoxP3	Forkhead box P3
g	Gravity
G_0	Quiescent Phase
G_1	Gap Phase 1
G_2	Gap Phase 2

HEPES	n-2-Hydroxyethylpiperazine-N-2ethanesulfonic acid
h	Hours
HER2	Human epidermal growth factor receptor 2
HMEC	Human mammary epithelial cells
HRP	Horseradish peroxidase
IBC	Inflammatory breast carcinoma
IDC	Infiltrating ductal carcinoma
IFN-γ	Interferon-gamma
IFN-γR1	Interferon-γ receptor 1
IgSF	Immunoglobulin superfamily
Iκβ	I kappa B Kinase β
IL-	Interleukin-
ILC	Infiltrating lobular carcinoma
iNOS	Inducible nitric oxide synthase
ITAMs	Immunoreceptor tyrosine-based activation motifs
iTreg	Inducible regulatory T cell
JNK	c-Jun N-terminal kinases
KCl	Potassium chloride
kg	Kilogram
LAT	Linker of activated T cells
LCIS	Lobular carcinoma in situ
LPS	Lipopolysaccharide
MAPK	Mitogen-activated protein kinase

MEGM	Mammary epithelial growth medium
M	Molar
MFI	Median/Mean (as indicated in text) fluorescence intensity
mg	Milligram
MHC	Major histocompatibility complex
min	Minute
mL	Milliliter
mM	Millimolar
MMP	Matrix metalloproteinase
MRI	Magnetic resonance imaging
mRNA	Messenger ribonucleic acid
MTT	3-(4,5-Dimethylthiazol-2-yl)-2,5-diphenyltetrazolium bromide
NAC	n-Acetylcysteine
NaCl	Sodium chloride
NK	Natural killer
NKT	Natural killer T
NFAT	Nuclear factor of activated T cells
NF-κB	Nuclear factor kappa light chain enhancer of activated B cells
ng	Nanogram
NOS	Nitric oxide synthase

nm	Nanometer
nM	Nanomolar
NMR	Nuclear magnetic resonance
NS	Non-significant
nTreg	Natural regulatory T cell
OVA	Ovalbumin
PBS	Phosphate buffered saline
PFA	Paraformaldehyde
pH	Power of hydrogen (measure of acidity)
PI	Propidium iodide
PI3K	Phosphatidylinositol-3-kinase
PKC	Protein kinase C
PLCγ1	Phospholipase Cγ1
PR	Progesterone receptor
PR+	Progesterone receptor positive
PTK	Protein tyrosine kinase
rmGM-CSF	Recombinant murine granulocyte/macrophage-colony stimulating factor
RNase	Ribonuclease
ROR	Retinoic acid receptor related orphan receptor
ROS	Reactive oxygen species
rpm	Revolutions per minute
RPMI	Roswell Park Memorial Institute 1640

S	Synthesis Phase
SEM	Standard Error of the Mean
SD	Standard Deviation
SDS	Sodium dodecylsulphate
STAT	Signal transducer and activator of transcription
SubG1	Sub Gap 1 phase
T-bet	T-box expressed in T cells
TCR	T cell receptor
TGF-β	Transforming growth factor
Th	T helper
TNF	Tumor necrosis factor
TNFRSF	Tumor necrosis factor receptor superfamily
Treg	Regulatory T cell
Tris-HCl	Tris-Hydrochloric acid
Triton-X 100	Octylphenolpoly(ethyleneglycolether)$_x$
TrypLE	Phenol red negative trypsin replacement
TTBS	Tween Tris-buffered saline
U	Units
µCi	Microcurie
µg	Microgram
µL	Microlitre
µM	Micromolar
v	Volume

VEGF	Vascular endothelial growth factor
WHO	World Health Organization
γ	Gamma
ZAP-70	ζ-associated protein
ZVAD-FMK	Benzyloxycarbonyl-Val-Ala-Asp (OMe) fluoromethylketone

Acknowledgments

A heartfelt thanks to my supervisor and all the members of the Hoskin Lab for their help over the last few years. A special thanks to my parents and grandmother for their support throughout my life.

CHAPTER 1

INTRODUCTION

1.1 Overview of the Inflammatory Process

Inflammation is a protective mechanism that is initiated in response to an invasion by a pathogen or to tissue injury and is orchestrated by the immune system[1,2]. There are two main branches of the immune system that work in concert to protect the host from anything considered "non-self" (or foreign) and to repair lingering damage: the innate immune response and the adaptive immune response[1]. The innate immune response is composed of chemical, physiological, cellular, and microbiological barriers and is the host's first line of defense[1–3]. The innate immune response is immediate and not highly specific to the pathogen or damage, whereas the adaptive immune response is slower to develop, long-lasting, and develops immunologic memory specific to the invading pathogen[1,4]. Among the primary cells of the innate immune response are neutrophils, macrophages, natural killer (NK) cells, and dendritic cells (DCs), while T cells and B cells are highly involved in the adaptive immune response[1].

Upon tissue damage or infection, pathogen-activated cells (for example, macrophages and DCs) employ pattern recognition receptors (PRRs; such as toll-like receptors, RIG-I-like receptors, and Nod-like receptors) on their cell surfaces to recognize invading pathogens as foreign and/or endogenous molecules from necrotic cells[1,3]. Macrophages and DCs of the innate immune response are also known as professional antigen-presenting cells (APCs) as, in the case of pathogenic invasion, they engulf pathogens, degrade the pathogen into antigenic peptides, and display to T cells the

peptides within the cleft of the major histocompatibility complex (MHC) on the APC surfaces. APCs, macrophages, and local epithelial cells also mediate the release of pro-inflammatory mediators that induce physiological changes that recruit additional inflammatory cells, including T cells of the adaptive immune response.

In sterile inflammation, in which tissue damage occurs and no infectious stimuli is involved, APCs promote changes that activate T cells and initiate a response specific to antigens associated with dying cells, similar to the process that occurs when APCs contact antigens from infectious stimuli. Sterile inflammation is triggered by crystals, minerals, toxins, antigens, chemicals, ischemia, and mechanical trauma, amongst other things[5]. A myocardial infarct is an example of sterile inflammation, in which tissue injury occurs without infectious stimuli and necrotic cells release chemical mediators, such as chemokines and interleukins, and express danger-associated molecular patterns (DAMPs) to induce inflammation[6]. In both pathogenic and sterile inflammation, activation of the innate immune response leads to the stimulation of the adaptive immune response.

1.1.1 T Cell Activation

T cells will traffic from where they develop in the thymus (primary lymphoid organ) to the lymph nodes and spleen (secondary lymphoid organs), where they are encountered by APCs displaying antigen[4]. T cells become activated through a series of events that begins with the recognition of foreign or harmful antigens presented by APCs. Antigens that are inside the cell (endogenous antigens) are displayed on MHC-I complexes on most nucleated cells and are presented to a subset of T cells that are positive for the cluster of differentiation (CD)8 cell surface molecule ($CD8^+$)[4,7]. Antigens from the extracellular environment are usually displayed on MHC-II complexes, which

are only expressed on APCs, and are presented to T cells that are positive for CD4 cell surface molecules ($CD4^+$)[4,7]. Cross-presentation may also occur, where extracellular antigens are picked up by APCs displaying MHC-I and presented to $CD8^+$ T cells. CD4 and CD8 surface markers act as co-receptors and stabilize T cell interactions between MHC-I and MHC-II, respectively, by binding to their nonpolymorphic constant regions[4].

Antigens that are presented in the context of a peptide-MHC complex interact with a T cell receptor (TCR) on the surface of T cells[8,9]. The TCR is a complex that consists of α and β chains that are antigen specific and non-covalently associated with CD3 proteins[8]. Instead of α and β chains, TCRs may possess γ and δ chains, which recognize non-peptide antigens[10]. The CD3 portion of the TCR is nonpolymorphic and has three possible dimer arrangements: γε, δε, or ζζ. While the αβ heterodimer subunit of the TCR is responsible for antigen recognition and binding, the CD3 portion, with a long cytoplasmic tail, is important for signal transduction[11].

1.1.2 Co-Stimulation

In addition to the interaction between the TCR with the antigen on the MHC, a co-stimulatory signal is required for full T cell activation. Most co-stimulatory molecules are members of the immunoglobulin superfamily (IgSF) or tumor necrosis factor receptor superfamily (TNFRSF)[12]. The most common co-stimulatory signals are provided by the CD28 receptor (a member of the IgSF) on the T cell, which interacts with CD80 (also known as B7.1) or CD86 (also known as B7.2) on the APC[8,13]. The interaction between CD28 and CD80/CD86 enhances T cell activation more robustly than other co-stimulatory molecules[4].

CD28 is constitutively expressed on 100 % of human $CD4^+$ T cells, approximately 50 % of human $CD8^+$ T cells, and almost all mouse T cells ($CD4^+$ and $CD8^+$); its expression is upregulated with the initiation of T cell activation[14]. CD80 and CD86 are expressed on activated B cells, activated monocytes, activated T cells (in small amounts), a variety of tumor cell lines, macrophages and DCs, and their expression is modulated by certain cytokines (IL-2, IL-6, tumor necrosis factor [TNF]-α)[13]. The interaction between CD28 and CD80/CD86 is thought to be mainly responsible for inhibiting T cell anergy and apoptosis and prolonging the T cell proliferative response[13,15]. Additionally, while TCR binding to MHC complexes is important for antigen specificity, co-stimulation is important for T cell survival, energy metabolism, proliferation, and differentiation into T cell subsets[15].

Another molecule that is important for mediating co-stimulation is CD40 on B cells, APCs, and certain non-immune cells and tumors. CD40 binds CD40 ligand which is expressed on T cells and several non-immune cells during inflammation to enhance cellular and humoral inflammatory responses[16]. Additionally, OX40 on activated APCs and endothelial cells binds OX40 ligand on T cells in acute inflammation and increases T cell expansion, cytokine production, and overall T cell survival[17]. Furthermore, inducible co-stimulator (ICOS) is also important in regulating T cell proliferation, the production of cytokines, and mediating other T cell responses to antigen presentation, including superinduction of the production of IL-10; however, ICOS does not upregulate the production of IL-2[18].

1.1.3 Activated T Cell Signal Transduction

Signal transduction begins with tyrosine phosphorylation of the cytoplasmic immunoreceptor tyrosine-based activation motifs (ITAMs) by the Src family protein tyrosine kinase (PTK) Lck[4]. ITAMs are present in the CD3 chains and PTK Lck is associated with $CD4^+$ and $CD8^+$ T cells. This leaves ITAM phosphotyrosines open for recruitment of ζ-associated protein, 70 kd (ZAP-70) that phosphorylates numerous molecules, including adaptive proteins linker of activated T cells (LAT) and SH2-containing leukocyte protein, 76 kd (SLP-76)[4]. Additionally, ZAP-70 will recruit phospholipase Cγ1 (PLCγ1), which, through the interaction of many intermediates, culminates in the activation of nuclear factor kappa light chain enhancer of activated B cells (NF-κB), nuclear factor of activated T cells (NFAT), and activator protein-1 (AP-1) transcription factor[4]. Each of these transcription factors is involved in the expression of genes that are extremely important for developing highly functional T cells[4].

1.1.4 $CD4^+$ T Cell Differentiation

Although T cells are activated by similar mechanisms, the resulting action of the activated T cells can be quite diverse. T helper (Th) and regulatory T (Treg) cells are $CD4^+$ T cell subsets that have different effects on the immune system; Th1, Th2, Th9, Th17, and Treg cells are the most commonly studied $CD4^+$ T cell subsets. The differentiation of $CD4^+$ T cells occurs after interaction with peptide displayed in context of MHC-II and the type of $CD4^+$ T cell subset that develops depends upon the cytokine milieu and on stabilization by specific transcription factors[4].

Th1 and Th2

The differentiation of Th1 or Th2 cells is influenced by the type of antigen(s) present, binding of co-stimulatory molecules, and, most importantly, the cytokine milieu[4,19]. Th1 cells are defined based on their ability to secrete interferon (IFN)-γ and IL-2[4]. $CD4^+$ T cells are induced to differentiate into Th1 cells through the influence of IL-12 which generates differentiation signals through the Signal Transducer and Activator of Transcription (STAT)4 signaling pathway; Th1 cells also express the transcription factor T-box expressed in T cells (T-bet)[4,19]. Th2 cells are defined by their production of IL-4, IL-5, IL-10, and IL-15. The differentiation of naïve $CD4^+$ T cells into Th2 cells occurs under the influence of IL-4, which signals through the STAT6 pathway. Th2 cells express the transcription factor GATA-3[4]. Th1 cells are important for the eradication of intracellular pathogens by activating APCs, NK cells, and CTLs, while Th2 cells are critical for defending against helminthes and other extracellular parasites[4]. Additionally, Th2 cells provide support to B cells and thereby enhance antibody production. Notably, the production of Th1 cytokines inhibits the differentiation of Th2 cells, and vice versa[19].

Th9 and Th17

Th9 cells produce IL-9 and are derived from Th2 cells under the influence of IL-4 and transforming growth factor (TGF)-β[20]. IL-9 is an important cytokine for mast cell growth and, like Th2 cells, is significant for strengthening immunity against helminthes[20]. Th17 cells produce IL-17A, B, C, D, E, and F, as well as IL-25, and additionally express retinoic acid receptor related orphan receptor (ROR)γt, RORα, and STAT3[21]. Th17 cells are differentiated from $CD4^+$ T cells by exposure to IL-6 and/or IL-21 and TGF-β, and their growth is stabilized and maintained by IL-23. IL-17A, IL-17F, and IL-22 are the

most abundantly produced Th17 cytokines and are involved in promoting autoimmune and inflammatory disease, and in the development of tissue inflammation for host defense.

Regulatory T Cells

Treg cells act by suppressing the function of effector T cells and other immune cells by their production of inhibitory molecules such as IL-10 and TGF-β, thereby preventing over-activation of the immune response and inflammatory disorders such as autoimmune disease and allergies[22]. Treg cells also interfere with cancer-associated inflammation and reduce the immune response against tumors. Two generally accepted types of Treg cells are the inducible Treg (iTreg) and natural Treg (nTreg) cells. iTreg cells are generated in the peripheral in the presence of TGF-β and the absence of IL-6 and IL-21; most express the forkhead box P3 (FoxP3) transcription factor[23]. The majority of nTreg cells also express FoxP3, and are generated in the thymus as a result of high affinity TCR interactions with self antigens[24]. Upon generation, nTreg cells are antigen-primed and ready to mediate immune suppression.

1.1.5 $CD8^+$ T Cell Differentiation

$CD8^+$ T cells differentiate into cytotoxic T lymphocytes (CTL) after interaction with peptide displayed in the context of MHC-I and are important for mounting an anti-tumour response, and for developing immunological memory and the direct killing of infected or damaged cells. Approximately 5-10 % of CTL become memory cells that can amount a rapid recall response should the memory CTL be re-exposed to its cognate antigen[25]. CTL express Fas ligand that binds Fas on infected, damaged, or malignant cells and induces apoptosis upon antigen recognition. CTL also secrete granzymes and

perforin into the intracellular space between the effector cell and target cells, triggering apoptosis in infected or malignant cells[25].

1.1.6 IL-2 and the IL-2 Receptor in T Cell Activation

IL-2 is produced mainly by activated $CD4^+$ T cells, but also by $CD8^+$ T cells, NK cells, natural killer T cells (NKT cells), and some DCs in response to antigen stimulation[26,27]. IL-2 functions in T cell homeostasis and promotes T cell generation and survival[28]. This cytokine binds to the high-affinity IL-2 receptor (IL-2R), which consists of three subunits: 1) IL-2Rα (CD25), 2) IL-2Rβ (CD122), and 3) IL-2Rγ[29]. There are three classes of IL-2R that have been described: low affinity (that consists of only the IL-2α unit), intermediate affinity (consisting of IL-2β and IL-2γ), and high-affinity (consisting of IL-2Rα, IL-2Rβ, and IL-2Rγ)[30]. High-affinity IL-2R is expressed upon antigen presentation and subsequent activation of T cells[31].

1.1.7 CD69 and the IFN-γ Receptor in T Cell Activation and Inflammation

The expression of CD69 on activated T cells is induced within 1-2 h post-stimulation, making it the earliest T cell activation marker[32]. CD69 expression can be induced by a variety of factors, including the activation of PKC with prolonged elevation of intracellular calcium levels. CD69 expression results in various processes, including platelet aggregation, T cell proliferation, production of TNF-α, and neutrophil degranulation. CD69 complexes with sphingosine 1-phosphate receptor-1 ($S1P_1$; a molecule responsible for lymphocyte egress) and retains lymphocytes in lymphoid organs and functions downstream from IFN-α/-β[33].

The IFN-γ receptor (IFN-γR) is composed to two subunits, IFN-γR1 and IFN-γR2[34]. CD119 is the ligand-binding component for IFN-γR1, also known as the α chain[34].

IFN-γR1 is highly specific for IFN-γ, a cytokine important for upregulating MHC-I, MHC-II, and regulating the production of pro-inflammatory and immunomodulatory cytokines. This receptor is expressed ubiquitously on immune cells and many epithelial and endothelial cells. Mutations in IFN-γR1 result in a dampened immune response. For example, it has been documented that an IFN-γR1 deficiency results in an increased susceptibility to mycobacterial disease[35].

1.1.8 The Involvement of T Cells in Inflammation

T cells have many beneficial roles in the inflammatory process, including eradicating infectious stimuli that have escaped the innate immune response (for example, T helper cells promote the elimination of pathogens such as bacteria, viruses, and helminthes[19]), resolving the inflammatory response after eradication of infectious stimuli (for example, Treg cells secrete IL-10 which is an anti-inflammatory cytokine[22]), direct destruction and removal of pathogen-infected, transformed, and/or damaged cells (for example, $CD8^+$ T cells induce apoptosis of virus-infected cells through Fas/Fas ligand interactions or through the release of perforin or granzyme[25]), and in many cases are important for mounting an anti-tumor immune response (for example, $CD8^+$ T cells also induce apoptosis of malignant cells through Fas/Fas ligand interactions and the release of granzyme/perforin[25]). TCR gene rearrangement during T cell development allows T cells to recognize and destroy an infinite number of antigens, and cytokines produced by T cells are important for modulating and controlling other cells and immunomodulatory factors of the immune system[4].

Improper control and activation of T cells are responsible for the development of chronic inflammation and chronic immune disorders, such as autoimmune disease, which

is caused by uncontrolled, autoreactive T cells[36]. Furthermore, T cells play an important role in mediating graft versus host disease, in which host APCs activate donor T cells[37], and allograft rejection, in which host T cells attack the foreign tissue[38]. Chronic inflammation is often accountable for the initiation of many different types of cancer[39]. These factors and more make T cells of central importance in the development of inflammation and in immunomodulation.

1.2 An Overview of the Links Between Cancer and Inflammation

Although acute immune responses are required for eliminating pathogens and restoring homeostasis to damaged tissues, long-lasting inflammation and associated reactive oxygen species (ROS) production can lead to further tissue damage and the development of chronic diseases, such as cancer. Cancer develops in stages driven by tumor initiators and tumor promoters. Tumor initiators are mutagens and carcinogens that begin abnormal transformations within a cell[40]. Sometimes, these transformed cells are removed by the body's natural innate and adaptive defenses; however, tumor promoters, including excessive inflammation, overcome the natural defenses of the body that normally eliminate the transformed cells, or act to foster the continuation of changes within the cells[41]. As these cells change, they acquire several biological capabilities that facilitate tumor growth and the ability to metastasize. These are described by Hanahan and Weinberg as the hallmarks of cancer and include sustained proliferative signaling by the transformed cell, resistance of cell death, release of factors that induce angiogenesis, replicative immortality of the transformed cell, activation of invasion and metastasis, and evasion of growth repressors[42,43]. Additionally, Hanahan and Weinberg have described

several emerging hallmarks, which are deregulating cellular energetics and avoiding immune destruction[42].

During chronic inflammation, cells involved in the healing process are constantly changing, and at the same time, tissue damage is occurring. The microenvironment consists of inflammatory cells that foster proliferation, cell survival, angiogenesis, and migration - all processes with dual involvement in promoting the neoplastic process and the metastasis of cancer cells[44]. NF-κB is a transcription factor that has strong ties to both the inflammatory and carcinogenic processes[45]. NF-κB is activated in response to various stresses such as pro-inflammatory cytokines, viruses, bacteria, or chemotherapeutic agents, and can lead to the activation of over 400 different genes[44]. Many of these genes code for anti-apoptotic, pro-angiogenic, and pro-invasion proteins, all of which are cancer-promoting[45].

Inflammation-induced cancer develops through an intrinsic pathway of genetic alterations that switch on pro-inflammatory processes, or, from an extrinsic pathway of genetic alterations that occurs in response to inflammatory processes[46]. These inflammatory processes ultimately initiate angiogenesis, tissue remodeling, inflammatory cell infiltration, and the release of pro-inflammatory cytokines – all of which are activities linked to cancer development and progression[46]. The RET gene is linked to the development of thyroid cancer and is an example of the intrinsic pathway in cancer development. The RET gene activates a set of genes that encode for chemokines (CCL2, CCL20, CXCL8, and CXCL12), chemokine receptors (CXCR4), and cytokines (IL-1β, colony-stimulating factor [CSF]-1, granylocyte/macrophage colony-stimulating factor

[GM-CSF], and granulocyte-colony-stimulating factor [G-CSF]) that are involved in inflammation and the development of thyroid tumors[47].

Autoimmune disease and infections induce genetic alterations through the extrinsic pathway, which can lead to inflammation-induced cancer. Colitis, an autoimmune disease that has been associated with the development of colon cancer, leads to the activation of the NF-κB transcription factor, which is an essential component in multiple inflammatory and carcinogenic pathways[48]. Additionally, another autoimmune disease, Hashimoto's thyroiditis, is strongly linked to the development of thyroid cancer[49,50]. A previous study discovered that patients with Hashimoto's thyroiditis were three times more likely to develop thyroid cancer, and that the expression of PI3K/Akt were increased in patients with Hashimoto's thyroiditis, as well as well-differentiated thyroid cancer, suggesting a possible molecular mechanism for carcinogenesis[50]. Moreover, human papillomavirus infection can block the normal functioning of tumor suppressor genes, p53 and retinoblastoma, leading to unchecked cellular proliferation and eventually cervical cancer[51]. Furthermore, the risk of developing gastric cancer significantly increases in *Helicobacter pylori*-colonized individuals that express high levels of IL-1β polymorphisms, who have polymorphisms that increase TNF-α expression, and who have polymorphisms that decrease IL-10 expression[52]. *Helicobacter pylori* infection also induces oxidative DNA damage and activates cyclooxygenase (COX) enzymes.

1.2.1 T Cells in Cancer Development and Tumor Regression

Immune surveillance of tumors is a process of immune cells identifying cancerous and/or precancerous cells and eliminating them from the body before any damage

occurs[53]. Sometimes the involvement of the innate immune system is enough to eradicate transformed tumor cells, but usually recognition of tumor-specific antigens by the adaptive immune system is required[41]. Additionally, adoptive T cell transfers using autologous tumor-infiltrating T cells are effective for the treatment of metastatic melanoma[54] and post-transplant lymphomas[55]. In adoptive T cell transfers, the patient's T cells with anti-tumor properties are identified *ex vivo* then injected back into the cancer patient with the appropriate growth factors and stimulants to encourage the survival and expansion of this population of T cells[55]. These T cells then target and destroy tumor cells.

$CD4^+$ and $CD8^+$ T cells have demonstrated numerous anti-tumor abilities. T helper cells are responsible for priming $CD8^+$ T cells to achieve full activation and function, especially for the eradication of non-hematopoietic tumors that mostly display MHC-I[56]. Additionally, several studies have demonstrated tumoricidal activity of $CD4^+$ T cells that is independent of $CD8^+$ T cells[57,58]. For example, the secretion of Th1 and Th2 cytokines and the recruitment of other innate immune cells, such as macrophages, granulocytes, and NK cells, are important for the eradication of tumors[59,60]. The secretion of IFN-γ by Th1 cells recruits macrophages that produce ROS, which causes tumor cell death[56]. T helper cells also directly kill tumor cells by secreting TNF-α and expressing TNF-related apoptosis-inducing factor (TRAIL) and/or Fas ligand[61].

Unfortunately, immune surveillance can result in the selection of tumor cell variants with reduced immunogenicity, since T cells target some tumor cells for elimination, but are incapable of eliminating all tumor cells[41]. This population of surviving cells expand until most tumor cells become hard to kill[41]. This concept is

known as cancer immunoediting. The cancer immunoediting concept suggests that the immune system has an involvement in determining tumor quantity and quality[41]. Cancer immunoediting occurs in three steps: elimination, equilibrium, and escape. The elimination step involves tumor immune surveillance. Equilibrium is a stage where tumor cells that escaped immune surveillance lay dormant, as the components of the adaptive immune system discourage tumor cell growth and sculpts the immunogenicity of the tumor[41]. IL-12, IFN-γ, and the involvement of $CD4^+$ and $CD8^+$ T cells in immunomodulation are believed to account for the dormancy of tumor cells. In the last step, tumor cells escape immune surveillance because they have acquired abilities that allow them to avoid destruction by the immune system; including 1) the expression of tumor antigens that do not promote tumor rejection, 2) the loss of MHC-I molecules needed to present tumor antigens, and 3) the inability to produce antigenic peptide epitopes for display on MHC-I molecules for immune recognition[41].

1.3 Breast Cancer and Inflammation

A lot of evidence has been accumulated demonstrating the negative impact that the immune system has during the initiation and promotion stages of breast cancer. Consider the following: 1) long-term non-steroidal anti-inflammatory drug (NSAID) use has been linked to a decreased risk of developing primary breast cancer[62], 2) the presence of macrophages have been shown to have a negative influence on breast cancer prognosis[63], 3) immune-compromised women demonstrate a reduced risk of developing breast cancer[64,65], 4) elevated c-reactive protein and serum amyloid levels (markers of low-grade chronic inflammation) are associated with reduced overall survival in breast cancer patients[66], and 5) tamoxifen, a potent breast cancer chemotherapeutic, has anti-

inflammatory effects in mice[67,68] and may have similar anti-inflammatory effects in humans[69]. The first four of these observations have linked the presence of inflammation with an increased risk of developing breast cancer or an increased severity of breast cancer. The observation regarding tamoxifen suggests that this chemotherapeutic drug may be efficiently treating cancer by reducing inflammation, in addition to its anti-estrogenic properties.

Although many tumor initiators that lead to the development of breast cancer have been discovered, breast cancer is still the most commonly diagnosed cancer in Canadian women over 20 years old[70]. It is estimated that in 2012, 14 women died from breast cancer every day[71]. Breast cancer in men is commonly diagnosed around 60 years of age and accounts for less than 1 % of breast cancer cases; however, men are less likely to survive than women, as male breast cancer is commonly not diagnosed until the disease is at an advanced stage[72]. The five-year relative survival rate in 2012 for breast cancer was 88 % for women, and 80 % for men[70].

1.4 Breast Cancer Classifications

The majority of breast cancers (greater than 95 %) occur as an abnormal change in the glandular cells of the breast tissue, described as a cancerous growth or tumour in the lobules (the glands where milk is produced) or ducts (important for the transportation of the milk from the lobules to the nipple) of the breast[73,74]. The most common histopathological classifications of breast cancer are ductal and lobular carcinoma[75]. Ductal and lobular carcinomas can be further classified as carcinoma in situ or invasive (infiltrating) carcinoma, depending upon the severity of the condition. Carcinoma in situ consists of abnormal cells that are contained within the ducts or lobules by the basement

membrane, whereas invasive carcinoma consists of neoplastic cells that have invaded beyond the basement membrane into the surrounding stroma[74]. Invasive carcinoma has the capacity to invade into the vascular and lymphatic systems and spread (metastasize) to other areas of the body.

Lobular carcinoma in situ (LCIS) and ductal carcinoma in situ (DCIS) are abnormal cell growths contained within the breast lobules and ducts, respectively[76]. Both increase the risk of invasive (infiltrating) lobular carcinoma (ILC) or invasive ductal carcinoma (IDC)[77]. IDC is the most common form of breast cancer[77]. IDC can be further differentiated by histological examination as tubular, medullary, metaplastic, colloid, and adenoid cystic[76].

A third classification of breast cancer is inflammatory breast cancer (IBC), which is caused by cancerous and inflammatory cells blocking nearby lymph vessels. IBC presents clinically as an enlarged erythematous breast due to extensive involvement of the dermal lymphatics[74]. The carcinoma is usually underlying and does not present as a palpable mass. IBC accounts for only 1-3 % of breast cancers but is highly metastatic with a worse prognosis than ductal or lobular carcinomas[78].

Breast cancer can be further classified through immunohistochemical staining for the presence of estrogen receptor (ER), progesterone receptor (PR), or the overexpression of human epidermal growth receptor (HER)2[76]. Generally, 70-75 % of breast cancers are positive for ER (i.e. ER+), and 50 % of these are positive for PR (PR+)[79]. Approximately 25 % of breast cancers overexpress HER2[80]. Appropriate classification of breast cancers is important for developing the most effective treatment strategies for patients. ER+ and PR+ breast cancers have the best prognosis, with generally 80 % of patients that will

respond to treatment[74]. Cancers that are negative for ER, PR, and HER2 overexpression (i.e. "triple-negative") have the worst prognosis, as they initially respond well to chemotherapy but later develop resistance to the treatment.

1.5 Breast Cancer Treatments

Common modalities of breast cancer treatment include biological interventions, hormone therapies, surgery, radiation, and chemotherapy, each of which has its own adverse side effects. A common biological intervention used in the treatment of breast cancer overexpressing HER2 is trastuzumab, which is a monoclonal antibody against HER2[81]. Although extremely effective for treating metastatic HER2 overexpressing breast cancer, this treatment is expensive[82], patients are prone to relapse[81], and trastuzumab has adverse effects, especially on the heart[83].

Hormonal therapy in breast cancer specifically targets estrogen and progesterone, which drive the growth of ER+ and PR+ breast cancer cells[84]. In hormone therapy, hormone receptor antagonists are used to block the activity of estrogen and progesterone and inhibit the growth of breast cancer cells. Antagonists can act by binding the hormone receptor and blocking its interaction with the hormone (such as tamoxifen), down-regulating the receptor by targeting the receptor for degradation (such as fulvestrant), or inhibiting the activity of aromatase and diminishing the conversion of androgen precursors into estrogen (such as anastrozole)[84]. As with biological interventions, administration of hormone therapy has several adverse side effects, including thromboembolic events, decreased bone mineral density, joint stiffness and pain, increased risk of endometrioid cancer, and patient-elected discontinuation of therapy[85].

Surgery is another treatment option for patients with invasive breast carcinoma. Surgical treatments of breast cancer range from slightly invasive lumpectomies to the complete removal of the breast (mastectomy)[77]. Additionally, dissection of the auxiliary lymph nodes is recommended if the sentinel lymph nodes are palpable or contain cancerous cells. Unfortunately, like other interventions, surgery has adverse side effects. Many patients report decreased body image[86]; extreme distress pre-surgery[87]; post-operative pain, nausea, and fatigue; and recurrence of the tumour[87].

Surgery is almost always performed in conjunction with chemotherapy and/or radiation treatment. Chemotherapy is a standard of care for women with node-positive breast cancer or tumors greater than one centimeter in diameter[77]. Also, women with hormone receptor negative-tumours derive a greater benefit from chemotherapy than women with hormone receptor-positive tumours[77]. Radiation treatment is most often recommended with breast-conservation therapy. Both chemotherapy and radiation treatment are not targeted towards only cancerous cells, and because of this have adverse effects on rapidly dividing normal cells. The most common side effects of chemotherapy and radiation treatment are nausea, fatigue, heart problems, and the development of new malignancies[88].

Although earlier detection and the therapies described above have dramatically increased the 5-year survival rate of women with breast cancer, new therapies are constantly being sought after due to the detrimental side effects of current breast cancer treatments. Additionally, new insights into the mechanisms behind cancer development and progression have sparked interest in researching not only cancer treatments, but also cancer prevention. Fruits, vegetables, grains, herbs, and spices are functional foods

containing non-nutrient natural chemical compounds called phytochemicals that have known disease-preventative and disease-fighting properties, and may therefore be useful in cancer prevention/treatment.

1.6 Phytochemicals

It is estimated that over 5000 types of phytochemicals can be found in functional foods, many of which have health-promoting properties that are yet to be scientifically explored[89]. Nevertheless, the phytochemicals that have been studied have demonstrated anti-mutagenic, anti-carcinogenic, and antioxidant activities, to name only a few[90]. Moreover, the health benefits of functional foods have also been demonstrated outside the laboratory. The World Health Organization (WHO) has identified decreased nutritional intake as one of the foremost factors in the development of chronic disease[91]. Additionally, numerous fruits, vegetables, grains, herbs, and spices have successfully been used for centuries in traditional medicine to prevent and treat disease[90].

Phytochemicals can be broadly classified as phenolic, carotenoid, alkaloids, nitrogen-containing compounds, and organosulfur compounds on the basis of their chemical structures[89]. Within these categories are several sub-groups that are also based on particular components of their structure, such as rings, attached functional groups, and side chains. Phytochemicals often behave differently depending upon their chemical structure, but many phytochemicals from different structural categories have shown similar inhibitory effects on inflammatory and carcinogenic pathways. In cancer therapy research, phytochemicals have many similar mechanisms, such as the disruption of cancer cell cycle progression, the mitogen-activated protein kinase (MAPK) signaling cascade, and the phosphatidylinositide 3-kinases (PI3K)/Akt/mTOR pathway[92].

Capsaicin, piperine, and gingerol are commonly studied phytochemicals that are structurally similar.

Capsaicin

Capsaicin (of the genus *Capsicum*) is the active ingredient in red (hot/chili) pepper that allows for the spicy taste[93]. Capsaicin is a vanillic compound, under the classification of phenolics and is structurally similar to gingerol[89]. Capsaicin is particularly well known for its pain-relieving properties[94,95], but several studies also elaborate on its anti-inflammatory and anti-cancer properties. Shin et al. demonstrated that capsaicin reduces inflammation induced in the salivary glands of mice by inhibiting the NF-κB pathway and TNF-α and IL-6 messenger ribonucleic acid (mRNA) transcription[96]. Furthermore, capsaicin significantly reduces the production of nitric oxide without affecting the number of lymphocytes[97]. Another study discovered that capsaicin reduces the number of Treg cells at the tumor site and enhances priming of anti-tumor T cells in tumor-bearing mice, overall modulating the tumor microenvironment to promote an anti-tumor response[98]. Also in the realm of anti-cancer facilitation, capsaicin inhibits IL-6-induced STAT3 activation in multiple myeloma cells[99], and induces apoptosis in colon[100], breast[101], hepatoma[102], and prostate[103] cell lines.

Piperine

The distinct biting taste of the fruits of *Piper nigrum* (black pepper) is attributed to the alkaloid, piperine. Piperine is classified structurally as a hydroxybenzoic acid and is the major constituent in this popular food flavouring spice. Piperine is thought to be responsible for many health-benefitting properties of black pepper, including enhancing digestive capacity, protecting against oxidative damage, enhancing the bioavailability of

therapeutic drugs, and has anti-inflammatory and anti-cancer properties[104]. Pretreatment of piperine reduces inflammation in cerebral ischemia-induced inflammation in rats by reducing the levels of IL-1β, IL-6, and TNF-α and the expression of COX-2, nitric oxide synthase (NOS)-2, and NF-κB[105]. Moreover, piperine inhibits the maturation of DCs by interfering with extracellular signal-related kinases (ERK) and c-Jun N-terminal kinases (JNK) activation[106]. Piperine interferes with rectal cancer cell growth by generating ROS to induce apoptosis and inhibit cell cycle progression[107]. Piperine also inhibits angiogenesis[108], which is a driving force in carcinogenesis and metastasis.

1.7 Ginger

Ginger (*Zingiber Officinale Roscoe,* Zingiberacae*)* originates from South-East Asia and is currently cultivated in various countries, including Brazil, the United States, Jamaica, Australia, China, India, and West Africa[109]. Ginger has a long history of medical use, dating back over 2500 years, in which the spice has been applied in Chinese and Ayurvedic medicine for its anti-pyretic, analgesic, anti-emetic, diuretic, and anti-inflammatory effects[110]. After black pepper, ginger is the world's most commonly used flavouring agent[111]. The constituents of ginger and their quantities vary, depending upon the origin or whether the ginger is dried or fresh; however, the main pharmacological components consist of the pungent phenolics: gingerol, shogaol, paradol, and zingerone[112].

Gingerol provides fresh ginger with its pungency[113]. Six homologs of gingerol have been described: [4]-, [6]-, [7]-, [8]-, [10]-, and [12]-gingerol[111]. Each differs by their unbranched alkyl side chain length (*n*). [6]-Gingerol is the most abundant gingerol, followed by [10]-gingerol, then [8]-gingerol[114,115], and are the focus of this study (Figure

1.1). One study analyzed the quantities of [6]-, [8]-, and [10]-gingerol in three commercial samples of ground ginger powder[114], and the corresponding concentrations (the amount of gingerol in milligrams [mg] per 100 grams [g] of ginger powder) of [6]-, [8]-, and [10]-gingerol are found in Table 1.1. Additionally, the concentrations (mg of gingerol per g of ginger) of [6]-, [8]-, and [10]-gingerol from samples of different varieties of ginger were measured in another study[115]. The samples of ginger that contained the lowest and highest gingerol concentrations are outlined in Table 1.2. Prolonged storage of ginger forms an abundance of [6]-, [8]-, and [10]-shogaols, which are the dehydrated form of gingerols, and zingerone co-occurs with shogaols in stored ginger[116]. Paradols are the reduced form of shogaols[116].

[6]-Gingerol

[6]-Gingerol, a phenolic phytochemical extract from ginger, is the most studied of all the gingerols. [6]-Gingerol exhibits numerous pharmacological properties, including antioxidant[117,118], anti-inflammatory[118], and anti-carcinogenic activities[44]. In particular, [6]-gingerol reduces the expression of tumor necrosis factor (TNF)-α, as well as inducible nitric oxide synthase (iNOS), by suppressing I kappa B Kinase (IKK) phosphorylation, NF-κB nuclear activation, and protein kinase C (PKC) translocation. Other anti-inflammatory effects of [6]-gingerol include the inhibition of phorbol 12-myristate 13-acetate (PMA)-induced cyclooxygenase (COX)-2 expression in mice upon topical application[119]. [6]-Gingerol also dose-dependently decreases the activities of matrix metalloproteinase (MMP)-2 and MMP-9, as well as human breast cancer cell migration and motility[120]. In addition, [6]-gingerol modulates AP-1 activation and transformation of murine epidermal cells[121]. *In vitro* administration of [6]-gingerol inhibits vascular

Figure 1.1 The Chemical Structures of (A) [6]-Gingerol, (B) [8]-Gingerol, and (C) [10]-Gingerol

A. [6]-Gingerol

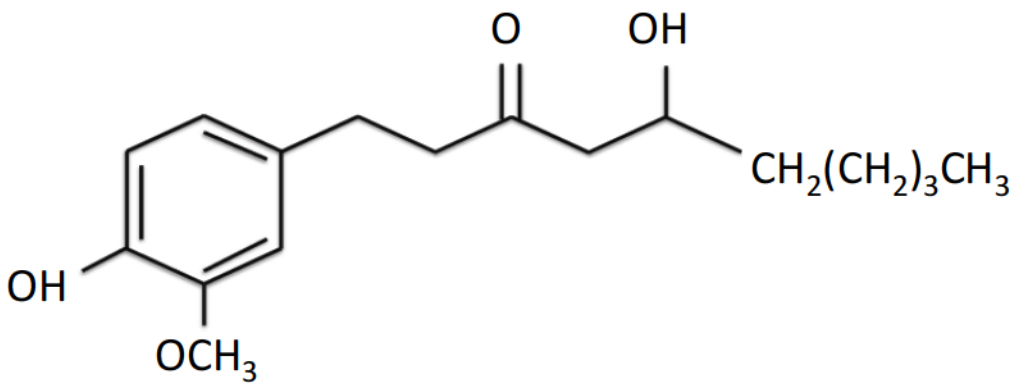

B. [8]-Gingerol

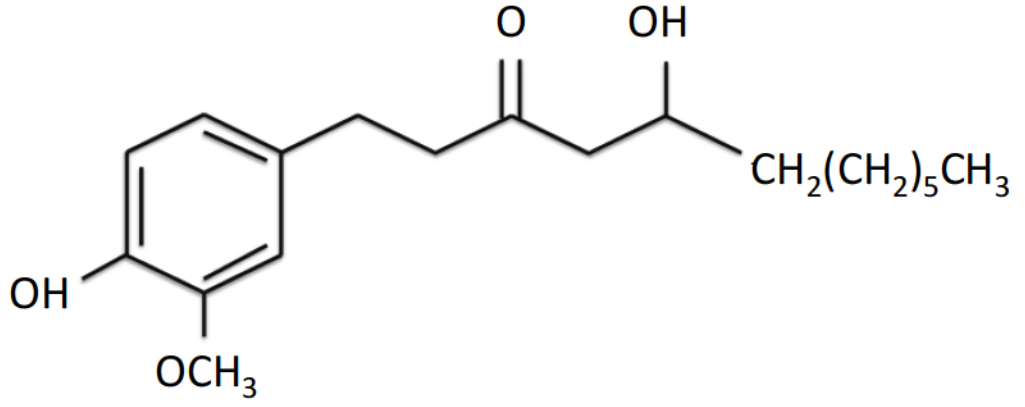

C. [10]-Gingerol

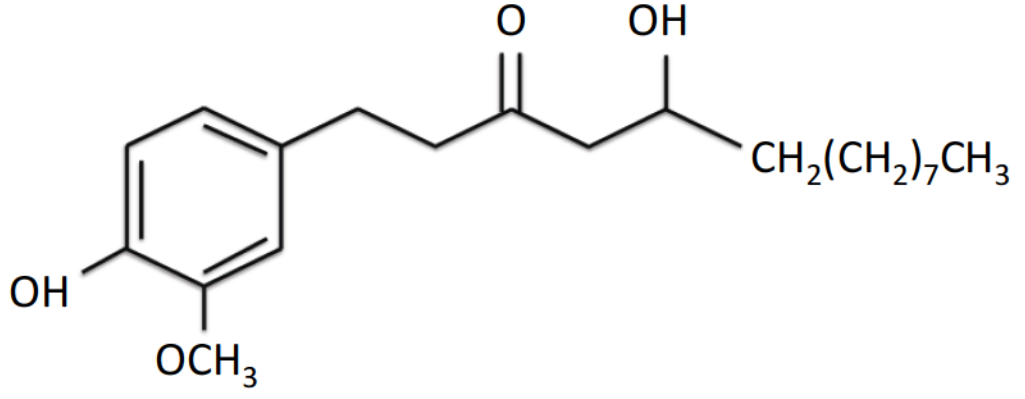

Table 1.1. The Concentrations (mg/100 g) of [6]-, [8]-, and [10]-Gingerol in Three Samples of Commercially Available Ground Ginger Powder[114].

Sample #	[6]-Gingerol (mg/100 g)	[8]-Gingerol (mg/100g)	[10]-Gingerol (mg/100g)
Sample 1	767.87	131.29	157.38
Sample 2	554.87	104.37	136.54
Sample 3	772.33	140.04	173.4

Table 1.2. The Highest and Lowest Concentrations (mg/g) of [6]-, [8]-, and [10]-Gingerol Taken from Several Ginger Samples[115].

	Sample Code	Source	[6]-Gingerol (mg/g)	[8]-Gingerol (mg/g)	[10]-Gingerol (mg/g)
Lowest Concentration	ZOO-12	Leuwiliang, Bogor, West Java	2.98 ± 0.06	0.52 ± 0.02	
Highest Concentration	ZOA-13	Ciampea, Bogor, West Java	18.83 ± 0.28	3.07 ± 0.03	
Lowest Concentration	ZOR-11	Leuwiliang, Bogor, West Java			0.79 ± 0.01
Highest Concentration	ZOA-3	Tegal Ombo, Pacitan, East Java			3.54 ± 0.02

endothelial growth factor (VEGF) and basic fibroblast growth factor-induced proliferation of endothelial cells, thereby displaying anti-angiogenic properties[122].

[8]-Gingerol and [10]-Gingerol

[8]-Gingerol and [10]-gingerol are also phenolic acids derived from ginger. Very little evidence has been gathered regarding the health benefits of [8]- and [10]-gingerol, especially regarding their potential anti-inflammatory and anti-cancer properties. Much of the information describes their modulation of calcium levels in muscle[123,124] and cancer cells[125] and their anti-emetic properties[126]. The mechanism behind the anti-emetic properties of ginger are thought to be in part due to the ability of [8]- and [10]-gingerol to bind to an unknown modulatory site on the 5- HT_3 (5-hydroxytryptamine) receptors[126]. Furthermore, [10]-gingerol modulates calcium levels to cause the death of human colorectal cancer cells[125]. Other evidence shows that [8]- and [10]-gingerol suppress human P450 enzyme activity in the hepatocellular carcinoma cell line, HepG2[127], implicating a potential negative impact of gingerol or ginger products on the efficacy of therapeutic drugs that are metabolized by cytochrome P450 enzymes. Moreover, [8]-gingerol suppresses splenocyte proliferation, possibly by decreasing the percentage of B cells and T cells in ovalbumin (OVA)-immunized mice[128].

1.4.1 Ginger Pharmacokinetics

Yu et al. conducted a study on oral administration of 2.0 g of ginger extracts to healthy human subjects. After 1 h, only low levels of free [10]-gingerol and [6]-shogaol were present in the plasma, and the majority of [6]-, [8]- and [10]-gingerol and [6]-shogaol existed as glucuronide and sulfate metabolites[129]. This was interesting, considering that [6]-gingerol was the most abundant component of the extracts (2.64%)

and [10]-gingerol accounted for 1.22% of the ginger extracts. [6]-Shogaol comprised 2.25% of the extract. The peak concentrations of [10]-gingerol and [6]-shogaol in the plasma were approximately 12 and 8 μM, respectively.

A second study on ginger metabolism in human subjects did not detect any free [6]-, [8]-, [10]-gingerol or [6]-shogaol in the plasma at several time intervals up to 72 h post-administration of 100 mg to 2.0 g of ginger as capsules[130]. Again, [6]-, [8]-, [10]-gingerol and [6]-shogaol glucuronides were detectable, as well as [6]- and [8]-gingerol sulfates.

Lv et al. cultured human lung cancer cells (H-1299) with [6]-gingerol in media for 48 h in order to isolate and establish the structures of the major metabolites. Major metabolites in these cells were shown to be the keto reduced metabolites of [6]-gingerol, (3S, 5S)-[6]-gingerdiol and (3R, 5S)-[6]-gingerdiol[131]. Urine samples collected from mice that were administered [6]-gingerol by oral gavage also contained [6]-gingerol, (3S, 5S)-[6]-gingerdiol, and (3R, 5S)-[6]-gingerdiol after 24 h[131]. These studies used high performance liquid chromatography (HPLC) and nuclear magnetic resonance (NMR) to measure metabolite levels.

In another study, zebrafish embryos were incubated with [10]-gingerol for 18-19 h. NMR determined that (3*R*, 5*S*)-[10]-gingerdiol, (3*S*, 5*S*)-[10]-gingerdiol, and an unknown compound were the resulting metabolized compounds[132]. The same study also found these metabolites at low levels in the urine of healthy human subjects who drank ginger tea.

Overall, it appears that gingerol is quickly metabolized into gingerdiols, glucuronides, and sulfate metabolites. According to the studies investigating the

administration of ginger extracts and ginger capsules to humans, the levels of gingerol are either extremely low or undetectable in comparison to other metabolites. This suggests that it is metabolites that provide the therapeutic benefits of ginger.

1.5 Rationale and Objectives

The overall objective of this investigation is a comparative study of the immunomodulatory and anti-breast cancer effects of three gingerol homologs, [6]-, [8]-, and [10]-gingerol, on mouse and human mammary carcinoma cell cultures and isolated mouse T cells. Since [6]-gingerol decreases cancer cell proliferation[110,120,133], induces cell death in several cancer cell lines[110,134], and inhibits various factors involved in the promotion of inflammation[135], I hypothesized that [8]- and [10]-gingerol may also have anti-cancer and anti-inflammatory properties.

The specific objectives of this study were to: 1) compare the anti-proliferative and cytotoxic effects of [6]-, [8]-, and [10]-gingerol on human and mouse cancerous and non-cancerous cell cultures; 2) establish whether gingerol-induced cancer cell death was dependent upon ROS production and/or the activation of caspases; 3) determine and compare the anti-proliferative effect of gingerol on mouse T cells *in vitro*; 4) determine the cytotoxicity of gingerol on isolated mouse T cells and DCs; and 5) determine the mechanism by which gingerol inhibits T cell proliferation.

CHAPTER 2

MATERIALS AND METHODS

2.1 Mice

Female C57BL/6 mice aged 6-8 weeks were purchased from Charles River Laboratory (Lasalle, PQ, Canada). Mice were housed at the Carleton Animal Care Facility of Dalhousie University where standard rodent chow and water were supplied *ad libitum*. Animal protocols were consistent with the Canadian Council on Animal Care guidelines and were approved by the Dalhousie University Committee on Laboratory Animals. All mice used in these experiments were 8-12 weeks old.

2.2 $CD3^+$ T Cell Isolation

C57BL/6 mice were sacrificed by cervical dislocation and spleens were harvested using aseptic technique. Tissues were homogenized in ice-cold phosphate buffered saline (PBS; pH 7.4) to yield a single-cell suspension (refer to Appendix Table 1 for the complete list of materials used in this study). Tissue debris was discarded and the cell suspension was centrifuged at 500 x gravity (*g*) for 5 minutes (min). 4 Milliliters (mL) of 0.2 % sodium chloride (NaCl) was added to the pellet for 20 seconds (causing the erythrocytes to undergo hypo-osmotic shock) followed by 4 mL of 1.6 % NaCl to restore isotonicity. Cell debris was discarded and cell suspensions were centrifuged at 500 x *g* for 5 min. Cells were resuspended in MACS® buffer (2 % BSA, 2 mM EDTA in PBS, pH 7.2) and run through a MACS® Pre-Separation Filter (30 µM; Miltenyi Biotec, Auburn, CA, USA) to remove any remaining debris. Cell suspensions were then centrifuged at 500 x *g* for 5 min. Pellets were resuspended in MACS® buffer and cell number was determined by trypan blue exclusion using a hemacytometer.

$CD3^+$ T cells (hereafter known as T cells) were isolated by negative selection using the Pan T Cell Isolation MACS® Kit II according to the manufacturer's instructions using slight modifications. 1.35 x 10^6 splenocytes were suspended in 450 microliters (µL) of MACS® buffer and treated with 50 µL of biotin-conjugated monoclonal antibody (mAb) beads against unwanted cells (anti-[α-]CD45R [B220], α-CD49b [DX5], α-CD11b [Mac-1], and α-Ter 119) for 10 min at 4 °C, following which an additional 400 µL of MACS® buffer and 100 µL of α-biotin microbeads were added and the cell suspension was incubated for an additional 15 min at 4 (°C). The volume was topped to 10 mL with MACS® buffer and the cell suspension was centrifuged at 500 x *g* for 5 min to remove excess beads and antibody. Pellets were resuspended in 1 mL of MACS® buffer, then run through a LS column (Miltenyi Biotec, Auburn, CA, USA) and placed in a magnetic field. The desired T cells were collected while the unwanted cells attached to the mAb beads were retained in the column. The column was washed 3 times with 3 mL of MACS® buffer and collected with desired cells. The cell suspension was washed 2 times with 5 mL of complete Roswell Park Memorial Institute 1640 (cRPMI) medium, then counted using Trypan Blue exclusion.

2.3 Bone Marrow-Derived Dendritic Cell Isolation and Culture

C57BL/6 mice were sacrificed by cervical dislocation and the tibia and femur were removed using aseptic technique. 10 mL of ice-cold PBS (pH 7.2) and a 27G1/2 PrecisionGlide® needle (Becton Dickinson & Co., Mississauga, ON, Canada) was used to flush bone marrow from the tibia and femur. The bone marrow was forced through an 18G1 PrecisionGlide® needle (Becton Dickinson & Co.) to create a single cell suspension then cells were centrifuged at 350 x *g* for 5 min. Cell pellets were

resuspended in 1 mL of bone marrow-derived dendritic cell (BMDC) media (the components of the media are described in Appendix Table 2) and a cell number was determined by Trypan Blue exclusion. 1.0 x 10^6 cells/well were seeded into 6-well tissue culture plates containing 5 mL of BMDC medium supplemented with 20 nanograms (ng)/mL of recombinant murine granulocyte/macrophage-colony stimulating factor (rmGM-CSF) to differentiate the cells into DCs. Plates were kept at 37 °C and 5 % CO_2. On day 3, an additional 5 mL of BMDC medium supplemented with 20 ng/mL of rmGM-CSF was added to each well. On day 6, half of the BMDC medium in each well was transferred to a new 6-well tissue culture plate while the other half of the BMDC medium was removed and centrifuged at 350 x *g* for 5 min then resuspended in 5 mL/well of fresh BMDC medium supplemented with 10 ng/mL of rmGM-CSF. This was then added on top of the previously transferred BMDC medium. Cells were transferred to another tissue culture plate to eliminate fibroblasts, which remain attached to the culture plates. On day 7 or 8, non-adherent cells were transferred into new 6-well plates for at least 1 hour (h) to remove remaining fibroblasts by allowing them to adhere. The BMDC medium in each well was centrifuged at 350 x *g* for 5 min then resuspended in fresh BMDC supplemented with 1 µg/mL of lipopolysaccharide (LPS) to mature the cells and 10 ng/mL of rmGM-CSF. On day 8 or 9, DC cultures were ready for use.

2.4 Cells and Cell Culture

4T1 and E0771 mouse mammary carcinoma cells were kindly donated by Dr. D. Waisman and Dr. R. Liwski, respectively (Dalhousie University, NS, Canada). The non-cancerous mouse epithelial cell line (HC11) was donated by Dr. Ro (Dalhousie University, NS, Canada). MDA-MB-231 and MDA-MB-468 triple-negative human

breast carcinoma cells were generously donated by Dr. S. Dover (Memorial University of Newfoundland, NL, Canada) and Dr. P. Lee (Dalhousie University, NS, Canada), respectively. Human mammary epithelial cells (HMEC) and the human dermal fibroblast cells were purchased from Lonza Inc. (Walkersville, MD, USA). The IL-2 dependent CTL cell line, CTLL-2, was donated by Dr. C. Too (Dalhousie University, NS, Canada).

4T1, E0771, MDA-MB-231, and MDA-MB-468 cell lines were cultured in complete Dulbecco's Modified Eagle's Medium (cDMEM) and maintained in a humidified incubator at 37 °C and 10 % CO_2. Their origin and known receptor expressions are described in Appendix Table 3. HMEC, HC11, human dermal fibroblasts, CTLL-2 cells, T cells, and DCs were cultured in Mammary Epithelial Growth Medium (MEGM), HC11 media, Fibroblast Growth Medium (FGM), CTLL-2 medium, cRPMI medium, and BMDC medium, respectively, and maintained in a humidified incubator at 37 °C and 5 % CO_2. The composition of these media are described in Appendix Table 2.

Adherent cell lines were passaged in a sterile environment and at 80 % confluence. For 4T1 and E0771 cell lines, this occurred approximately every 2 days. For HC11, MDA-MB-231, and MDA-MB-468 cell lines, this occurred every 3-4 days. For human dermal fibroblasts and HMECs, this occurred approximately every 5-8 days. To passage adherent cell lines, culture medium from the T75 flask was discarded and 3 mL of TrypLE was added at room temperature for approximately 5 min or until cells were detached. 7 mL of the appropriate medium was added to the flask containing the cell suspension, and a designated volume was added to the respective medium in a fresh T75 flask to a total volume of 10 mL. Specifically, 0.5 mL of 4T1 and E0771 cell suspension

and between 1.5-2 mL of HC11, HMEC, human dermal fibroblasts, MDA-MB-231, and MDA-MB-468 cell suspension were pipetted into fresh flasks.

CTLL-2 cells were passaged in a sterile environment every 3 days. For passaging, 1.5 mL of cell culture were added to 8.5 mL of CTLL-2 medium in a fresh T25 flask. 30 units (U)/mL of IL-2 was added to each flask.

2.5 Cell Seeding Conditions

The seeding densities of epithelial cells were based on plate size and species. Seeding densities were based on cell species because of similar growth rates and to maintain moderate consistency. Human cell cultures (MDA-MB-231, MDA-MB-468, HMEC, and human dermal fibroblasts) were seeded at 5000 cells/well in 96-well flat-bottom plates and 1.5×10^5 cells/well in 6-well flat-bottom plates. Mouse cell cultures (4T1, E0771, and HC11) were seeded at 1200 cells/well in 96-well flat-bottom plates and 2.5×10^4 cells/well in 6-well flat-bottom plates.

T cells were seeded at 2.5×10^5 cells/well in 96-well U-bottom plates for bead-activated tritiated thymidine ([^{3}H]TdR) incorporation and 2.0×10^5 cells/well for all other T cell experiments in 96-well U-bottom plates. T cells were added at 1.0×10^6 cells/tube in 5 mL tubes and 5.0×10^6 cells/tube in 1.5 mL microcentrifuge tubes. CTLL-2 cells were added at 1.0×10^6 cells/tube in in 5 mL tubes and at 2.0×10^5 cells/well in 96-well U-bottom plates.

When combined with T cells, DCs were seeded at 6.4×10^3 cells/well in 96-well U-bottom plates. Alone, DCs were seeded at 5.0×10^4 cells/well in 96-well U-bottom plates and 1.0×10^5 cells/well in 6-well flat-bottom plates.

2.6 T Cell Activation

For antibody-coated bead T cell stimulation, Dynabeads® Mouse T-Activator CD3/CD28 antibody-coated beads were used at a ratio of one bead for every two T cells. These beads are coated with α-CD3 and α-CD28 antibodies to mimic the stimulatory signals provided by APCs. α-CD3 antibody will bind to the CD3/TCR complex on the T cell while α-CD28 antibody will bind the co-stimulatory molecule CD28 on the T cell.

For T cell stimulation using DC cultures, cultures were seeded at 6400 DCs for every 200 000 T cells and pulsed with 20 µg/mL of α-TCR antibody. The α-TCR antibody will bind the CD3/TCR component of the T cell, while the B7 on the DCs bind CD28 on the T cell, providing sufficient stimulatory signals for T cell activation and expansion.

Ratios of beads or DCs to T cells and the concentration of α-TCR antibody were determined based on manufacturers' suggestions and numerous experiments by lab personnel who determined these quantities to be the most cost effective and efficient at inducing T cell activation (personal communication).

2.7 Gingerol Solutions

[6]-Gingerol (purity greater than [>] 95 %) was purchased from Dalton Pharma Services (Toronto, ON, Canada) and [8]- and [10]-gingerol (purity $\geq$ 98 %) were purchased from Chengdu Biopurify Phytochemicals Ltd. (Chengdu, Sichuan, China). Stock solutions were prepared at 0.3 Molar (M) concentration in dimethylsulfoxide (DMSO) and stored at -20 °C. The percentage of DMSO during treatment was maintained at $\leq$ 0.01% to avoid DMSO-induced cytotoxicity. In each individual experiment, the percentage of DMSO was kept constant between concentrations.

2.8 Trypan Blue Dye Exclusion Assay

To determine whether gingerol had a cytotoxic effect on T cell or DC cultures, the Trypan Blue dye exclusion assay was performed. Trypan Blue dye is a cell permeable dye that enters dead cells, staining them blue while live cells remain unstained due to active exclusion of the dye. The cells are then counted using a light microscope. T cells or DCs were seeded into 96-well plates, treated with gingerol, and T cells were left unstimulated or were stimulated with α-CD3/CD28 antibody-coated beads and DCs were pulsed with α-TCR at 30 min post-treatment. The Trypan Blue exclusion assay was performed by combining a suspension of medium, vehicle, or gingerol treated cells with Trypan Blue dye (1:1; v/v). Cells were counted at the designated time point using a hemacytometer at 10X resolution. The percentage of live cells was quantified by using the formula (C/T * 100 %), where C is the number of live unstained cells and T is the total number of cells.

2.9 MTT Assay

To determine if gingerol has an effect on the metabolic activities of several human and mouse mammary cancer and non-cancerous cell cultures, the MTT (3-(4,5-Dimethylthiazol-2-yl)-2,5-diphenyltetrazolium bromide) assay was performed. MTT is a tetrazolium salt that is reduced by succinate dehydrogenase within the mitochondria of living cells to form purple formazan crystals that can then be dissolved by DMSO and read on a spectrophotometer. The absorbance readings by the spectrophotometer are indicative of the number of metabolically active cells[136]. For experiments, cells were seeded in at least triplicate in 96-well flat-bottom plates and allowed to adhere overnight. Culture medium was removed and cells were treated with varying concentrations of [6]-,

[8]-, or [10]-gingerol. Between 2 and 6 h prior to the designated time point (depending upon the cell line), 20 µL of 0.5 milligram (mg)/mL of MTT solution (in PBS) was added to each well and incubated at 37 °C and 5 % or 10 % CO_2 (dependent upon the cell line) for the remainder of the time period. Plates were centrifuged at 500 x *g* for 5 min and supernatants were discarded. DMSO was added to each well (100 µL/well) and plates were shaken on a Microplate Genie (Montreal Biotech Inc., Montreal, PQ) for 5 min at 550 revolutions per minute (rpm). Absorbance was read at 570 nanometers (nm) on an Expert 96-well microplate reader (Biochrom ASYS, Cambridge, UK). Absorbance readings were normalized to the medium control and the percent metabolic rate was determined using the formula (100-[(E/C)*100%]) where E is the absorbance reading of the vehicle or gingerol treated cells and C is the absorbance of the medium treated cells.

As previously mentioned, MTT incubation times were dependent upon the cell line. This was due to the differing growth rates, mitochondrial activity, and production of succinate dehydrogenase, which are dependent upon the number of mitochondria within cells. Different cell cultures have varying numbers of mitochondria. Increasing MTT incubation times allows sufficient time for the reduction of MTT by mitochondrial succinate dehydrogenases in cell cultures that contain cells with lower numbers of mitochondria or fewer cells. MDA-MB-231, MDA-MB-468, 4T1, E0771, and HC11 cells were incubated with MTT solution for 2 h. Human fibroblasts were incubated with MTT solution for 4 h and HMECs were incubated for 6 h. These times were deemed sufficient from personal experimentation and from the experimentation of lab personnel.

2.10 Acid Phosphatase Assay

In the phosphatase assay, the phosphatase substrate, p-nitrophenyl phosphatase, is hydrolyzed in the presence of cytosolic phosphatases in living cells and initiates a colour change in the presence of a strong base (1 Normal [N] sodium hydroxide [NaOH]) that can be read by a spectrophotometer. Like the MTT assay, the absorbance readings are indicative of the number of metabolically active cells[137]. For experiments, MDA-MB-231 or 4T1 cells were seeded in quadruplicate in 96-well flat-bottom plates and allowed to adhere overnight. Culture medium was removed and cells were treated with varying concentrations of [6]-gingerol, then 2 h prior to the designated time point, plates were centrifuged at 500 x *g* for 5 min and supernatants were discarded. 100 µL of PBS and 100 µL of acid phosphatase solution (4 mg/mL phosphatase substrate tablet, 0.1% Triton-X-100 [v/v], 0.2 M sodium acetate) were added to each well and incubated for 2 h at 10 % CO_2 and 37 °C. After the incubation period, 10 µL of 1 N NaOH was added to the wells to stop the chemical reaction and plates were shaken on a Microplate Genie (Montreal Biotech Inc.) for 3 mins at 550 rpm. Absorbance was read at 405 nm on an Expert 96-well microplate reader (Biochrom ASYS). The percent phosphatase substrate activity was measured using the same formula as for the MTT assay.

2.11 Amplex Red Assay

The Amplex Red assay was performed to determine if gingerol reacts with sodium bicarbonate in media to produce hydrogen peroxide in a cell-free environment. The Amplex Red reagent ((10-acetyl-3, 7-dihydroxyphenoxazine) combines with horseradish peroxidase (HRP) to produce resorufin, a red-fluorescent oxidation product, which can be measured on a spectrophotometer. The absorbance readings are indicative

of the amount of hydrogen peroxide present. For this assay, 100 µL/well of medium, vehicle, and a final concentration of 200 µM of [6]-, [8]-, and [10]-gingerol (in phenol red-free cDMEM) were pipetted into a 96-well flat-bottom plate in triplicate. Additionally, a final concentration of 50 µM of myricetin (in phenol red-free cDMEM) was added in triplicate as a positive control. In the dark, 100 µL/well of master mix (at a final concentration of 25 µM Amplex Red and 0.005 U/mL HRP in phenol red-free cDMEM) was added on top of the treatments. At 90 min and 24 h post-treatment, the absorbance was read at 570 nm on an Expert 96-well microplate reader (Biochrom ASYS).

2.12 Tritiated Thymidine Incorporation Assay

Tritiated thymidine ([^{3}H]TdR) incorporates into newly synthesized DNA and becomes a radioactive label that can be quantified using a liquid scintillation counter. This provided a comparison of the proliferation of vehicle-treated to gingerol-treated cell cultures. CTLL-2 cells were IL-2 starved for 3 h before being seeded in triplicate in 96-well U-bottom plates, then treated with the indicated concentrations of [6]-, [8]-, and [10]-gingerol. At 30 min post-treatment, cells were stimulated with 50 U/mL of IL-2, then incubated at 37 °C and 5 % CO_2 for 24 h. Isolated T cells were seeded in triplicate into 96-well plates then treated with [6]-, [8]-, or [10]-gingerol, stimulated with α-CD3 and α-CD28 antibody-coated beads at 30 min post-treatment, and incubated at 37 °C and 5 % CO_2 for 48, 72, and 96 h. For assays involving DC co-culture, DCs were seeded in triplicate in 96-well U-bottom plates and kept at 37 °C and 5 % CO_2 until T cells were isolated and added (approximately 2.5 hours later). Next, DC and T cell co-cultures were treated with [6]-, [8]-, or [10]-gingerol and pulsed with α-TCR at 30 min. post-treatment.

Plates were incubated at 37 °C and 5 % CO_2 for 48, 72, and 96 h. For all [^{3}H]TdR incorporation assays, in the last 6 h of incubation, cells were pulsed with 0.2 microcurie (μCi) of methyl [^{3}H]TdR (MP Biomedicals, Irvine, CA) then harvested onto fiberglass filter mats with a Titertek® Cell Harvester (both from Skatron Instruments, Sterling, VA). [^{3}H]TdR- incorporation was measured using a Beckman LS6000IC liquid scintillation counter (Beckman Coulter Inc., Mississauga, ON). The raw counts per minute (cpm) were recorded.

2.13 Flow Cytometry

All flow cytometry was performed on a FACSCalibur flow cytometer using BD Cell Quest™ software (version 3.3; BD Biosciences, Mississauga, ON). Aside from cell cycle data, all data was analysed using FCS Express software (version 3.0; De Novo Software, Thornhill, ON). Cell cycle analysis was performed using ModFit LT software (Verity Software House, Topsham, ME). A minimum of 1.0 x 10^4 events were collected per sample and counts were gated on the live cell population, with the exception of Annexin-V-FLUOS and propidium iodide (PI) staining, where the counts included both live and dead cells.

2.14 Annexin-V-FLUOS and Propidium Iodide Staining

Annexin-V-FLUOS binds phosphatidylserine that has flipped to the outside of early apoptotic cells, and propidium iodide (PI; a cell impermeable DNA intercalating fluorescent dye) enters through pores in cell membranes that form upon necrotic cell death. Annexin-V-FLUOS positive and PI negative staining cells are indicative of early apoptosis, while PI positive and Annexin-V-FLUOS positive staining cells are indicative of late apoptosis/necrosis.

After completing the instructions specific to adherent or suspension cells that are given below, all sample pellets (from adherent cells and suspension cells) were resuspended in 50 µL of 1 µg/mL PI and 1 % Annexin-V-FLUOS (v/v) in incubation buffer (10 mM HEPES, 5 mM $CaCl_2$, 140 mM NaCl) and incubated at room temperature for 10-15 min in the dark. Following incubation, 200-500 µL of incubation buffer was added to each sample in preparation for fluorescence analysis by flow cytometry. Appropriate controls were collected (single-stained and an unstained sample) for appropriate compensation during acquisition of overlapping emission spectra of the two fluorescent dyes.

2.14.1 Adherent Cells

To determine whether gingerol induced cell death, Annexin-V-FLUOS/PI staining was performed on MDA-MB-231, MDA-MB-468, 4T1, E0771, and human dermal fibroblast cells. Cells were seeded in 6-well plates, allowed to adhere overnight, then treated with the desired concentrations of [6]-, [8]-, or [10]-gingerol. 24 h post-treatment, the contents of the wells were transferred to 15 mL polystyrene or polypropylene tubes and the cells were lifted by incubating in 1 mL/well of TrypLE EXPRESS for 5 min and added to respective 15 mL tubes. Samples were centrifuged at 500 x *g* for 5 min, the supernatants were discarded, and the pellets were washed with 5 mL of PBS. The samples were once again centrifuged at 500 x *g* for 5 min and the pellets were resuspended in 1 mL of 1X PBS and transferred to 5 mL tubes. The samples were again centrifuged at 500 x *g* for 5 min and the supernatants were discarded in preparation for the staining protocol described above.

2.14.2 Suspension Cells

To determine whether gingerol induced cell death, Annexin-V-FLUOS/PI was performed on CTLL-2 cell, DC, and T cell cultures. CTLL-2 cell cultures were IL-2 starved for 3 h. T cells, dendritic cells, or CTLL-2 cells were seeded into 96-well U-bottom plates or 5 mL tubes and treated with desired concentrations of [6]-, [8]-, or [10]-gingerol. At 30 min post-treatment, the samples were either left unstimulated (T cells), or were stimulated with α-CD3/α-CD28 antibody-coated beads (T cells) or 50 U/mL of IL-2 (CTLL-2), or were pulsed with α-TCR (DCs cultured with T cells). At 8 or 24 h post-treatment, the samples were transferred to 5 mL tubes containing 1 mL PBS. Samples were centrifuged at 500 x *g* for 5 min, the supernatants were discarded, and the pellets were washed with 1 mL PBS. Samples were centrifuged at 500 x *g* for 5 min and the supernatants were discarded in preparation for the staining protocol described above.

2.15 Oregon Green 488 Cytofluorometric Assay

The Oregon Green 488 cytofluorometric assay was performed to determine if gingerol effected the proliferation of MDA-MB-231, 4T1, or T cell cultures. Oregon Green 488 (Cell Trace™ Oregon Green® 488 carboxylic acid diacetate) is a cell permeable fluorescent dye. The quantity of dye within a stained cell is halved with each cell division. Therefore, the number of cell divisions can be quantified by comparing the fluorescence of treatments to a stained, non-proliferating control. Fluorescence intensity is measured and analyzed by flow cytometry.

2.15.1 Adherent Cells

MDA-MB-231 or 4T1 cells were seeded into 6-well plates and allowed to adhere overnight. Culture medium was discarded and the wells were washed with 1 mL of warm

(37 °C) PBS. PBS was discarded and, in the dark, cells were incubated with 1.25 μM of Oregon Green in warm serum-free DMEM for 10-15 min at room temperature. Next, samples were washed 3 times (1 mL/wash) with warm cDMEM. A non-proliferative control was harvested and fixed in 1 % paraformaldehyde (PFA) and stored at 4 °C until further use. Remaining cells were treated with desired concentrations of [6]-, [8]-, or [10]-gingerol for 72 h.

Following culture, the cells were removed from the plates by transferring the culture medium from the wells to separate 5 mL tubes, incubating the cells in 1 mL/well of TrypLE EXPRESS for 5 min, then adding the detached cells to their respective 5 mL tubes. Samples were centrifuged at 500 x *g* for 5 min, washed with 1 mL of PBS, and fixed in 250-500 μL of 1 % PFA. Fluorescence intensity was measured and analyzed by flow cytometry.

The number of cell divisions was calculated on Microsoft® Excel® (version 14.2.5) using the formula ($\ln[MFI_{control}/MFI_{sample}]/\ln 2$) where MFI is the mean fluorescence intensity, $MFI_{control}$ is the MFI of the non-proliferative sample, and MFI_{sample} is the MFI of treated samples[108].

2.15.2 T Cells

T cells were harvested from the spleens of C57BL/6 mice using the described T cell isolation protocol. T cells were pooled in a 15 mL polystyrene or polypropylene tube, centrifuged at 500 x *g* for 5 min, and the pellets were resuspended in the dark in 1.25 μM of Oregon Green 488 in PBS and incubated at room temperature. After 10 min, T cells were centrifuged at 500 x *g* for 5 min and the pellets were resuspended in 4 mL of warm FBS to bind excess Oregon Green 488. Again, T cells were centrifuged at 500 x *g* for 5

min and the pellets were resuspended in 4 mL of warm cRPMI and incubated at 37 °C in 5 % CO_2 for 30 min with a loosened cap.

T cells were counted and plated in triplicate into 96-well plates and treated with varying concentrations of [6]-, [8]-, or [10]-gingerol. A non-proliferative control was collected and fixed in 1 % paraformaldehyde (PFA) and kept at 4 °C until further use. The remaining T cells were stimulated with α-CD3 and α-CD28 antibody-coated beads 30 min post-treatment. 48 and 72 h post-stimulation, T cells were transferred to 5 mL tubes containing 1 mL of PBS, centrifuged at 500 x *g* for 5 min, and washed with 1 mL/tube of PBS. Samples were centrifuged at 500 x *g* for 5 min and the pellets were fixed in approximately 300-500 µL of 1 % PFA for analysis by flow cytometry. Constructing a gate that excluded the non-proliferative control allowed analysis of the percent of live proliferating cells.

2.16 Cell Cycle Analysis

Cell cycle analysis was performed to determine the stage of gingerol-induced cell cycle arrest. PI is a DNA intercalating fluorescent dye. When performing cell cycle analysis, PI-binding is directly related to the amount of DNA within a cell. Therefore, the phase of the cell cycle can be determined by measuring the fluorescence of PI by flow cytometry. In the G1 (Gap Phase 1) phase of the cell cycle, the cells have one copy of their own DNA. Therefore, the same fluorescence should be detected from each G1 cell and the result is a sharp Gaussian peak. As cells enter the S (synthesis) phase, the amount of DNA begins to double as the cells are undergoing replication, but not all of the cells synthesize DNA at the same rate. Therefore, the fluorescence begins to double and the peak is spread over a wider area. In the G2 (Gap Phase 2) phase, cells have completed

DNA synthesis and the cells have double the amount of DNA compared to the G1 phase, showing approximately double the mean Gaussian peak position as seen in the G1 phase.

To synchronize cell cycles into the G0 (quiescent) phase, MDA-MB-231 and 4T1 cell cultures were incubated in serum-free cDMEM for approximately 24 h before seeding into 6-well plates. Cells were allowed to adhere overnight before treatment with [6]-, [8]-, or [10]-gingerol. At 48 and 72 h post-treatment, culture medium containing treatments were removed from wells and transferred to separate 15 mL polystyrene or polypropylene tubes. TrypLE EXPRESS (1 mL/well) was added for 5 min at room temperature to detach cells. Cells were then added to their respective supernatants. Samples were centrifuged at 500 g for 5 min then washed in 5 mL of ice-cold PBS, and centrifuged at 500 x *g* for 5 min. Pellets were resuspended in 500 µL of ice-cold PBS. While vortexing, 4.5 mL of 70 % ethanol was slowly added to samples in a drop-wise fashion to permeabilize and fix the cells. Samples were stored at -20 °C for at least 24 h. Prior to analysis, samples were centrifuged at 1000 x *g* for 5 min and washed with 5 mL of PBS. Samples were again centrifuged at 1000 x *g* for 5 min. In the dark, pellets were resuspended in 0.5-1 mL of cell cycle solution (0.1 % Triton X-100 [v/v] in PBS, 0.2 mg/mL DNase-free RNase A, and 0.02 mg/mL PI) and transferred to separate 5 mL tubes. Samples were incubated for 30 min at room temperature in the dark. Samples were collected at 40 to 80 events/second by flow cytometry and analyzed using ModFit LT Software (Verity Software House). Gates were constructed on a single cell population to exclude cell debris and cell aggregates during collection. Apoptosis data was collected as represented by cells in the sub G1 peak.

2.17 Cell Surface Antibody Staining

Antibody staining was used to assess the effects of gingerol on the expression of early activation markers (CD25 and CD69) and the IFN-γR1 (CD119). CTLL-2 cells were IL-2 starved for 3 h. T cells or CTLL-2 cells were seeded into 5 mL tubes and treated with [6]-, [8]-, or [10]-gingerol. 30 min post-treatment, T cell samples were stimulated with α-CD3- and α-CD28 antibody-coated beads and CTLL-2 cells were stimulated with 50 U/mL of IL-2 and incubated at 37 °C and 5 % CO_2 for 24 h. Samples were centrifuged twice at 500 x *g* and 4 °C for 5 min and washed with 1 mL/well of fluorescence-activated cell sorting (FACS) buffer (0.2 % sodium azide [w/v], 1 % BSA [w/v], in PBS). Cell pellets were incubated in antibody (α-CD25-PE, α-CD69-FITC, or α-CD119-FITC) or isotype antibody control for 30 min on ice in the dark. Following incubation, cells were centrifuged twice at 500 x *g* and 4 °C for 5 min and washed with 1 mL/well of FACS buffer. Pellets were fixed in approximately 200-500 µL of 1 % PFA and the fluorescence intensity was analyzed by flow cytometry. Analysis was performed using FCS Express Software.

The median fluorescence intensity (MFI) of cells expressing the antibody is a measurement of the amount of antibody being expressed by each cell. This was determined by subtracting the MFI of the isotype from the respective MFI of the antibody. The percent of cells expressing the antibody was acquired by graphing the percent of gated cells as determined by constructing a gate that excluded the isotype control.

2.18 Enzyme-Linked Immunosorbent Assay

To measure the effects of gingerol on the production of select cytokines, T cells were seeded into 96-well plates, treated with indicated concentrations of [6]-, [8]-, or [10]-gingerol, and stimulated with α-CD3- and α-CD28 antibody-coated beads for 15 min post-treatment. Samples were transferred to 5 mL tubes and centrifuged at 500 x *g* for 5 min. Supernatants were then collected and analyzed for IFN-γ, IL-2, and IL-4 concentrations at 24 h post-stimulation using a sandwich enzyme-linked immunosorbent assay (ELISA) kit from BD biosciences (IL-2 and IL-4) or eBioscience (IFN-γ) according to the manufacturer's instructions with slight modifications. Costar® 96-well flat-bottom high binding chemistry enzyme immunoassay plates (Corning Inc, Corning, NY) were coated with capture enzyme antibody diluted in coating buffer (0.1 M sodium carbonate [pH 9.5]) and incubated overnight at 4 °C. Plates were washed 5 times with washing buffer (0.05% Tween-20 [v/v] in PBS) before blocking with assay diluent (10 % BSA in PBS) at room temperature. After 1 h, plates were washed 5 times in washing buffer and supernatants and recombinant cytokine standards were added and incubated at 4 °C for 24 h. Again, plates were washed 5 times and biotinylated detection antibody was added for 1 h at room temperature. Plates were washed 5 times before the addition of streptavidin-HRP for 45 min. 7 washes were performed before adding substrate solution (tetromethylbenzidine [TMB]). When a sufficient amount of colour was observed (after 10-30 mins), the reaction was stopped by adding 1 M sulfuric acid and the absorbance readings were recorded at 450 nm on an Expert 96 well microplate reader. From the absorbance readings, SOFTmax® Pro software (version 4.3; Biotek Instruments Inc.,

Winooskin, VT) was used to further acquire the average concentration of each cytokine in pg/mL.

2.19 Statistical Analysis

Statistical analysis was performed using a one-way analysis of variance (ANOVA) with a Tukey-Kramer multiple parameters post-test using GraphPad Prism analysis software (GraphPad Software Inc., La Jolla, CA). Data were considered statistically significant when p was less than 0.05 ($p < 0.05$) and were denoted by *.

CHAPTER 3

THE IMMUNOMODULATORY EFFECTS OF [6]-, [8]-, AND [10]-GINGEROL

3.1 [6]-Gingerol, [8]-Gingerol, and [10]-Gingerol Inhibit α-CD3 and α-CD28 Antibody-Coated Bead-Stimulated T Cell DNA Synthesis

Several phytochemicals mediate anti-inflammatory effects by affecting the proliferation and differentiation of T cells[101,138,139]. To examine the effects of gingerol on T cell proliferation, mouse splenic T cell DNA synthesis was measured by the [^{3}H]TdR incorporation assay. In [^{3}H]TdR incorporation, a decrease in cpm is indicative of a decrease in DNA synthesis and therefore the number of proliferating cells. For this experiment, T cells were isolated from the spleens of C57BL/6 mice, treated with gingerol or a vehicle control, and at 30 min post-treatment were stimulated with α-CD3 and α-CD28 antibody-coated beads, mimicking the signals of APCs to induce T cell proliferation.

T cell proliferation was decreased at 48 and 72 h post-stimulation by [6]-, [8]-, and [10]-gingerol, and additionally after 96 h by [6]- and [8]-gingerol with 100 μM (Figure 3.1). After 72 and 96 h, 50 μM of [6]- and [8]-gingerol induced a significant decrease in T cell proliferation. Furthermore, [6]-gingerol significantly inhibited T cell proliferation at 50 μM after 48 h. Additionally, [6]-gingerol induced a significant dose-dependent decrease in T cell proliferation with 50 μM compared to 2.5 μM (72 h), 50 μM compared to 10 μM (72 h), 100 μM compared to 2.5 μM (48 and 72 h), and 100 μM compared to 10 μM (72 h). [8]-Gingerol induced a significant dose-dependent decrease in T cell proliferation with 100 μM compared to 2.5 μM, 100 μM compared to 10 μM, and 100 μM compared to 50 μM at all time points. [10]-Gingerol induced a significant dose-

Figure 3.1. Gingerol Inhibits Antibody-Coated Bead-Stimulated Pan T Cell Proliferation. T cells were isolated from the spleens of C57BL/6 mice, incubated with vehicle or [6]-, [8]-, or [10]-gingerol, and stimulated with α-CD3 and α-CD28 for 48, 72, and 96 h. Cell samples were pulsed with [^{3}H]TdR for the last 6 h of incubation and harvested for liquid scintillation counting. Data shown are the average cpm of $\geq$ 3 independent experiments $\pm$ SEM; * $p < 0.05$ when compared to the vehicle at the corresponding time point by one-way ANOVA with a Tukey-Kramer multiple parameters post-test.

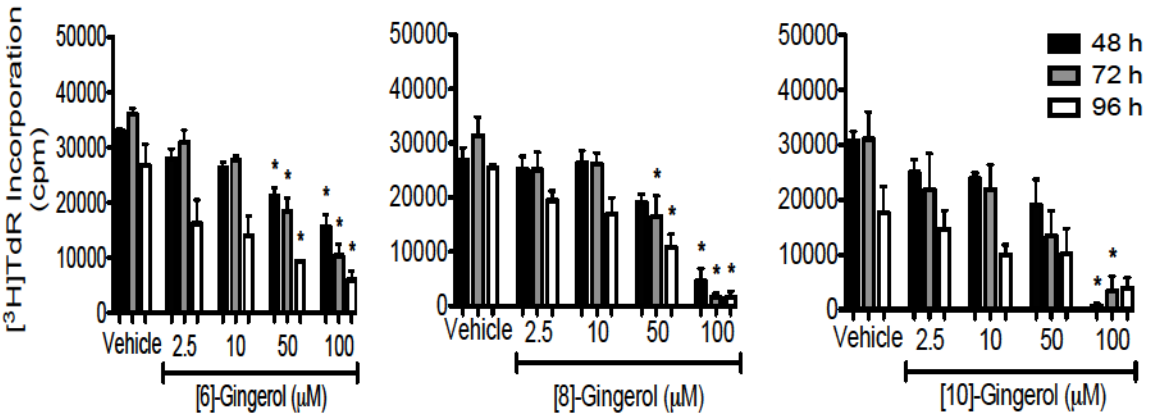
[³H]TdR Incorporation (cpm)
50000
40000
30000
20000
10000
0
Vehicle
2.5
10
50
100
[6]-Gingerol (μM)
[8]-Gingerol (μM)
[10]-Gingerol (μM)
48 h
72 h
96 h

Figure 3.1

dependent decrease in T cell proliferation with 100 μM compared to 2.5 μM, 10 μM , and 50 μM at 48 h post-stimulation. Overall, following gingerol treatment, a significant dose-dependent decrease in T cell proliferation was observed. This reduction in T cell levels was evident as early as 48 h post-stimulation. Interestingly, at the highest dose tested, [8]- and [10]-gingerol exhibited a stronger suppressive activity than [6]-gingerol, as indicated by lower cpm readings.

3.2 [6]-Gingerol, [8]-Gingerol, and [10]-Gingerol Inhibit T Cell DNA Synthesis After Stimulation With Dendritic Cells and α-TCR Antibody.

The [^{3}H]TdR incorporation assay was repeated using DC cultures and α-TCR antibody for T cell stimulation in the place of antibody-coated beads. DCs more closely mimic the interactions that occur *in vivo*, although it represents only a small part of the many complex interactions that occur *in vivo*. T cells were isolated from the spleens and DCs were derived from the bone marrow of C57BL/6 mice were treated with gingerol or a vehicle control, and pulsed with α-TCR antibody. The proliferation of [6]-gingerol-treated T cells was significantly inhibited with 50 μM at 48 and 96 h post-stimulation and with 100 μM at 48, 72, and 96 h post-stimulation (Figure 3.2). [6]-Gingerol also induced a significant dose-dependent decrease in T cell proliferation at 48 and 72 h with 100 μM compared to 2.5 μM and 10 μM. [8]-Gingerol (50 and 100 μM) significantly decreased T cell proliferation after 48 and 72 h. Additionally, 100 μM of [8]-gingerol inhibited T cell proliferation after 96 h. [8]-Gingerol also induced a significant dose-dependent decrease in T cell proliferation with 50 μM compared to 2.5 μM (48, 72, and 96 h), 50 μM compared to 10 μM (48 h), 100 μM compared to 2.5 μM (48, 72, and 96 h), 100 μM compared to 10 μM (48, 72, and 96 h), and 100 μM compared to 50 μM (96 h). [10]-

Figure 3.2. Gingerol Inhibits Pan T Cell Proliferation After Stimulation With Dendritic Cells and α-TCR Antibody. T cells were isolated from the spleens and DCs were harvested from the bone marrow of C57BL/6 mice. T cell and DC co-cultures were incubated with vehicle or [6]-, [8]-, or [10]-gingerol and pulsed with α-TCR antibody for 48, 72, and 96 h. Cell samples were pulsed with [^{3}H]TdR for the last 6 h of incubation and harvested for liquid scintillation counting. Data shown are the average cpm of $\geq$ 3 independent experiments $\pm$ SEM; * $p < 0.05$ when compared to the vehicle at the corresponding time point by one-way ANOVA with a Tukey-Kramer multiple parameters post-test

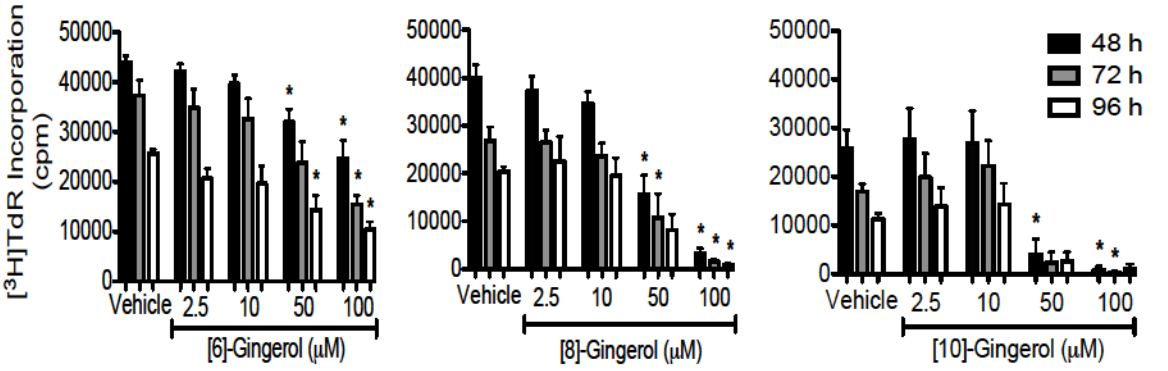
[3H]TdR Incorporation (cpm)
50000
40000
30000
20000
10000
0
Vehicle
2.5
10
50
100
[6]-Gingerol (μM)
[8]-Gingerol (μM)
[10]-Gingerol (μM)
48 h
72 h
96 h

Figure 3.2

Gingerol inhibited T cell proliferation after 48 h at concentrations of 50 and 100 μM, and after 72 h at a concentration of 100 μM. Moreover, [10]-gingerol induced a significant dose-dependent decrease in T cell proliferation with 50 μM compared to 2.5 μM (48 and 72 h), 50 μM compared to 10 μM (48 and 72 h), 100 μM compared to 2.5 μM (48 and 72 h), and 100 μM compared to 10 μM (48, 72, and 96 h). Overall, gingerol treatment caused a dose-dependent reduction in α-TCR and DC-stimulated T cell proliferation. As also observed in the antibody bead-stimulated T cell cultures, significant inhibition of proliferation was seen as early as 48 h with high doses of gingerol. Similar to previous experiments, [8]- and [10]-gingerol were more potent suppressors of T cell proliferation than [6]-gingerol, as indicated by lower cpm readings.

3.3 100 μM of [8]- and [10]-Gingerol, But Not [6]-Gingerol, Inhibit CTLL-2 DNA Synthesis

The effect of gingerol on the IL-2-dependent cytotoxic T cell line, CTLL-2, was also assessed by [^{3}H]TdR incorporation. CTLL-2 cell cultures were IL-2-starved for 3 h, treated with gingerol or a vehicle control, and stimulated with 50 U/mL of IL-2 at 30 mins post-treatment. [8]-Gingerol and [10]-Gingerol at 100 μM concentrations were found to significantly reduce CTLL-2 proliferation at 24 h post-stimulation with IL-2 (Figure 3.3). Interestingly, [6]-gingerol had no effect on CTLL-2 proliferation.

3.4 [8]-Gingerol and [10]-Gingerol, But Not [6]-Gingerol, Inhibit the Proliferation of Oregon Green 488-Stained T Cells

Inhibition of splenic T cell proliferation was further investigated by fluorescence quantification of Oregon Green 488-stained T cell cultures. T cell cultures were treated

Figure 3.3. [8]-Gingerol and [10]-Gingerol, But Not [6]-Gingerol, Inhibit CTLL-2 Proliferation. CTLL-2 cell cultures were IL-2-starved for 3 h, incubated with vehicle or [6]-, [8]-, or [10]-gingerol, then treated with IL-2 (50 U/mL) for 24 h. Cell samples were pulsed with [^{3}H]TdR for the last 6 h of incubation and harvested for liquid scintillation counting. Data shown are the average cpm of $\geq$ 3 independent experiments $\pm$ SEM; * $p < 0.05$ when compared to the vehicle at the corresponding time point by one-way ANOVA with a Tukey-Kramer multiple parameters post-test

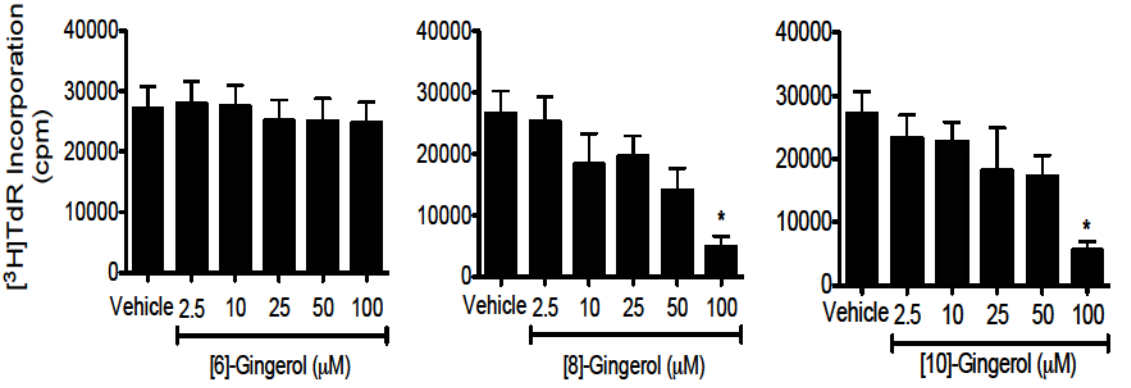
[3H]TdR Incorporation (cpm)
40000
30000
20000
10000
0
Vehicle
2.5
10
25
50
100
[6]-Gingerol (μM)
*
[8]-Gingerol (μM)
[10]-Gingerol (μM)

Figure 3.3

with gingerol or a vehicle control in the presence or absence of α-CD3 and α-CD28 antibody-coated beads. After the indicated time-points, T-cell culture fluorescence was measured by flow cytometry. No significant decrease in the percent of live proliferating T cells or the rounds of T cell division were viewed upon [6]-gingerol treatment (Figure 3.4). [8]- and [10]-gingerol (100 μM) caused a significant decrease in the percent of live proliferating T cells and rounds of division after 48 and 72 h. Additionally, [10]-Gingerol (50 μM) showed a significant decrease in the percent of live proliferating cells and T cell divisions after 48 h, and [8]-gingerol (50 μM) significantly decreased the rounds of T cell divisions after 72 h. Representative histograms from an experiment performed at 72 h are displayed in Figure 3.4B.

3.5 Gingerol Does Not Reduce Viable Cell Counts of Dendritic Cell Cultures or Stimulated or Unstimulated T Cell Cultures at Concentrations Less Than 100 μM

To determine whether gingerol also induced T cell and DC cytotoxicity, Trypan Blue counts and Annexin-V-FLUOS/PI staining were performed. Trypan Blue counts were performed to quantify viable cells, whereby stained cells were counted as dead cells and unstained cells were counted as live cells. No significant decrease in T cell live counts was viewed in unstimulated gingerol-treated T cell cultures at 8 (Figure 3.5A) or 24 h (Figure 3.5B) post-treatment with Trypan Blue staining. Trypan Blue staining of T cells only indicated a significant decrease in viable T cell counts with 100 μM of [10]-gingerol at 24 h post-antibody-coated bead stimulation (Figure 3.6). The viability of DCs cultured with α-TCR antibody and examined by Trypan Blue staining indicated no change in viable cell counts at 8 (Figure 3.7A) or 24 h (Figure 3.7B) post-treatment with [6]- [8]-, or [10]-gingerol.

Figure 3.4. High Concentrations of [8]- and [10]-Gingerol, But Not [6]-Gingerol, Inhibit T Cell Proliferation. T cells were isolated from the spleens of C57BL/6 mice and stained with Oregon Green 488. Cells were then treated with vehicle (Veh) or [6]-, [8]-, or [10]-gingerol and cultured for 48 and 72 h with or without α-CD3 and α-CD28 antibody-coated beads. Cells were fixed and the fluorescence was measured by flow cytometry. Histograms depict a representative experiment at 72 h (A). Data shown are the mean percentage of proliferating cells $\pm$ SEM (B) and the average rounds of division of $\geq$ 3 independent experiments $\pm$ SEM; * $p < 0.05$ when compared to the vehicle at the corresponding time point by one-way ANOVA with a Tukey-Kramer multiple parameters post-test.

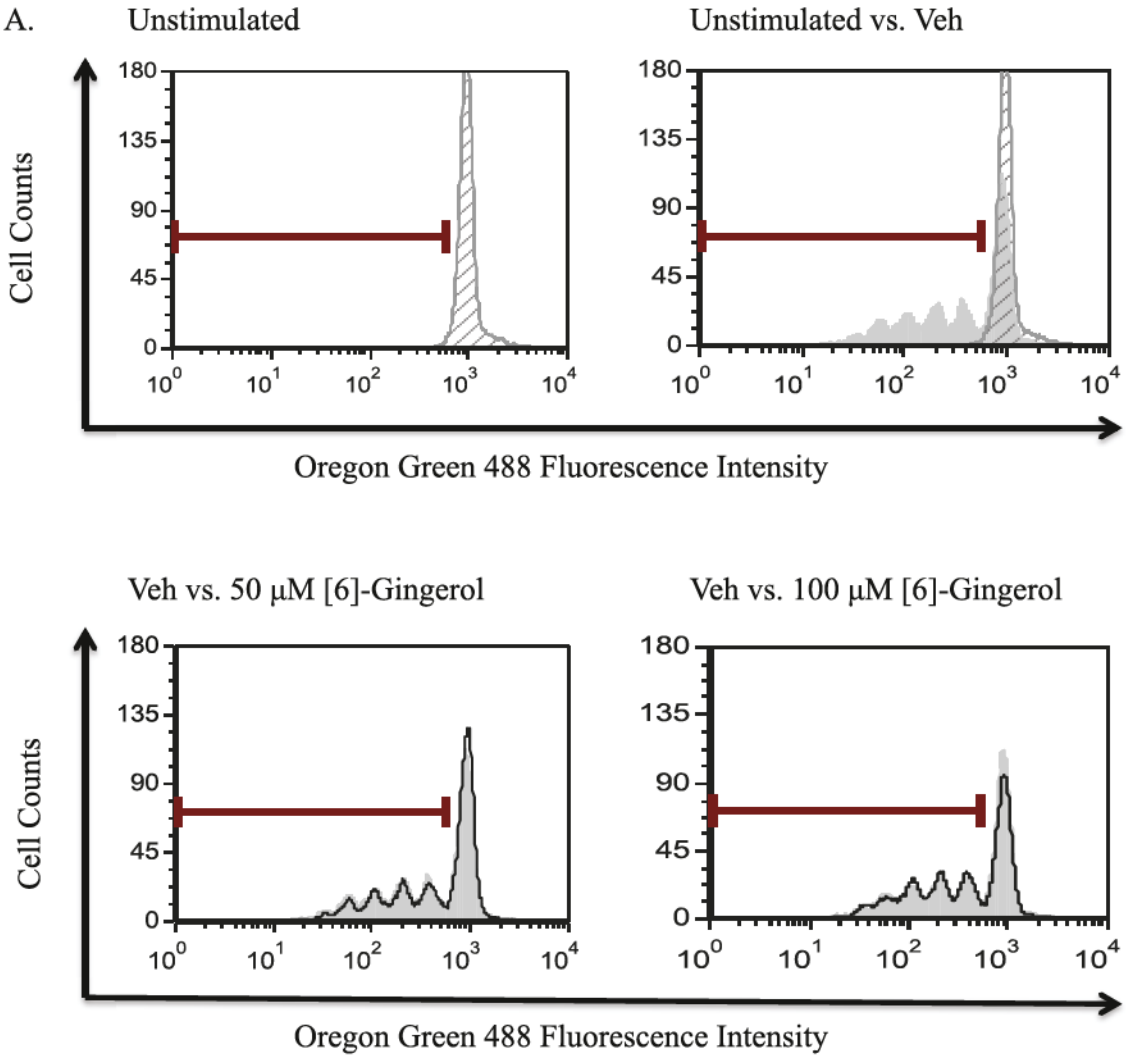
A.
Unstimulated
Unstimulated vs. Veh
Cell Counts
180
135
90
45
0
10^0
10^1
10^2
10^3
10^4
Oregon Green 488 Fluorescence Intensity
Veh vs. 50 µM [6]-Gingerol
Veh vs. 100 µM [6]-Gingerol
Cell Counts
Oregon Green 488 Fluorescence Intensity

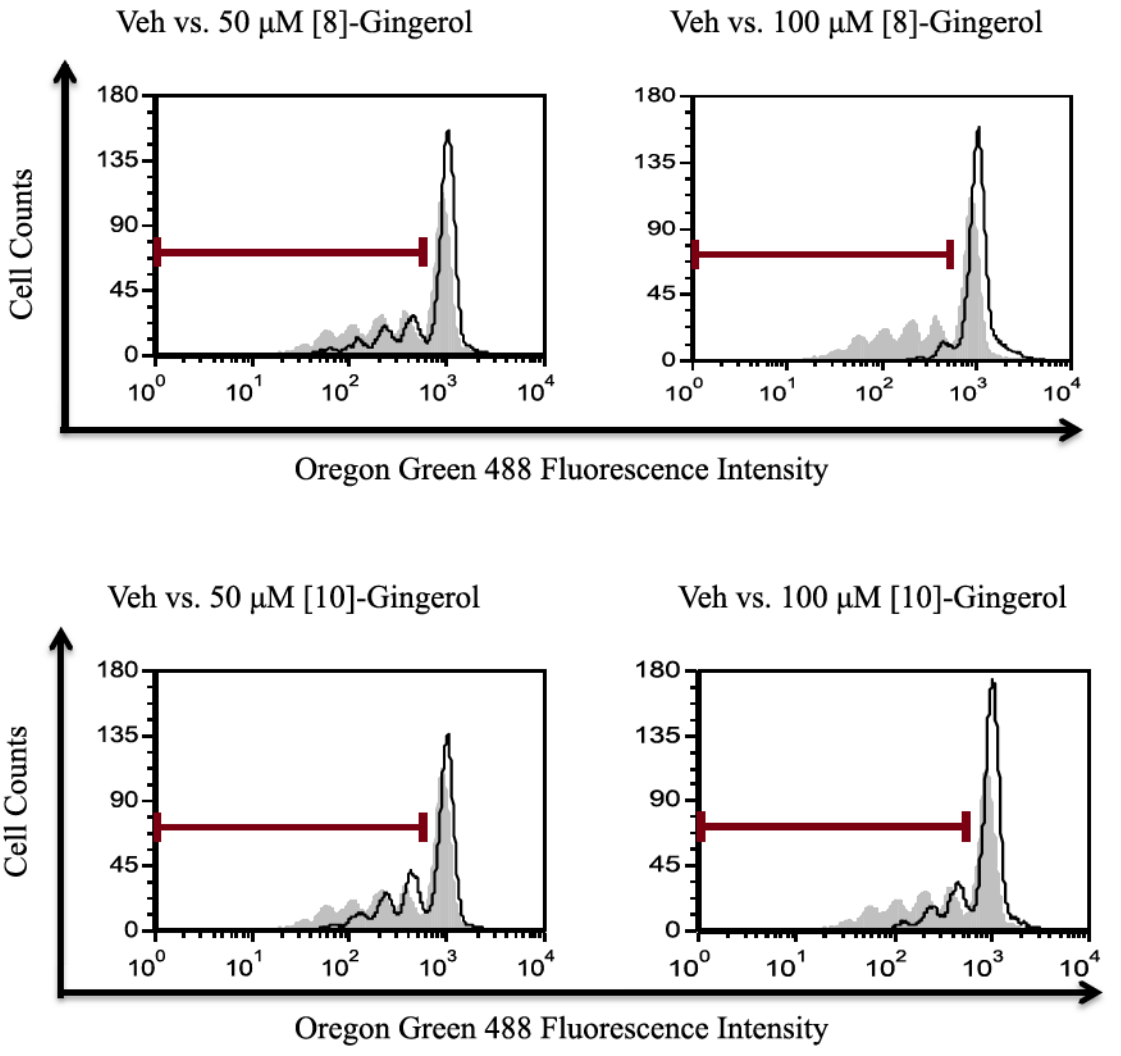

Figure 3.4 (continued)

B.

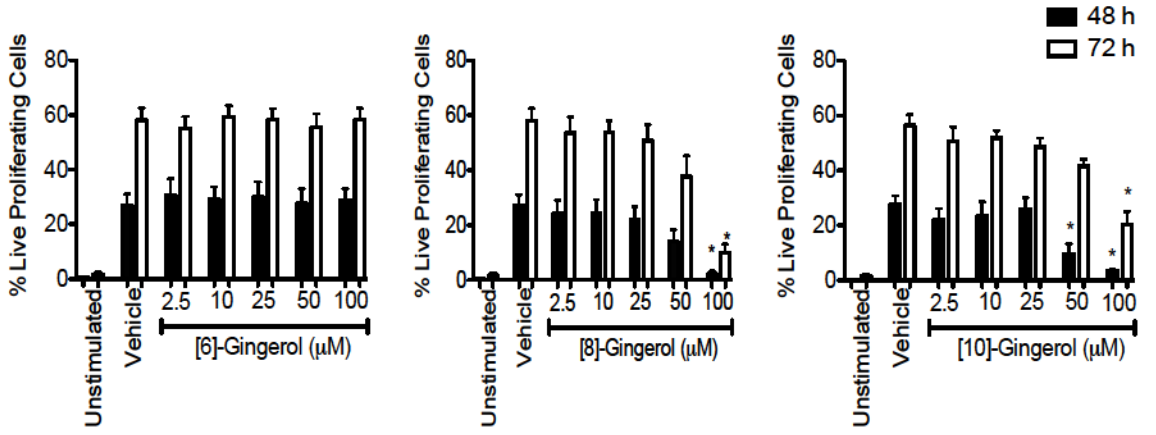

C.

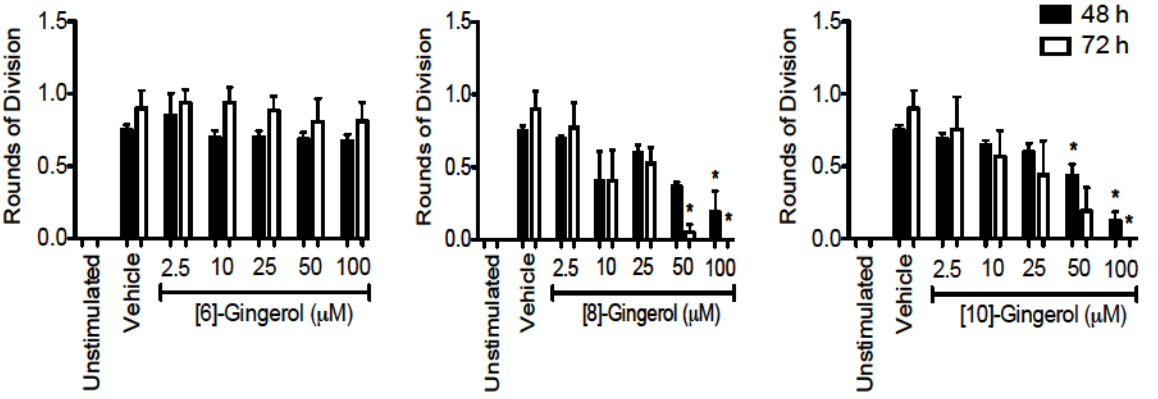

Figure 3.4 (continued)

Figure 3.5. Gingerol Does Not Significantly Decrease Live Cell Counts in Unstimulated Pan T Cell Cultures After 8 or 24 h. Pan T cells were isolated from the spleens of C57BL/6 mice and treated with vehicle or [6]-, [8]-, or [10]-gingerol. After 8 (A) or 24 (B) h, cells were stained with Trypan Blue dye (1:1; v/v) and counted using a hemacytometer. Data shown are the mean percentages of live cell counts of ≥ 3 independent experiments $\pm$ SEM; * $p < 0.05$ when compared to the vehicle at the corresponding time point by one-way ANOVA with a Tukey-Kramer multiple parameters post-test.

A. Unstimulated T Cells, 8 h

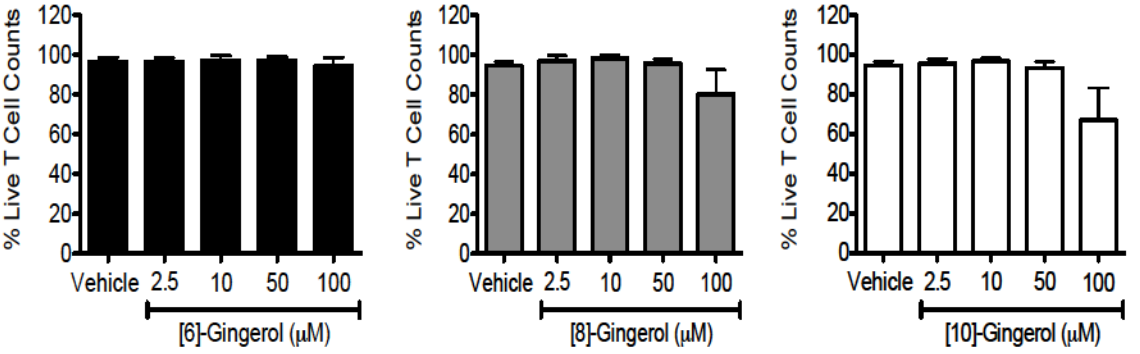

B. Unstimulated T Cells, 24 h

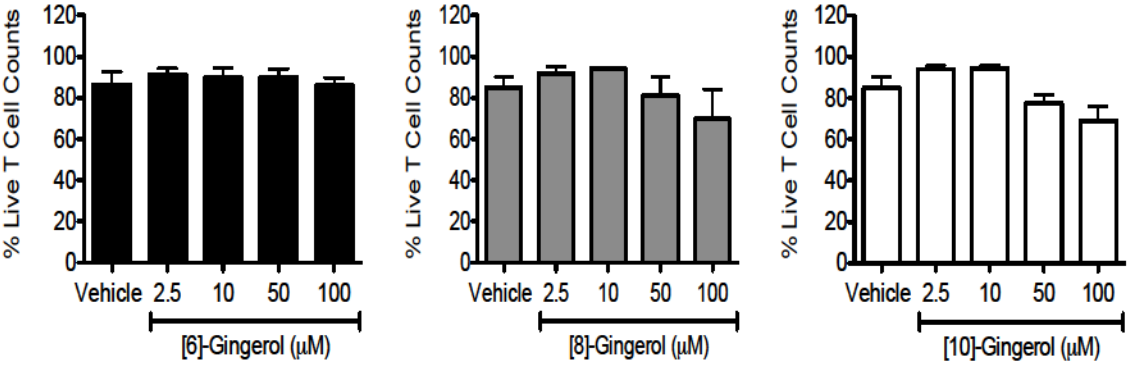

Figure 3.5

Figure 3.6. Low Concentrations of Gingerol Do Not Significantly Decrease Live Cell Counts in Antibody-Coated Bead-Stimulated T Cell Cultures After 24 h. Pan T cells were isolated from the spleens of C57BL/6 mice, treated with vehicle or [6]-, [8]-, or [10]-gingerol, and stimulated with α-CD3 and α-CD28 antibody-coated beads. After 24 h, cells were stained with Trypan Blue dye (1:1; v/v) and counted using a hemacytometer. Data shown are the mean percentages of live cell counts of $\geq$ 3 independent experiments $\pm$ SEM; * $p < 0.05$ when compared to the vehicle at the corresponding time point by one-way ANOVA with a Tukey-Kramer multiple parameters post-test.

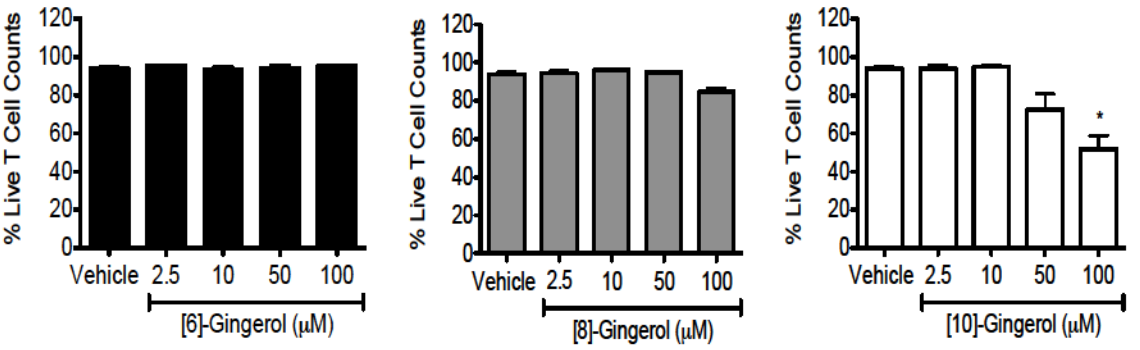
% Live T Cell Counts
120
100
80
60
40
20
0
Vehicle
2.5
10
50
100
[6]-Gingerol (μM)
% Live T Cell Counts
120
100
80
60
40
20
0
Vehicle
2.5
10
50
100
[8]-Gingerol (μM)
% Live T Cell Counts
120
100
80
60
40
20
0
*
Vehicle
2.5
10
50
100
[10]-Gingerol (μM)

Figure 3.6

Figure 3.7. Gingerol Does Not Significantly Decrease Live Cell Counts in Dendritic Cell Cultures. DCs derived from the bone marrow of C57BL/6 mice were treated with vehicle or [6]-, [8]-, or [10]-gingerol and cultured with α-TCR antibody. After 8 (A) or 24 (B) h, cells were stained with Trypan Blue dye (1:1; v/v) and counted using a hemacytometer. Data shown are the mean percentages of live cell counts of $\geq$ 3 independent experiments $\pm$ SEM; * $p < 0.05$ when compared to the vehicle at the corresponding time point by one-way ANOVA with a Tukey-Kramer multiple parameters post-test.

A. Dendritic Cells, 8 h

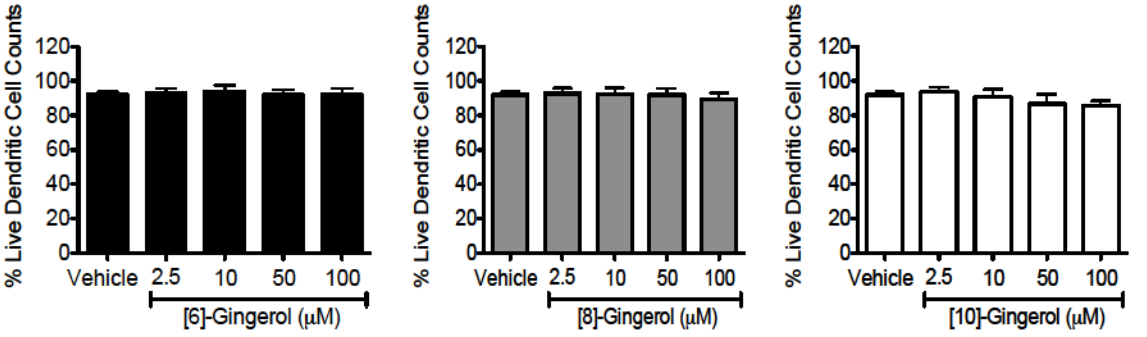

B. Dendritic Cells, 24 h

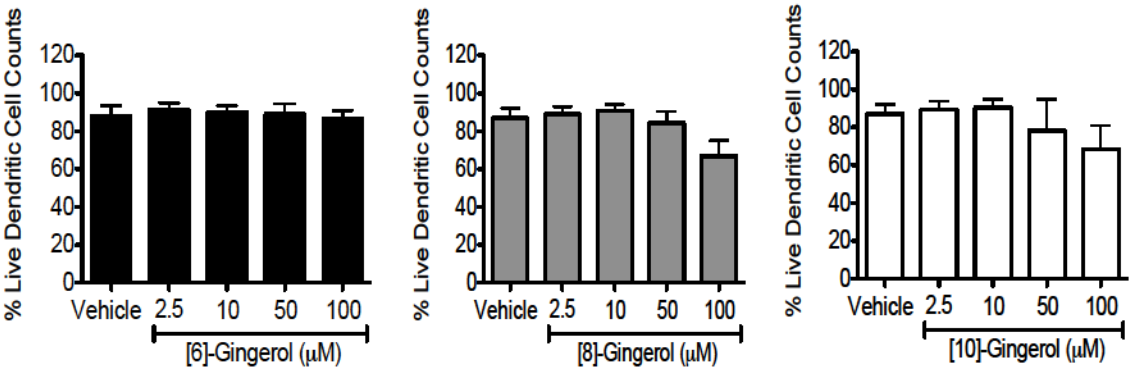

Figure 3.7

3.6 [8]-Gingerol and [10]-Gingerol, But Not [6]-Gingerol, Induce Late Apoptosis/Necrosis in T Cell and Dendritic Cell, But Not CTLL-2 Cell, Cultures

Annexin-V-FLUOS/PI staining was performed to assess apoptosis/necrosis of gingerol-treated pan T cells and DCs. Annexin-V-FLUOS can be used to detect phosphatidylserine membrane translocation and PI can be used to detect a loss in membrane integrity, both which occur upon cell death. No significant change in the percentage of cells undergoing early apoptosis, late apoptosis/necrosis, or the percent of total cell death in unstimulated T cells was seen with gingerol treatment after 8 h (Figure 3.8A). At 100 μM of [8]-gingerol and 50 and 100 μM of [10]-gingerol, an increase in the percentage of cells undergoing late apoptosis/necrosis and the percent of total cell death in unstimulated T cells was observed after 24 h (Figure 3.8B). A high percentage of dead cells was seen in the vehicle control; however, this can be expected as the T cells were not receiving stimulation signals to maintain a proper homeostatic environment. After 24 h, antibody-coated bead-stimulated T cells showed a significant increase in the percentage of cells undergoing late apoptosis/necrosis and the percent of total cell death with 100 μM of [8]-gingerol and [10]-gingerol in comparison to their respective vehicles (Figure 3.9).

Annexin-V-FLUOS and PI staining of DC cultures was performed at 8 and 24 h post-treatment. No cytotoxicity was found in DCs treated with gingerol and cultured with α-TCR antibody after 8 h (Figure 3.10A). Treatment with 100 μM of [8]- and [10]-gingerol were found to significantly increase the percentage of cells undergoing late apoptosis/necrosis in comparison to the respective vehicle controls at 24 h post-treatment

Figure 3.8. Low Concentrations of Gingerol Do Not Increase Cytotoxicity in Unstimulated Pan T Cell Cultures After 8 or 24 h. Pan T cells were isolated from the spleens of C57BL/6 mice and treated with vehicle or [6]-, [8]-, or [10]-gingerol. After 8 (A) or 24 (B) h, cells were stained with Annexin-V-FLUOS and PI and the fluorescence intensity was measured by flow cytometry. Data shown are the mean percentages of cells in early apoptosis, of cells in late apoptosis/necrosis, or of total cell death of ≥ 3 independent experiments $\pm$ SEM; * $p < 0.05$ when compared to the vehicle at the corresponding time point by one-way ANOVA with a Tukey-Kramer multiple parameters post-test.

A. Unstimulated T Cells, 8 h

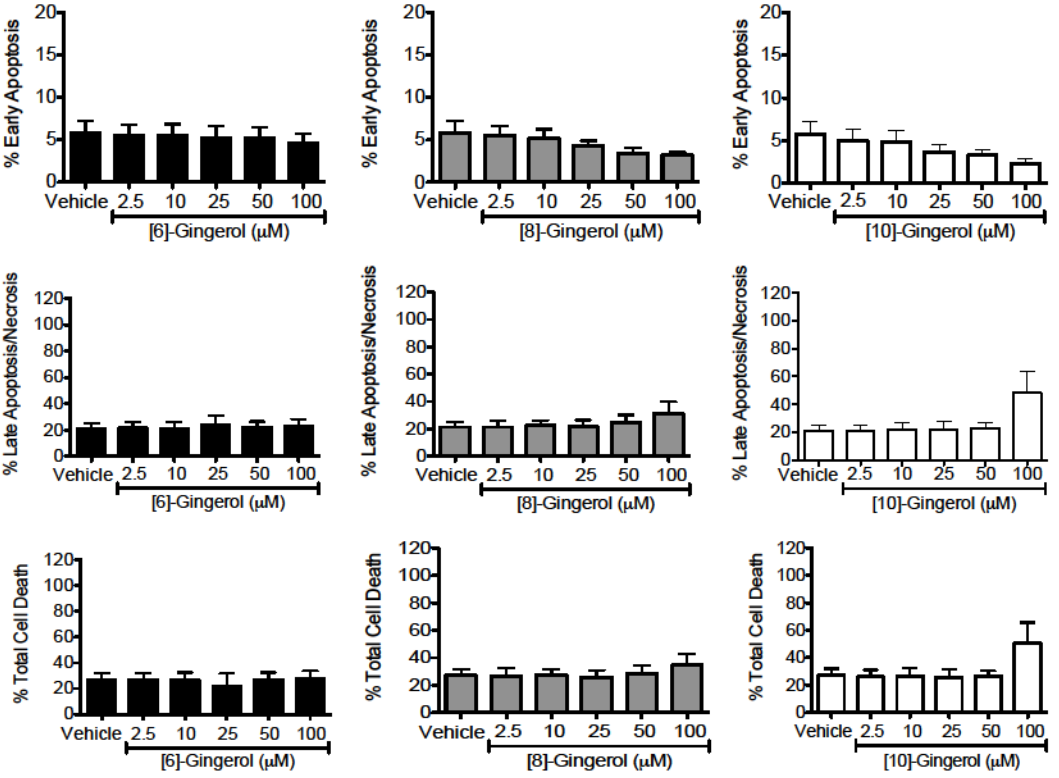

B. Unstimulated T Cells, 24 h

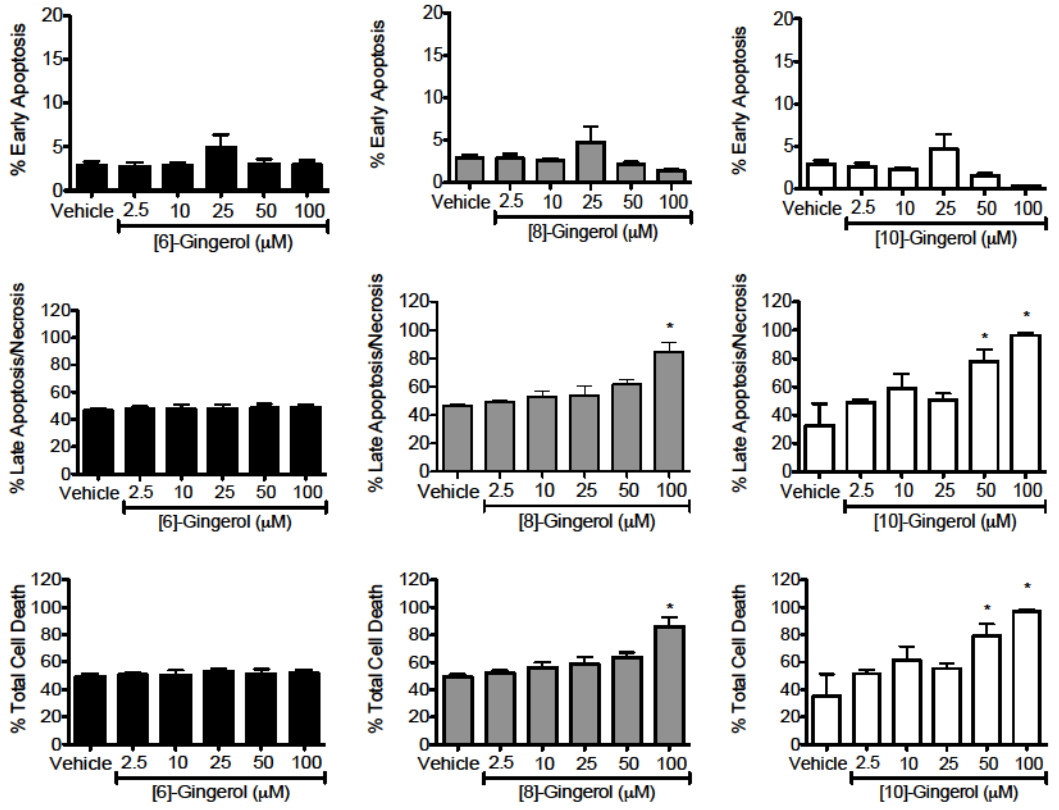

Figure 3.9. Low Concentrations of Gingerol Do Not Significantly Increase Cytotoxicity in Antibody-Coated Bead-Stimulated Pan T Cell Cultures After 24 h. T cells were isolated from the spleens of C57BL/6 mice, treated with vehicle or [6]-, [8]-, or [10]-gingerol, and stimulated with α-CD3 and α-CD28 antibody-coated beads. After 24 h, cells were stained with Annexin-V-FLUOS and PI and the fluorescence was measured by flow cytometry. Data shown are the mean percentages of cells in early apoptosis, of cells in late apoptosis/necrosis, or of total cell death of $\geq$ 3 independent experiments $\pm$ SEM; * $p < 0.05$ when compared to the vehicle at the corresponding time point by one-way ANOVA with a Tukey-Kramer multiple parameters post-test.

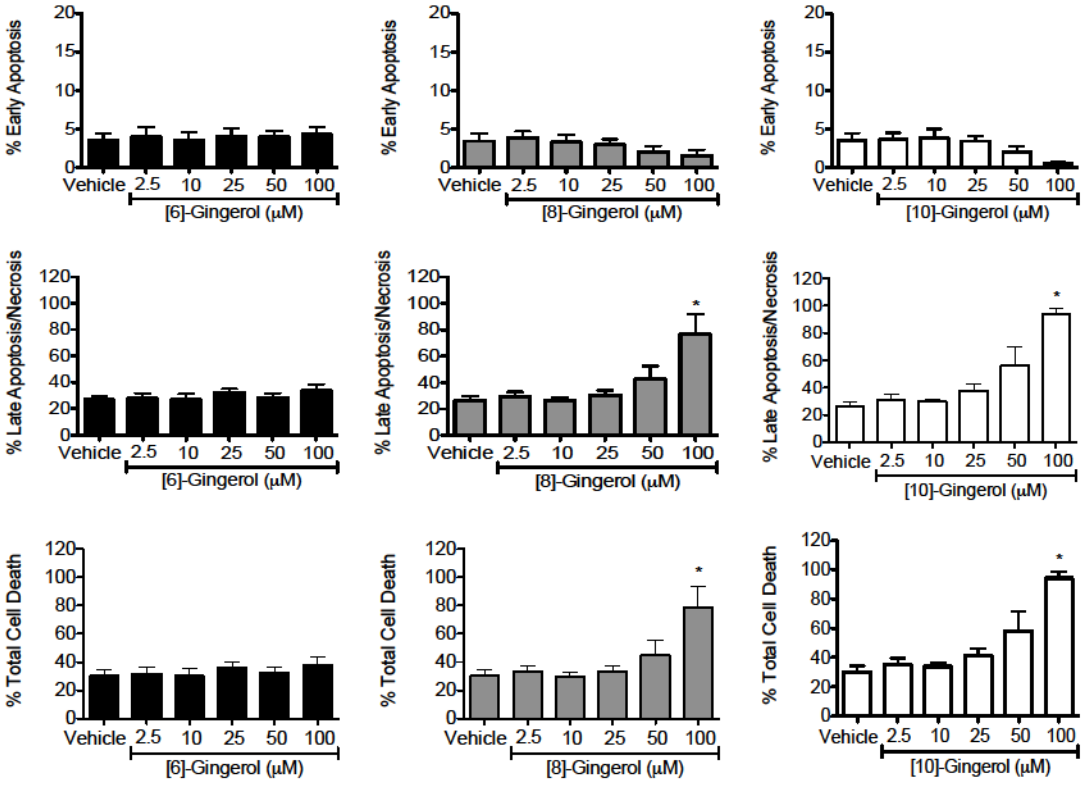
% Early Apoptosis
% Late Apoptosis/Necrosis
% Total Cell Death
Vehicle 2.5 10 25 50 100
[6]-Gingerol (μM)
[8]-Gingerol (μM)
[10]-Gingerol (μM)
*

Figure 3.9

Figure 3.10. [8]- And [10]-Gingerol, But Not [6]-Gingerol, Induce Late Apoptosis/ Necrosis in Dendritic Cell Cultures After 24 h. DCs were derived from the bone marrow of C57BL/6 mice, treated with vehicle or [6]-, [8]-, or [10]-gingerol, and stimulated with α-TCR antibody. After 8 (A) or 24 (B) h, cells were stained with Annexin-V-FLUOS and PI and the fluorescence was measured by flow cytometry. Data shown are the mean percentages of cells in early apoptosis, of cells in late apoptosis/ necrosis, or of total cell death of $\geq$ 3 independent experiments $\pm$ SEM; * $p < 0.05$ when compared to the vehicle at the corresponding time point by one-way ANOVA with a Tukey-Kramer multiple parameters post-test.

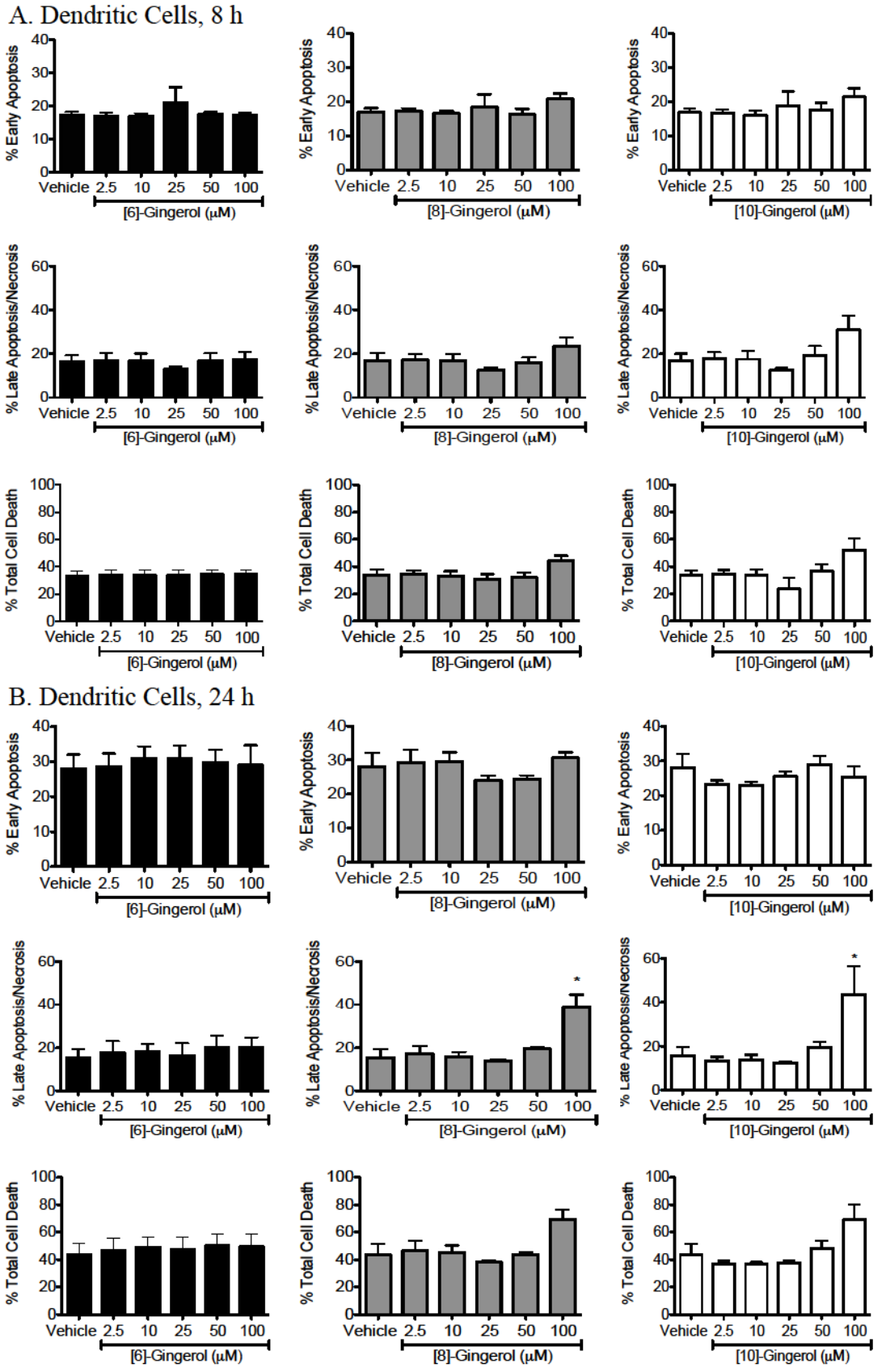
A. Dendritic Cells, 8 h
% Early Apoptosis
% Late Apoptosis/Necrosis
% Total Cell Death
Vehicle 2.5 10 25 50 100
[6]-Gingerol (μM)
[8]-Gingerol (μM)
[10]-Gingerol (μM)
B. Dendritic Cells, 24 h
*

(Figure 3.10B), although no significant change in the percent of total cell death was observed.

CTLL-2 cell cultures were IL-2 starved for 3 h before being treated with gingerol or a vehicle control, stimulated with 50 U/mL of IL-2, and stained with Annexin-V-FLUOS/PI. There was no indication of any significant increase in cytotoxicity with 10, 25, or 50 μM concentrations after 24 h (Figure 3.11). Consistent with the previous findings, these data indicate that [8]- and [10]-gingerol are more potent than [6]-gingerol, exhibiting not only the greatest anti-proliferative effects on T cell, DC, and CTLL-2 cell cultures, but also being the most cytotoxic, particularly at 100 μM concentrations.

Early activation markers CD25 and CD69 are expressed on the surface of T cells upon activation[140]. CD25 is the α-chain of the IL-2 receptor and CTLL-2 cells constitutively express the IL-2 receptor. Consequently, inhibition of the expression of these cell surface markers would indicate a suppression of T cell activation, leading to a decrease in proliferation. The effects of gingerol on receptor expression of T cells stimulated with α-CD3 and α-CD28 antibody-coated beads and of IL-2-stimulated CTLL-2 cells were investigated by staining for CD69 (T cells) and CD25 (T cells and CTLL-2 cells).

Compared to the vehicle control, treatment with 50 μM (a non-cytotoxic concentration) of both [8]- and [10]-gingerol significantly decreased the expression of CD25 on T cells (i), but not the percentage of T cells expressing CD25 (ii) at 24 h post-stimulation (Figure 3.12A). Compared to the vehicle control, 50 μM of [8]- and [10]-gingerol also decreased the expression of CD69 (i), but not the percentage of T cells expressing CD69 (ii) at 24 h post-stimulation (Figure 3.12B). [6]-Gingerol did not affect

Figure 3.11. Gingerol Does Not Induce Cytotoxicity After 24 h in CTLL-2 Cell Cultures at Concentrations Up To 50 µM. CTLL-2 cells were treated with vehicle or [6]-, [8]-, or [10]-gingerol, and stimulated with IL-2 (50 U/mL). After 24 h, cells were stained with Annexin-V-FLUOS and PI and the fluorescence was measured by flow cytometry. Data shown are the mean percentages of cells in early apoptosis, of cells in late apoptosis/necrosis, or of total cell death of $\geq$ 3 independent experiments $\pm$ SEM; * $p < 0.05$ compared to the vehicle at the corresponding time point by one-way ANOVA with a Tukey-Kramer multiple parameters post-test.

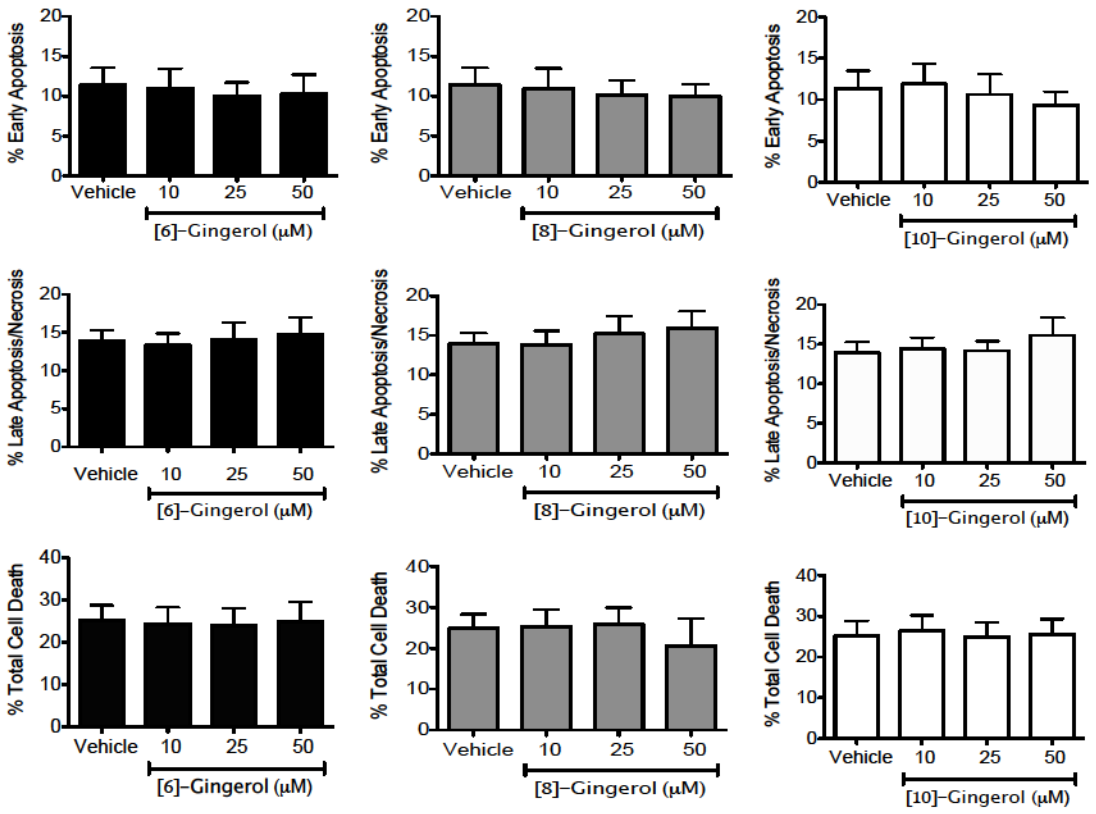
% Early Apoptosis
% Late Apoptosis/Necrosis
% Total Cell Death
Vehicle
10
25
50
[6]-Gingerol (μM)
[8]-Gingerol (μM)
[10]-Gingerol (μM)

Figure 3.11

Figure 3.12. [8]-Gingerol and [10]-Gingerol, But Not [6]-Gingerol, Inhibit the Expression of CD25 and CD69 on T Cells. T cells were isolated from the spleens of C57BL/6 mice and treated with vehicle or [6]-, [8]-, or [10]-gingerol. After 30 min, samples were either stimulated with α-CD3 and α-CD28 antibody-coated beads or left unstimulated as a control. At 24 h post-stimulation, samples were stained with anti-CD25-PE (A), anti-CD69-FITC (B), or the respective isotype antibody controls, fixed in PFA, and the fluorescence was measured by flow cytometry. Data shown are the median fluorescence intensities (MFI; i) or the % of T cell expression (ii) of $\geq$ 3 independent experiments $\pm$ SEM; * $p < 0.05$ when compared to the vehicle at the corresponding time point by one-way ANOVA with a Tukey-Kramer multiple parameters post-test. Histograms depict corresponding representative experiments (iii).

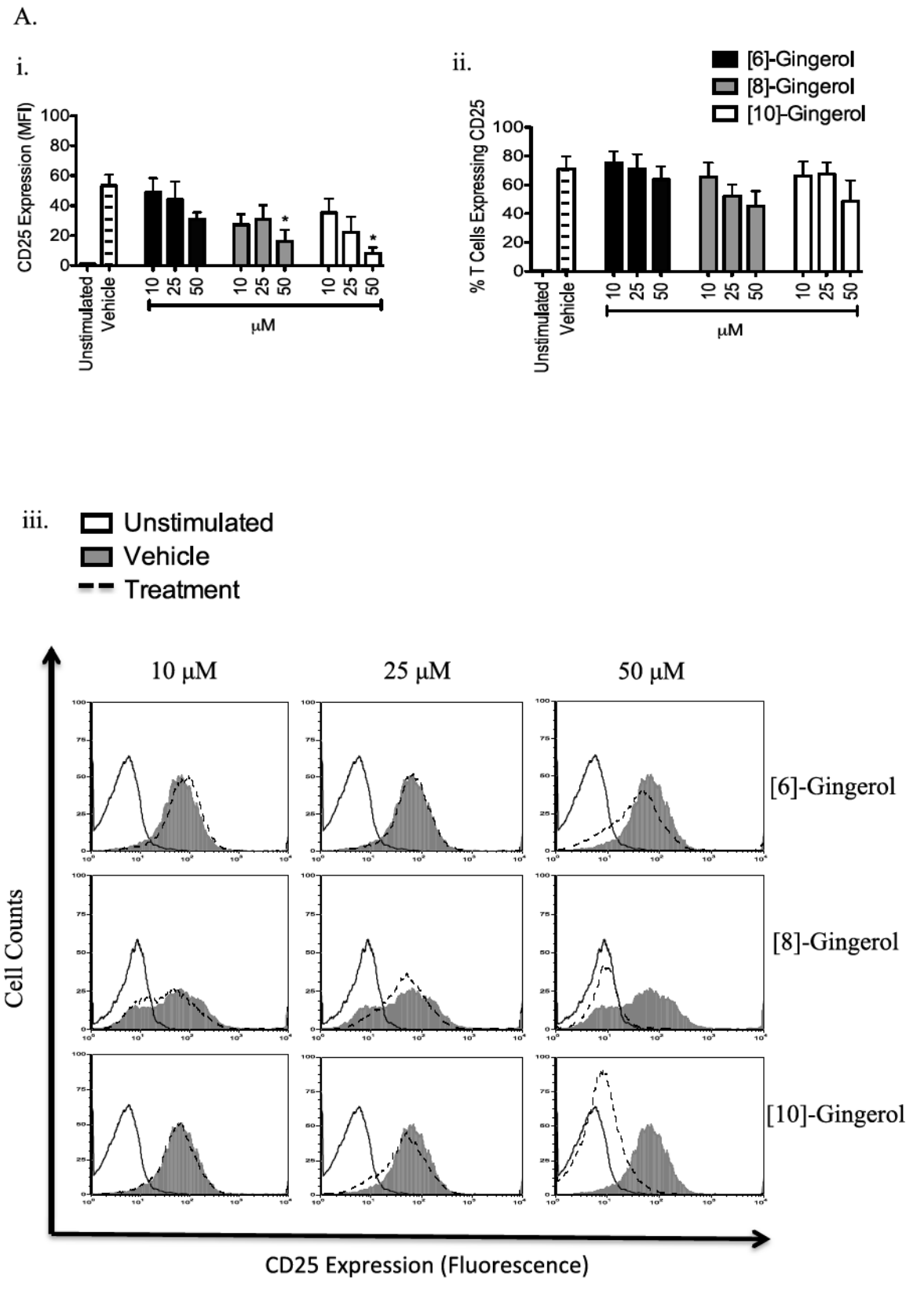
A.
i.
CD25 Expression (MFI)
100
80
60
40
20
0
Unstimulated
Vehicle
10
25
50
10
25
50
10
25
50
μM
*
*
ii.
[6]-Gingerol
[8]-Gingerol
[10]-Gingerol
% T Cells Expressing CD25
100
80
60
40
20
0
Unstimulated
Vehicle
10
25
50
10
25
50
10
25
50
μM
iii.
Unstimulated
Vehicle
Treatment
10 μM
25 μM
50 μM
[6]-Gingerol
[8]-Gingerol
[10]-Gingerol
Cell Counts
CD25 Expression (Fluorescence)

Figure 3.12

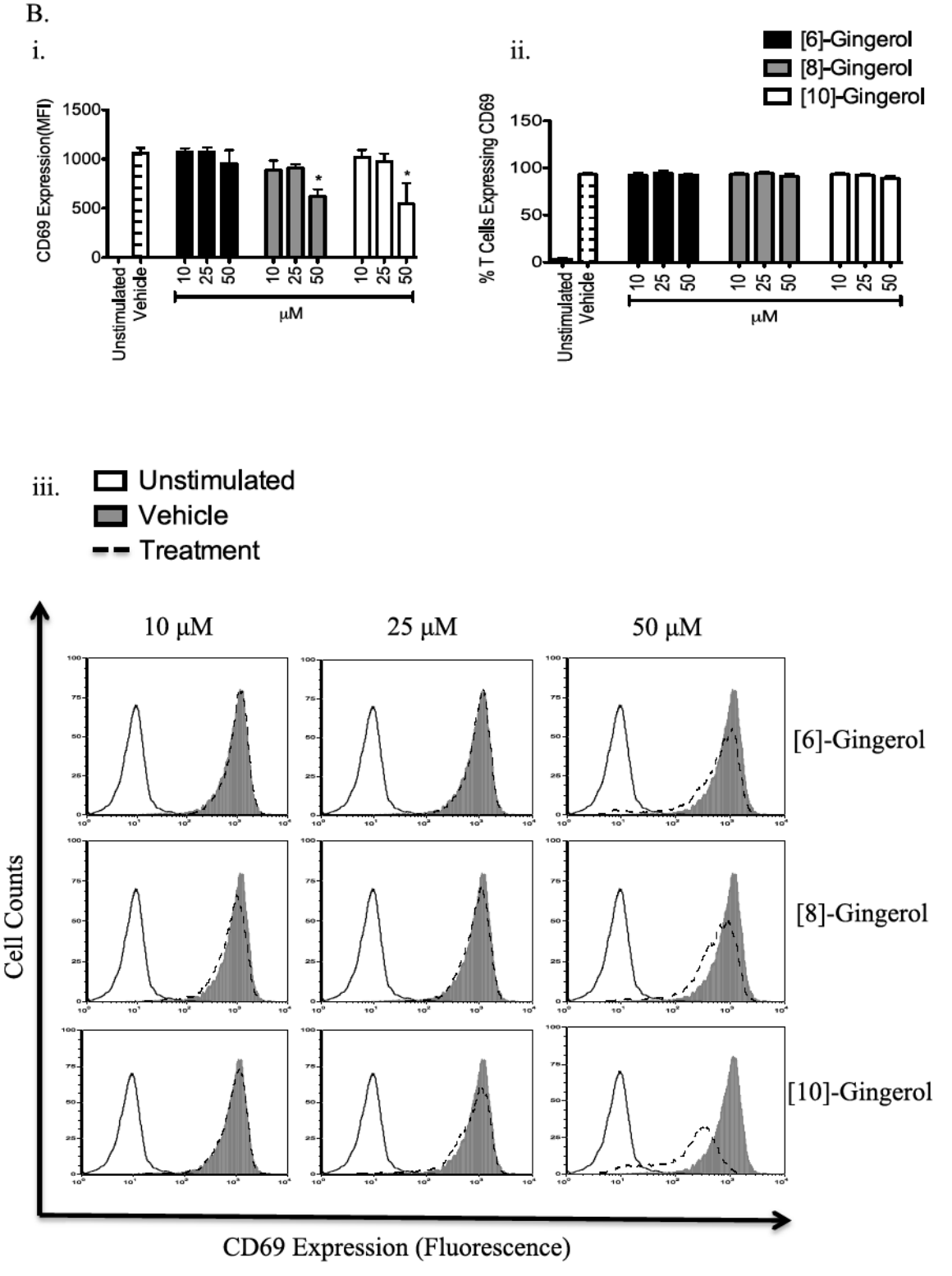

Figure 3.12 (continued)

the expression of CD25 or CD69 on pan T cells or the percentage of T cells expressing CD25 or CD69 (Figure 3.12A and B). Gingerol did not affect the expression of CD25 on CTLL-2 cells (Figure 3.13). This data suggests that [8]- and [10]-gingerol inhibit the signals that induce CD25 and CD69 surface expression in pan T cells, but act through another pathway in CTLL-2 cells that does not affect the CD25 early activation marker, or, does not induce any effect on CTLL-2 cell cultures. Histograms depict a representative experiment (iii).

A decrease in the expression of CD119 (IFN-γ R1) could result in a diminished ability to react to IFN-γ and a possible decrease in an inflammatory response. No decrease in CD119 on pan T cells stimulated with α-CD3 and α-CD28 antibody-coated beads was discovered upon investigation by flow cytometry (Figure 3.14), indicating that gingerol does not effect the expression IFN-γ R1.

3.7 [6]-Gingerol, [8]-Gingerol, and [10]-Gingerol Inhibit IFN-γ Synthesis, While [8]- and [10]-Gingerol, But Not [6]-Gingerol, Inhibit IL-2 Synthesis

The cytokines IFN-γ and IL-4 are important for the differentiation of T helper cells into Th1 and Th2 cells, respectively[141]. Therefore, the influence of gingerol on the differentiation of T cells into either Th1 or Th2 T helper cell subsets was investigated by using sandwich-ELISA to measure cytokines produced by T cells. At 25 and 50 μM, all three gingerols demonstrated significant decreases in IFN-γ levels at 24 h post-stimulation (Figure 3.15A). No significant change in IL-4 production was observed after 24 h from gingerol-treated T cells (Figure 3.15B).

Figure 3.13. Gingerol Does Not Inhibit the Expression of CD25 on IL-2-Dependent CTLL-2 Cells. CTLL-2 cell cultures were IL-2-starved for 3 h and then treated with vehicle or [6]-, [8]-, or [10]-gingerol. After 30 min, samples were stimulated with IL-2 (50 U/mL) or left unstimulated as a control. 24 h post-stimulation, CTLL-2 cell cultures were stained with α-CD25-PE or the respective isotype antibody control. Data shown are the median fluorescence intensities (MFI; i) and the % of CTLL-2 cells expressing CD25 (ii) of $\geq$ 3 independent experiments $\pm$ SEM; * $p < 0.05$ when compared to the vehicle at the corresponding time point by one-way ANOVA with a Tukey-Kramer multiple parameters post-test. Histograms depict a corresponding representative experiment (iii).

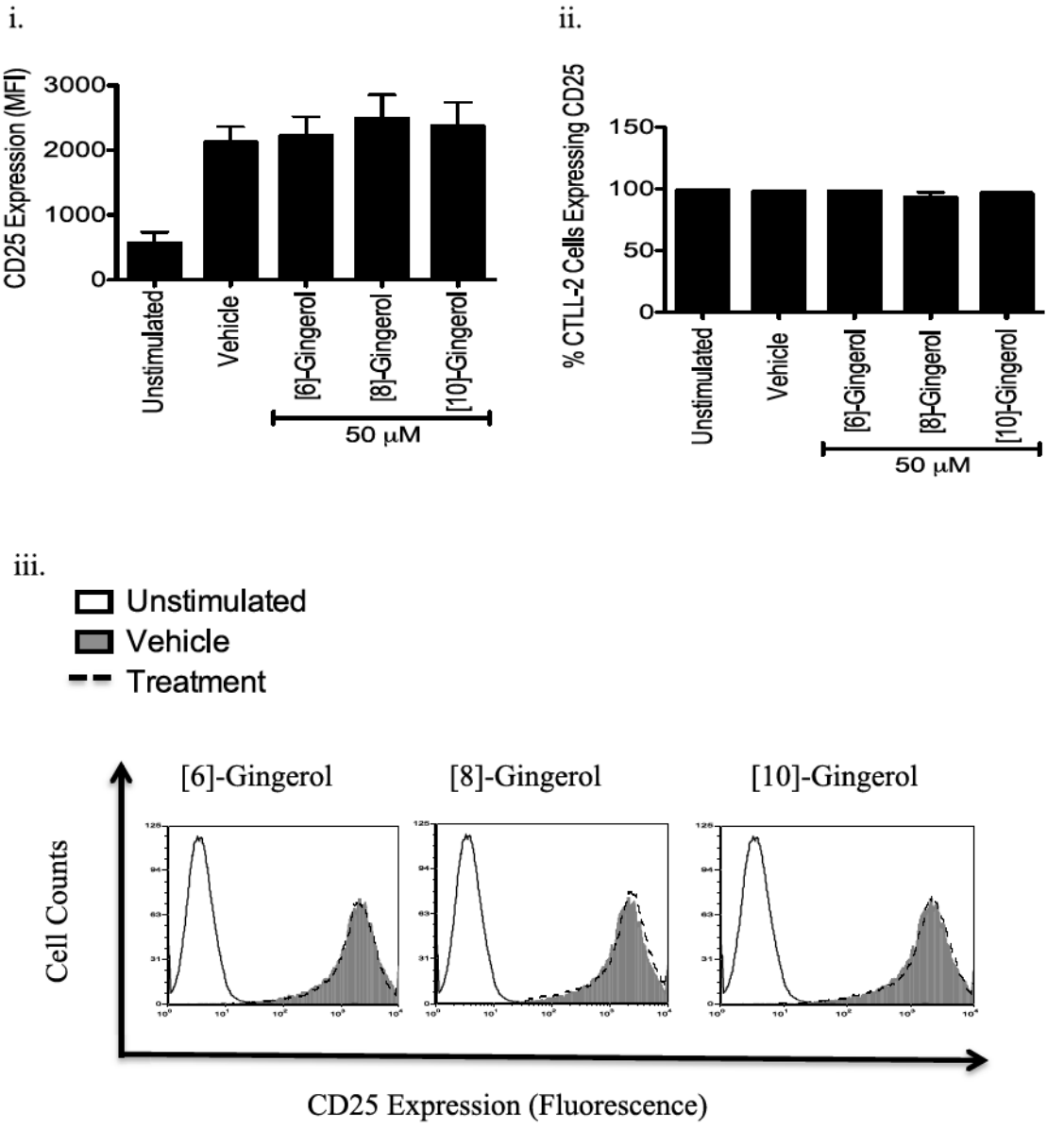
i.
CD25 Expression (MFI)
3000
2000
1000
0
Unstimulated
Vehicle
[6]-Gingerol
[8]-Gingerol
[10]-Gingerol
50 μM
ii.
% CTLL-2 Cells Expressing CD25
150
100
50
0
Unstimulated
Vehicle
[6]-Gingerol
[8]-Gingerol
[10]-Gingerol
50 μM
iii.
Unstimulated
Vehicle
Treatment
[6]-Gingerol
[8]-Gingerol
[10]-Gingerol
Cell Counts
CD25 Expression (Fluorescence)

Figure 3.13

Figure 3.14. Gingerol Does Not Affect CD119 Expression on Pan T Cells. Pan T cells were isolated from the spleens of C57BL/6 mice and treated with vehicle or [6]-, [8]-, or [10]-gingerol. After 30 min, samples were either stimulated with α-CD3 and α-CD28 antibody-coated beads or left unstimulated as a control. 24 h post-stimulation, samples were stained with anti-CD119-FITC or the respective isotype antibody control, fixed in PFA, and the fluorescence was measured by flow cytometry. Data shown are the median fluorescent intensities (MFI; i) or the % of T cells expressing CD119 (ii) of $\geq$ 3 independent experiments $\pm$ SEM; * $p < 0.05$ independent experiments when compared to the vehicle at the corresponding time point by one-way ANOVA with a Tukey-Kramer multiple parameters post-test. Histograms depict corresponding representative experiments (iii).

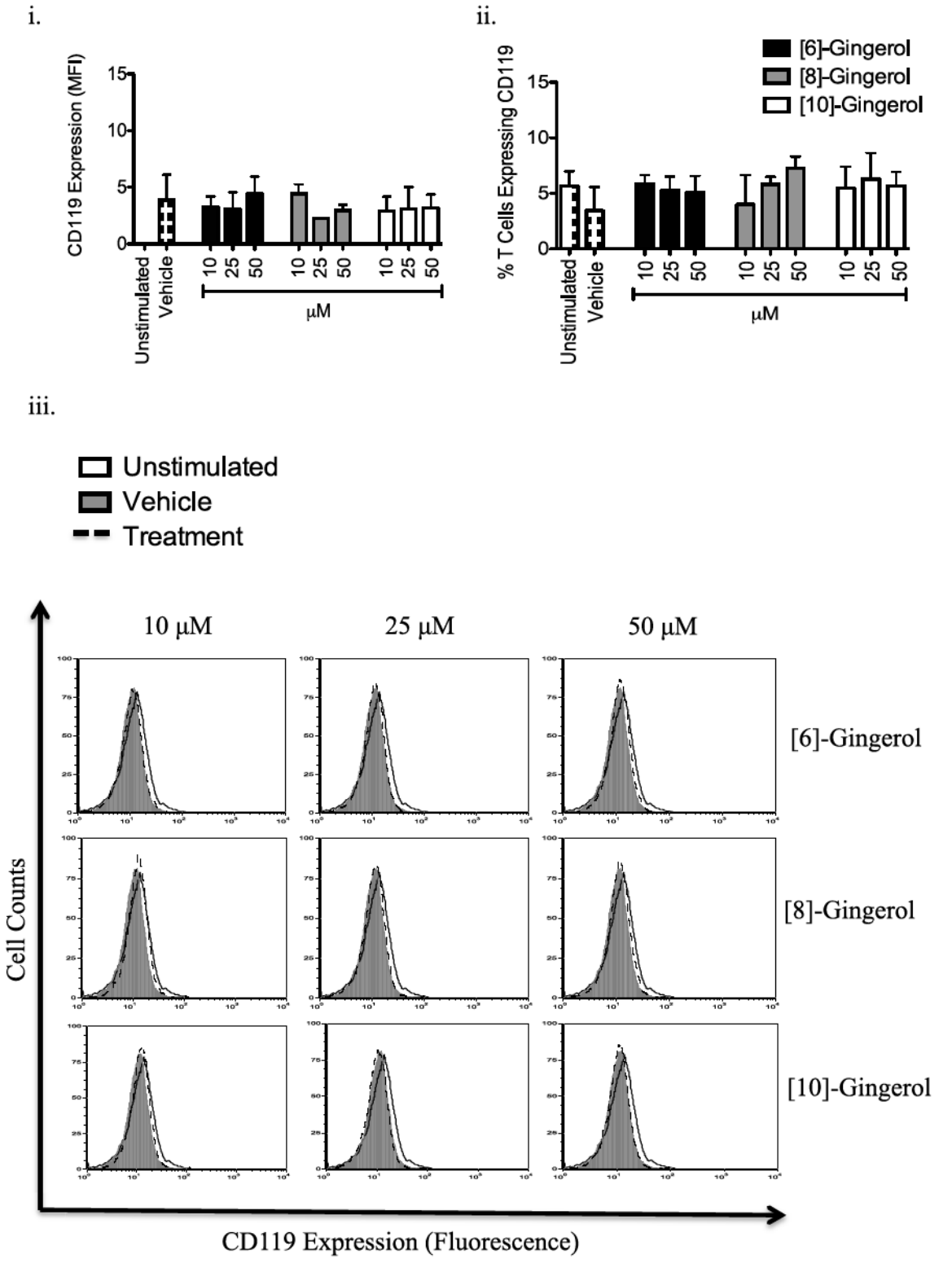
i.
CD119 Expression (MFI)
15
10
5
0
Unstimulated
Vehicle
10
25
50
10
25
50
10
25
50
μM
ii.
% T Cells Expressing CD119
[6]-Gingerol
[8]-Gingerol
[10]-Gingerol
iii.
Unstimulated
Vehicle
Treatment
10 μM
25 μM
50 μM
[6]-Gingerol
[8]-Gingerol
[10]-Gingerol
Cell Counts
CD119 Expression (Fluorescence)

Figure 3.14

Figure 3.15. Gingerol Has Differential Effects on Cytokine Production. T cells were isolated from the spleens of C57BL/6 mice, treated with vehicle or [6]-, [8]-, or [10]-gingerol, and stimulated with α-CD3 and α-CD28 antibody-coated beads. 24 h post-stimulation, supernatants were collected for analysis by sandwich-ELISA. Data shown are the mean cytokine production of (A) IFN-γ, (B) IL-4, and (C) IL-2 normalized to the media of $\geq$ 3 independent experiments $\pm$ SEM; * $p < 0.05$ when compared to the vehicle at the corresponding time point by one-way ANOVA with a Tukey-Kramer multiple parameters post-test.

A.

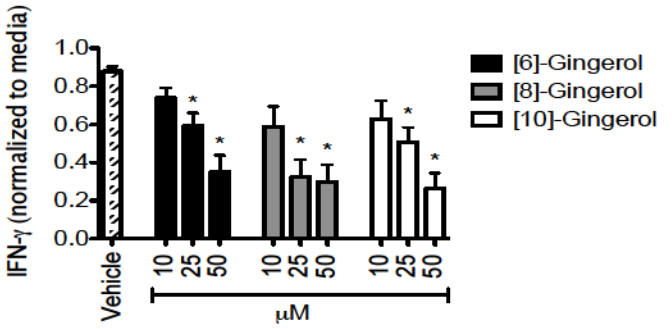

B.

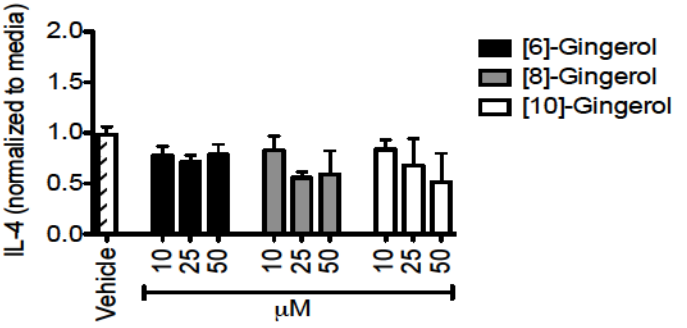

C.

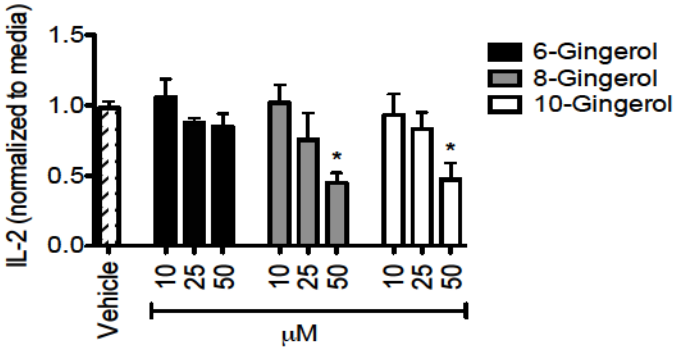

Figure 3.15

In addition, the cytokine IL-2 is important for driving the proliferation of T cells *in vitro*[31]. Therefore, as gingerol was seen to diminish T cell proliferation and the expression of CD25 and CD69, it was suspected that the levels of IL-2 might also decrease with gingerol treatment. Levels of IL-2 in the supernatants of gingerol-treated T cells were measured by sandwich-ELISA. With 50 μM, both [8]- and [10]-gingerol were found to significantly decrease the production of IL-2 at 24 h post-stimulation (Figure 3.15C). [6]-Gingerol did not have an effect on IL-2 cytokine levels.

CHAPTER 4

THE CYTOSTATIC AND CYTOTOXIC EFFECTS OF [6]-, [8]-, AND [10]-GINGEROL ON MOUSE AND HUMAN MAMMARY CARCINOMA CELLS

4.1 [6]-, [8]-, and [10]-Gingerol Decrease the Mitochondrial Succinate Dehydrogenase Activity in Human Mammary Carcinoma Cell Cultures

[6]-Gingerol from ginger has previously been shown to inhibit the proliferation and invasion of numerous cancer cell types[142–144]. [8]-Gingerol and [10]-gingerol are also derived from ginger and differ only slightly in chemical structure to [6]-gingerol, but their effects on breast cancer have not been investigated extensively. Therefore, the effects of [6]-, [8]-, and [10]-gingerol on several human and mouse mammary carcinoma and non-cancerous cell cultures were investigated and compared using the MTT assay, which indicates the cell number relative to the mitochondrial activity of the cell cultures.

The inhibitory effects of gingerol on the metabolic activities of human mammary carcinoma cell cultures are seen in Figure 4.1A and B. As seen in Figure 4.1A, [6]-gingerol significantly decreased the relative metabolic activity of MDA-MB-231 cells with 100 and 200 μM concentrations (72 h). Interestingly, MDA-MB-231 cells were the most sensitive to [8]-gingerol (compared to the other gingerols), as seen by the significant reduction in the metabolic activity with 100 and 200 μM after 24, 48, and 72 h. [10]-Gingerol showed a significant decrease in the metabolic activity of MDA-MB-231 cells with 200 μM (48 and 72 h). In MDA-MB-468 cell cultures, [6]-gingerol significantly decreased the relative metabolic activity with 50 and 100 μM (48 and 72 h), and at all time points with 200 μM (Figure 4.1B). [8]-Gingerol significantly decreased the relative metabolic activity with 50 μM (72 h), 100 μM (48 and 72 h), and at all time points with

Figure 4.1. Gingerol Decreases the Mitochondrial Succinate Dehydrogenase Activities of Human and Mouse Mammary Carcinoma Cell Cultures. MDA-MB-231 (A), MDA-MB-468 (B), 4T1 (C), and E0771 (D) cells were seeded, allowed to adhere overnight, then treated with medium, vehicle, or the indicated concentrations of [6]-, [8]-, or [10]-gingerol. MTT assays were performed 24, 48, and 72 h post-treatment. Data shown are the average percent metabolic activities relative to the medium control of $\geq$ 3 independent experiments $\pm$ SEM; * $p < 0.05$ compared to the vehicle at the corresponding time point by a one-way ANOVA with a Tukey-Kramer multiple parameters post-test.

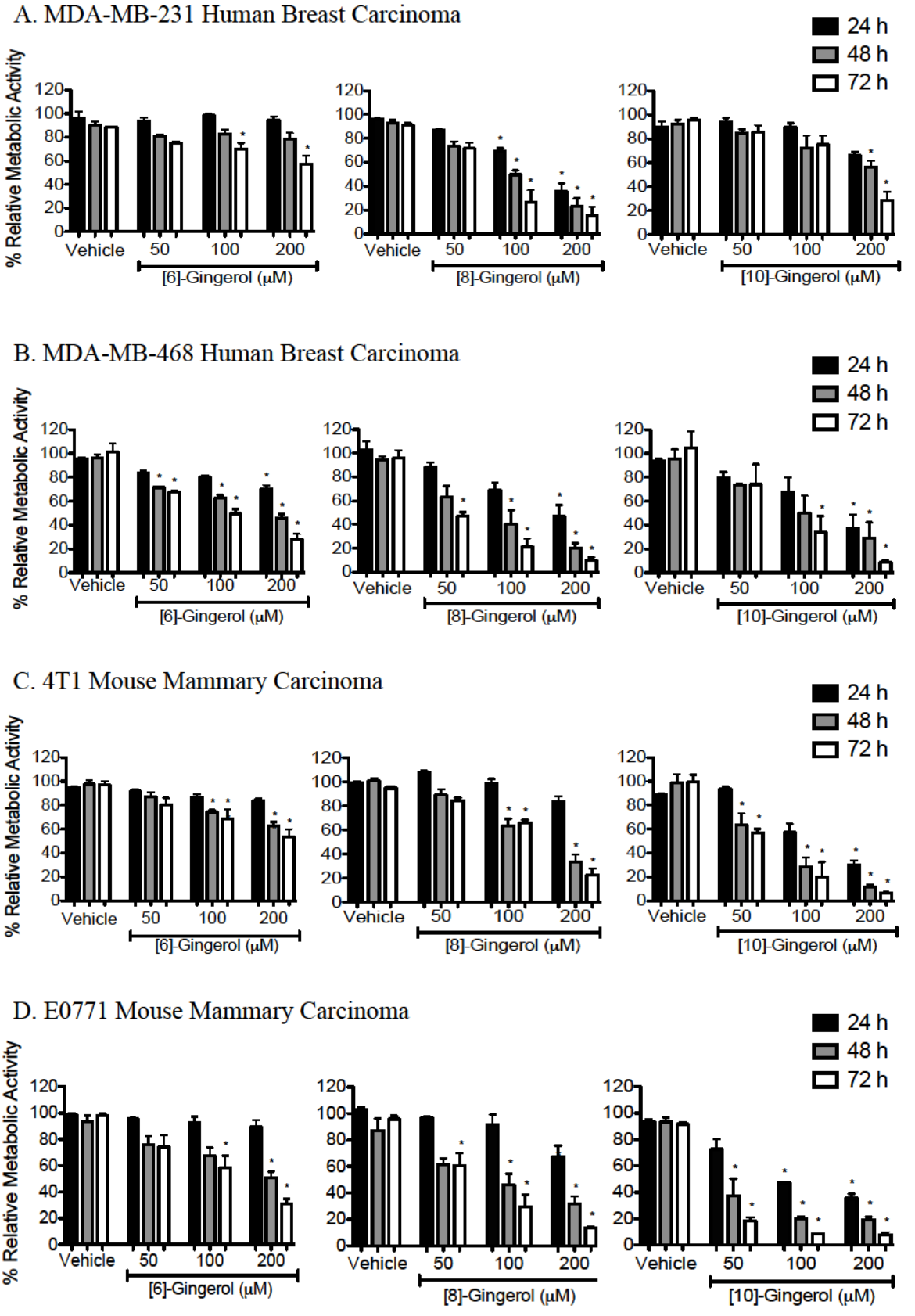
A. MDA-MB-231 Human Breast Carcinoma
B. MDA-MB-468 Human Breast Carcinoma
C. 4T1 Mouse Mammary Carcinoma
D. E0771 Mouse Mammary Carcinoma
24 h
48 h
72 h
% Relative Metabolic Activity
0
20
40
60
80
100
120
Vehicle
50
100
200
[6]-Gingerol (μM)
[8]-Gingerol (μM)
[10]-Gingerol (μM)

200 μM. [10]-Gingerol significantly decreased the relative metabolic activity with 100 μM (72 h) and all time points with 200 μM. Overall, these data reveal that [8]- and [10]-gingerol demonstrated similar effects on the relative metabolic activities of human breast carcinoma cells and that MDA-MB-468 cells are more sensitive to gingerol than are MDA-MB-231 cell cultures. Interestingly, [6]-gingerol showed the most significant decrease at the lowest concentration (50 μM) and earliest time point (48 h) in MDA-MB-468 cell cultures.

4.2 [6]-, [8]-, and [10]-Gingerol Decrease the Mitochondrial Succinate Dehydrogenase Activity in Mouse Mammary Carcinoma Cell Cultures

The inhibitory effects of gingerol on the relative metabolic activities of mouse mammary carcinoma cells, as examined by the MTT assay are shown in Figure 4.1C and D. [6]-Gingerol and [8]-gingerol treatments significantly decreased the metabolic activities of 4T1 cells with 100 and 200 μM (48 and 72h; Figure 4.1C). [10]-Gingerol significantly decreased the relative metabolic activity at 50 (48 and 72 h), 100 (48 and 72 h), and 200 μM (all time points). In E0771 cell cultures, [6]-gingerol significantly decreased the relative metabolic activity with 100 (72 h) and 200 μM (48 and 72 h; Figure 4.1D). [8]-Gingerol showed a significant decrease with 50 (72 h), 100 (48 and 72 h) and 200 μM (48 and 72 h). [10]-Gingerol had the greatest effect, with a significant decrease at 50 (48 and 72 h), 100 (all time points), and 200 μM (all time points). E0771 cell cultures were slightly more sensitive to gingerol than were 4T1 cell cultures.

Overall, analysis of the MTT data indicated that [8]- and [10]-gingerol caused similar decreases in the metabolic activities of human and mouse mammary carcinoma

cultures. Generally, this effect was much greater than that seen following treatment with [6]-gingerol.

4.3 [8]- Gingerol and [10]-Gingerol, But Not [6]-Gingerol, Decrease the Mitochondrial Succinate Dehydrogenase Activity in Non-Cancerous Human and Mouse Cell Cultures

The results of the MTT assays showed no significant change in the relative metabolic activities of human dermal fibroblasts, HMECs, or HC11 cells upon treatment with [6]-gingerol (Figure 4.2). [8]-Gingerol induced a significant decrease in the relative metabolic activity of HMEC cultures with 100 and 200 µM (48 and 72 h; Figure 4.2A). [10]-Gingerol at 100 µM (48 and 72 h) and 200 µM (all time points) significantly reduced the metabolic activity of HMECs. In human dermal fibroblast cultures, 200 µM of [8]-gingerol and 100 and 200 µM of [10]-gingerol caused a significant decrease in the relative metabolic activity at all time points (Figure 4.2B). [8]-Gingerol significantly reduced the relative metabolic activity of HC11 cells with 200 µM at all time points, while [10]-gingerol caused a significant decrease with 100 µM after 48 h and with 200 µM after 48 and 72 h (Figure 4.2C).

4.4 [6]-, [8]-, and [10]-Gingerol Do Not Reduce MTT in the Absence of Cells

As some phytochemicals have been shown to reduce MTT in the absence of cells[145], medium, vehicle, and [6]-, [8]-, and [10]-gingerol were incubated in the presence of MTT solution for 2 h without cells. No apparent change in optical density readings compared to the medium or vehicle was found, indicating that MTT was not converted to formazan by gingerol in the absence of cells (Table 4.1).

Figure 4.2. Gingerol Decreases the Mitochondrial Succinate Dehydrogenase Activities of Non-Cancerous Human and Mouse Cell Cultures. HMEC (A), human dermal fibroblasts (B), and HC11 mouse epithelial cells (C) were seeded, allowed to adhere overnight, then treated with medium, vehicle, or the indicated concentrations of [6]-, [8]- or [10]-gingerol. MTT assays were performed 24, 48, and 72 h post-treatment. Data shown are the average percent metabolic activities relative to the medium control of $\geq$ 3 independent experiments $\pm$ SEM; * $p < 0.05$ compared to the vehicle at the corresponding time point by a one-way ANOVA with a Tukey-Kramer multiple parameters post-test.

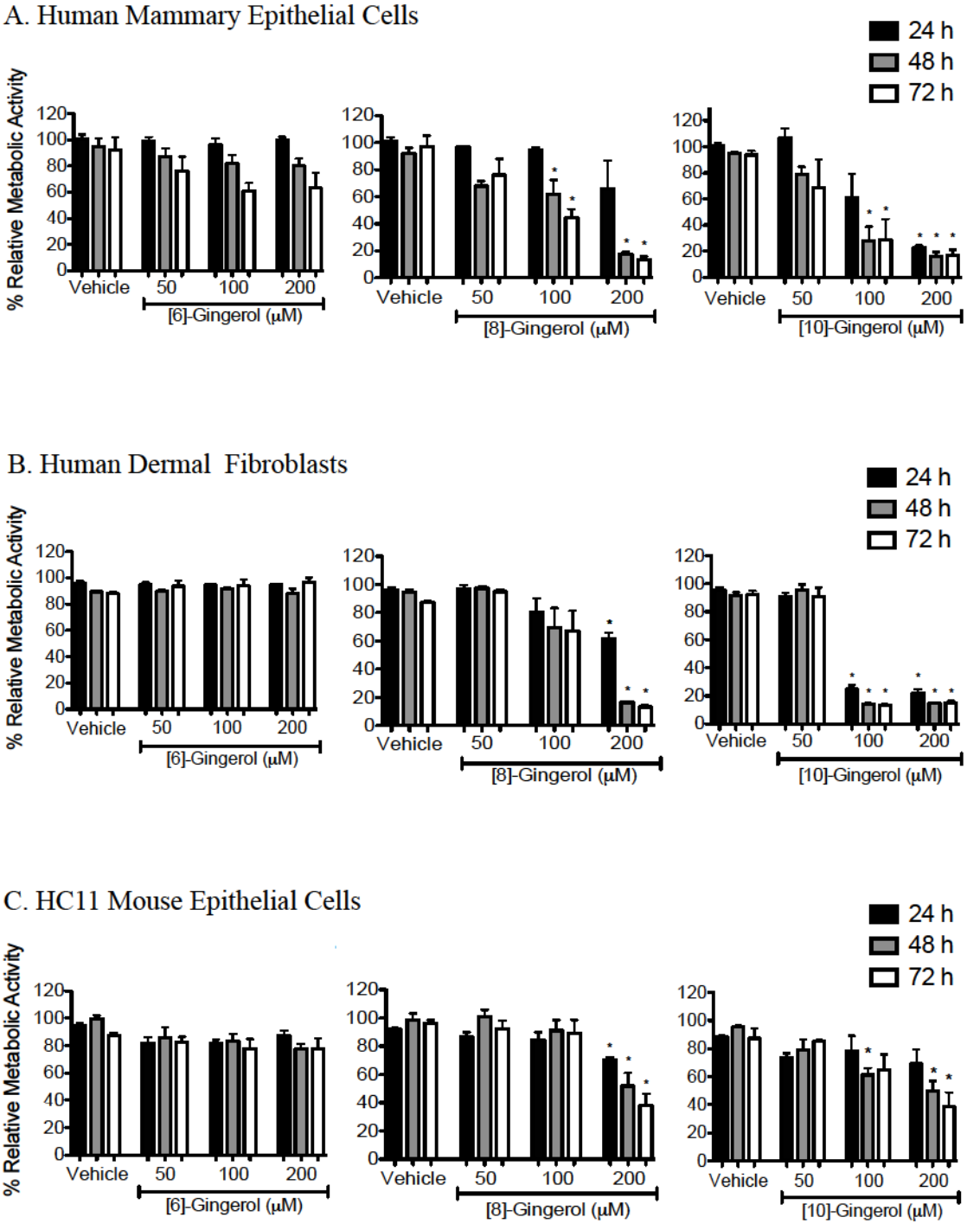
A. Human Mammary Epithelial Cells
B. Human Dermal Fibroblasts
C. HC11 Mouse Epithelial Cells
24 h
48 h
72 h
% Relative Metabolic Activity
Vehicle
50
100
200
[6]-Gingerol (μM)
[8]-Gingerol (μM)
[10]-Gingerol (μM)

Figure 4.2

Table 4.1. [6]-, [8]-, and [10]-Gingerol Do Not Reduce MTT in the Absence of Cells. Medium, vehicle, and indicated concentrations of gingerol were incubated with MTT solution. Data shown are the average optical density readings (OD) at 570 nm of triplicate wells ± standard deviation (SD). n=1.

Gingerol	Treatment	OD	SD
-	**Medium**	0.19	± 0.03
	Vehicle	0.19	± 0.04
[6]-	**50µM**	0.18	± 0.04
	100µM	0.22	± 0.04
	200µM	0.21	± 0.05
[8]-	**50µM**	0.22	± 0.04
	100µM	0.20	± 0.04
	200µM	0.20	± 0.05
[10]-	**50µM**	0.21	± 0.03
	100µM	0.20	± 0.04
	200µM	0.20	± 0.04

4.5 [6]-Gingerol Decreases the Cytosolic Phosphatase Activity in Human and Mouse Mammary Carcinoma Cultures

To confirm that [6]-gingerol did not cause an interaction with the mitochondrial dehydrogenases that would falsely indicate a decrease in the metabolic activity of the cell cultures, the acid phosphatase assay was performed on MDA-MB-231 and 4T1 cell cultures to investigate the effect of [6]-gingerol on the cytosolic phosphatases as an additional indication of cell number. These cell lines grow well in mice and were chosen for further experimentation instead of MDA-MB-468 and E0771 cells because of their potential use in *in vivo* experiments. Like the MTT assay, the absorbance readings are indicative of the number of metabolically active cells. In MDA-MB-231 cell cultures, [6]-gingerol significantly decreased the metabolic activity with 200 μM at all time points (Figure 4.3A). In 4T1 cell cultures, [6]-gingerol significantly decreased the relative phosphatase activity at all time points with 200 μM (Figure 4.3B). The percent metabolic activity of each [6]-gingerol concentration was consistent between the MTT assay and the acid phosphatase assay.

4.6 [8]-Gingerol and [10]-Gingerol, But Not [6]-Gingerol, Inhibit Human and Mouse Mammary Carcinoma Cell Proliferation

Several phytochemicals inhibit the proliferation of cancer cells[142,144,146,147]. To determine whether the decrease in cell numbers observed using the MTT assay were the result of a decrease in cell proliferation or an increase in cell death (as the MTT assay does not distinguish between the two), the effects of gingerol on the proliferation of MDA-MB-231 and 4T1 cell cultures was investigated using the Oregon Green 488 cytofluorometric assay at 72 h post-treatment. Before treating with gingerol, the cell

Figure 4.3. [6]-Gingerol Decreases the Cytosolic Phosphatase Activities of Human and Mouse Mammary Carcinoma Cell Cultures. MDA-MB-231 (A) and 4T1 (B) cells were seeded, allowed to adhere overnight, then treated with medium, vehicle, or the indicated concentrations of [6]-gingerol. Acid phosphatase assays were performed 24, 48, and 72 h post-treatment. Data shown are the average percent metabolic activities relative to the medium control of $\geq$ 3 independent experiments $\pm$ SEM; * $p < 0.05$ compared to the vehicle at the corresponding time point by a one-way ANOVA with a Tukey-Kramer multiple parameters post-test.

A. MDA-MB-231 Human Breast Carcinoma

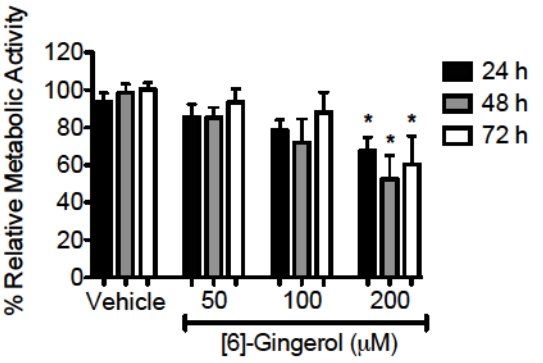

B. 4T1 Mouse Mammary Carcinoma

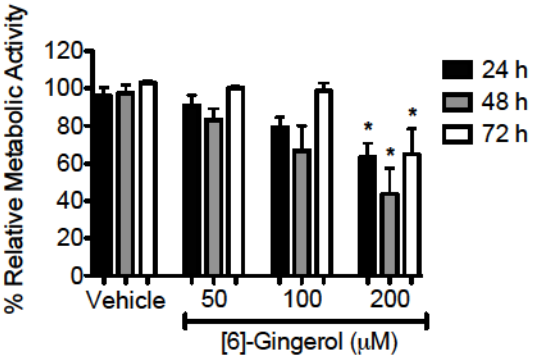

Figure 4.3

cultures were stained with the fluorescent dye, Oregon Green 488, and as the cells divided, the fluorescence intensity was halved with each cell division.

[6]-Gingerol treatment did not have a significant effect on the proliferation of MDA-MB-231 or 4T1 cell cultures (Figures 4.4A and B, respectively), while [8]-gingerol significantly decreased MDA-MB-231 and 4T1 proliferation with 200 μM. [10]-Gingerol also decreased MDA-MB-231 proliferation with 200 μM, and 4T1 proliferation with 100 and 200 μM. This data indicates that [8]- and [10]-gingerol have similar inhibitory effects on human and mouse mammary carcinoma cell proliferation, and that the decreased metabolic activities observed using the MTT assay is due in part to the anti-proliferative activity of these gingerols.

4.7 [8]-Gingerol and [10]-Gingerol, But Not [6]-Gingerol, Cause Human MDA-MB-231 and Mouse 4T1 Cells to Arrest in S Phase

To determine the phase of gingerol-induced cell cycle arrest, cell cycle analysis was performed at 48 and 72 h post-treatment. MDA-MB-231 and 4T1 cell cultures were treated with 50, 100, and 200 μM of [6]-, [8]-, and [10]-gingerol for the indicated time points and incubated with the fluorescent DNA-intercalating dye, PI. The phase of cell cycle arrest can be determined by quantifying the amount of DNA per cell.

Analysis showed a significant increase in the percentage of MDA-MB-231 cells in the S phase of the cell cycle and a corresponding decrease in the number of cells present in the G2 phase at 48 (i) and 72 h (ii) post-treatment with 200 μM of [8]-gingerol (Figure 4.5A). Treatment with 200 μM of [10]-gingerol had a similar effect, inducing an increase in the percentage of cells in the S phase of the cell cycle at 48 and 72 h post-

Figure 4.4. [8]-Gingerol and [10]-Gingerol, But Not [6]-Gingerol, Inhibit Human and Mouse Mammary Carcinoma Cell Proliferation. MDA-MB-231 (A) and 4T1 (B) cells were seeded, allowed to adhere overnight, stained with Oregon Green 488, and treated with medium, vehicle, or [6]-, [8]-, or [10]-gingerol for 72 h. Cells were fixed and the fluorescence was analyzed by flow cytometry to measure the rounds of cell division. (ii)Histograms depict a representative experiment. Data shown are the averages of $\geq$ 3 independent experiments $\pm$ SEM; * $p < 0.05$ compared to the respective vehicle at the corresponding time point by a one-way ANOVA with a Tukey-Kramer multiple parameters post-test.

A. MDA-MB-231 Human Breast Carcinoma

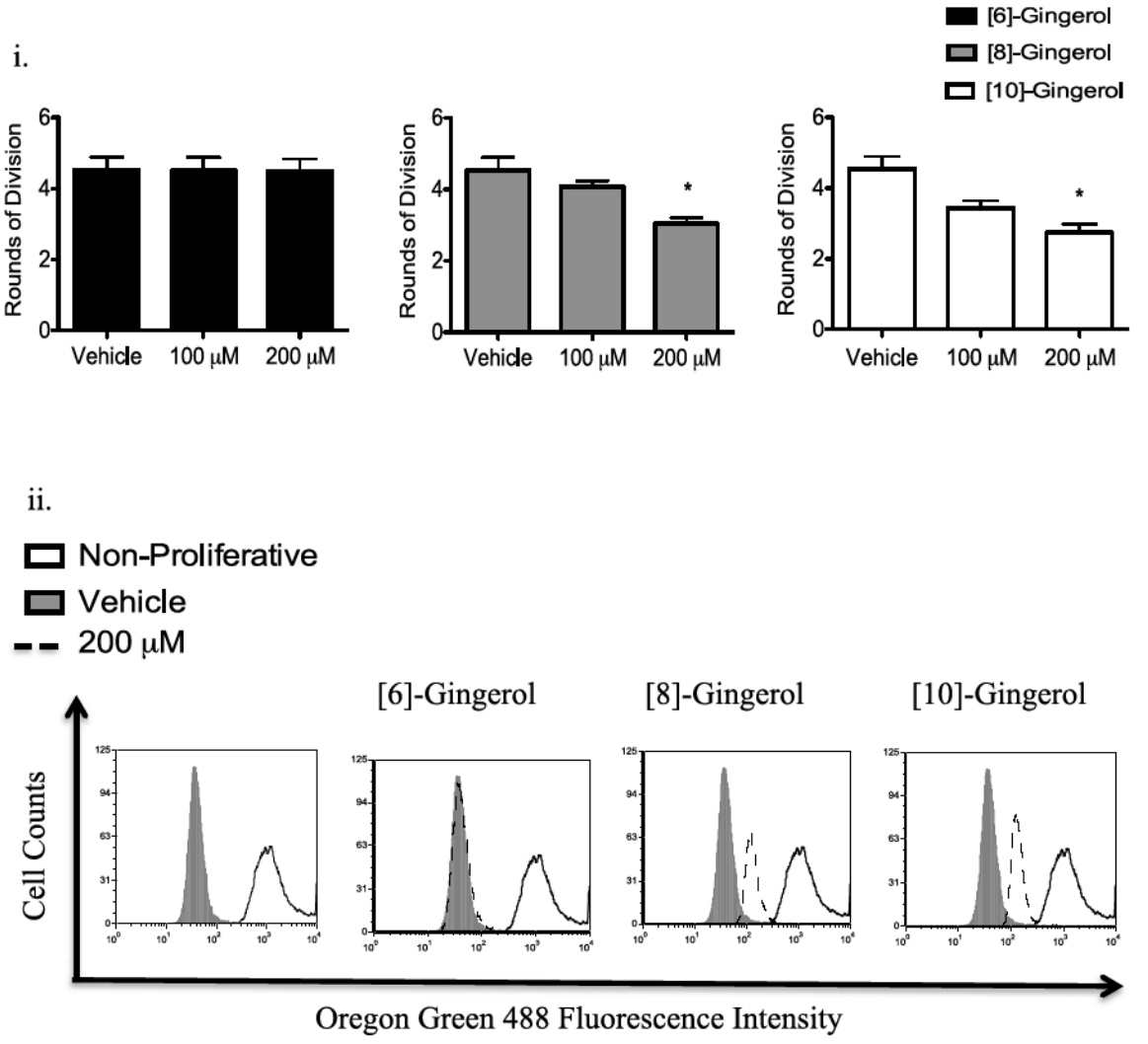

Figure 4.4

B. 4T1 Mouse Mammary Carcinoma

i.

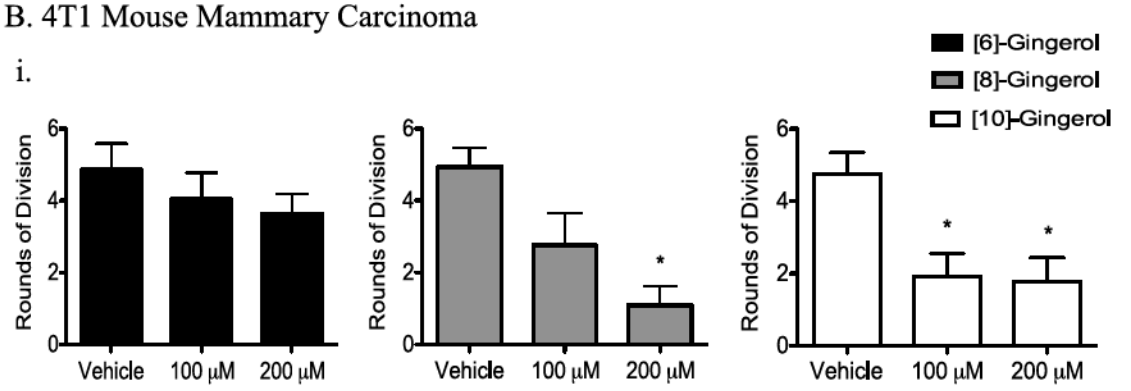

ii.

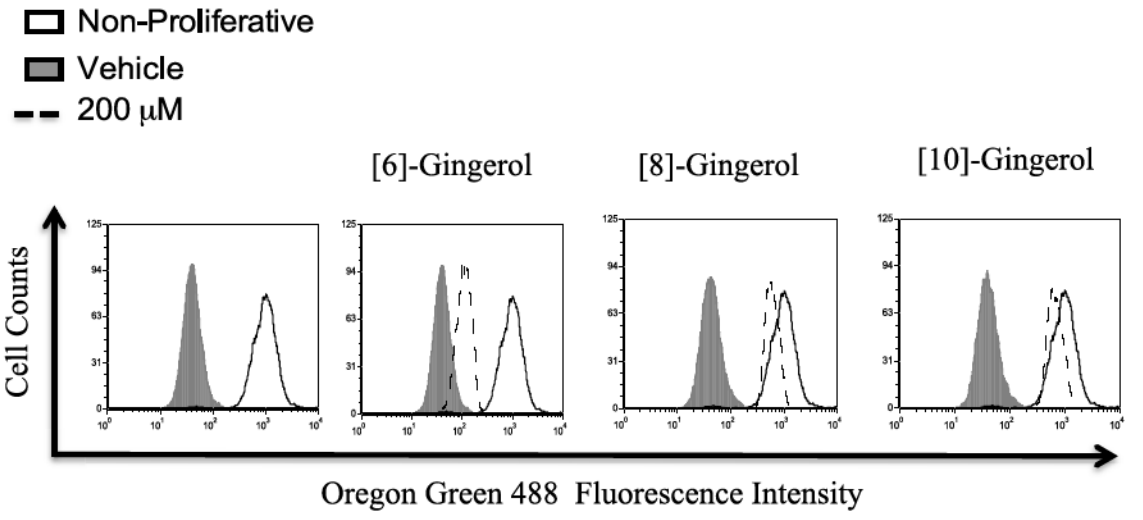

Figure 4.4 (continued)

Figure 4.5. [8]-Gingerol and [10]-Gingerol, But Not [6]-Gingerol, Cause S Phase Cell Cycle Arrest. MDA-MB-231 (A) and 4T1 (B) cells were seeded and allowed to adhere overnight. Next, samples were treated with vehicle or [6]-, [8]-, or [10]-gingerol for 48 (i) or 72 (ii) h, fixed and permeabilized in ethanol, then stored for a minimum of 24 h at -20 °C. Samples were then stained with PI and the fluorescence was analyzed by flow cytometry. Data shown are the averages of $\geq$ 3 independent experiments $\pm$ SEM; * $p < 0.05$ compared to the respective vehicle at the corresponding time point by a one-way ANOVA with a Tukey-Kramer multiple parameters post-test.

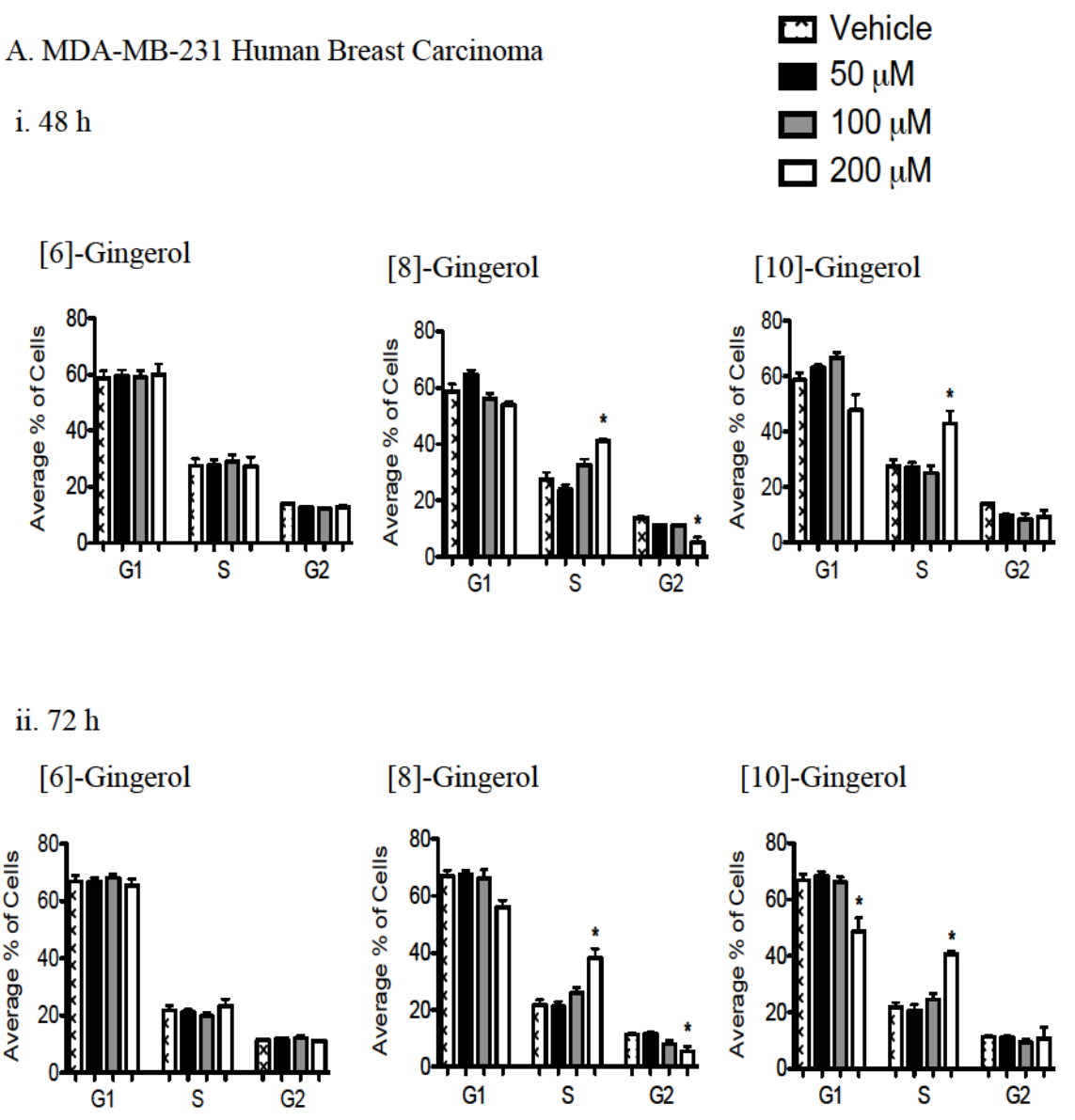
A. MDA-MB-231 Human Breast Carcinoma
i. 48 h
Vehicle
50 μM
100 μM
200 μM
[6]-Gingerol
[8]-Gingerol
[10]-Gingerol
Average % of Cells
0
20
40
60
80
G1
S
G2
*
ii. 72 h
[6]-Gingerol
[8]-Gingerol
[10]-Gingerol
Average % of Cells
G1
S
G2
*

Figure 4.5

B. 4T1 Mouse Mammary Carcinoma

i. 48 h

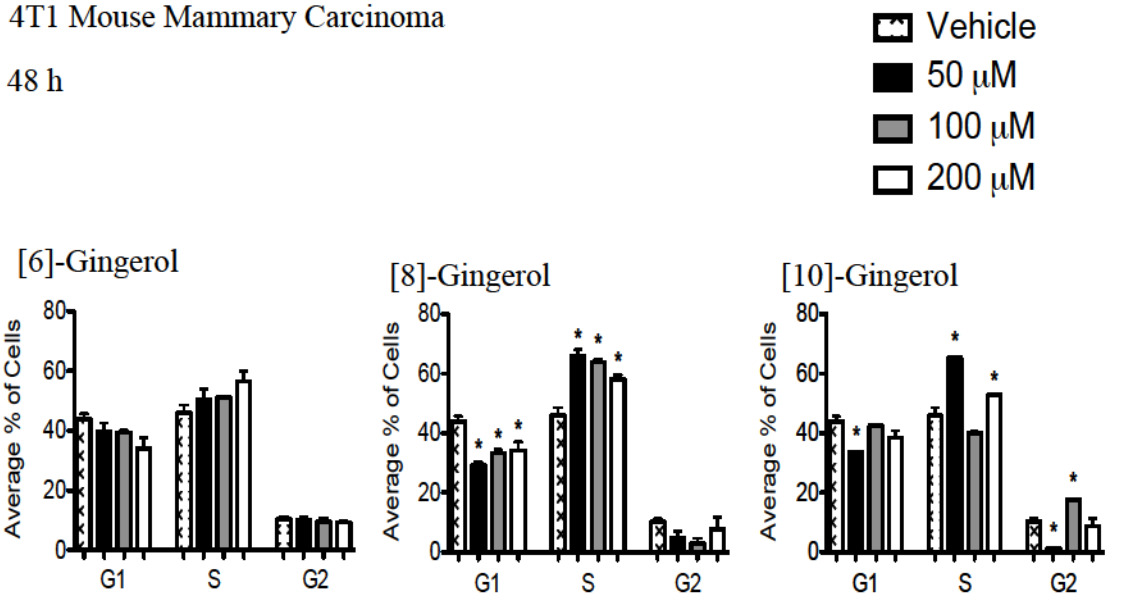

ii. 72 h

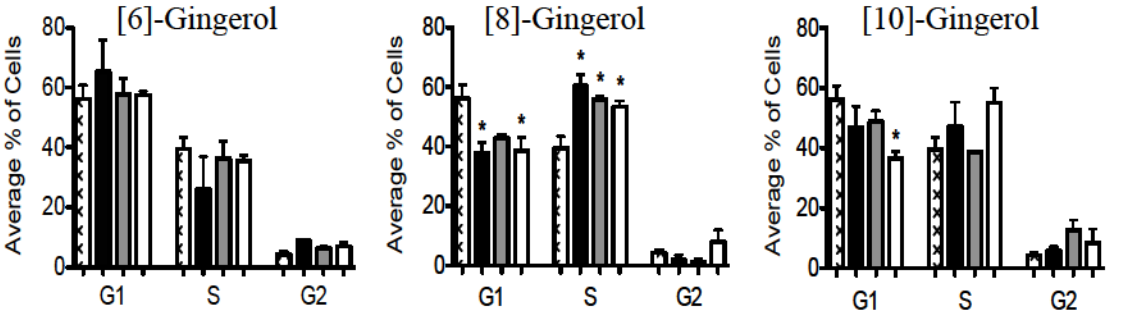

Figure 4.5 (continued)

treatment. However, unlike the effect of [8]-gingerol treatment, [10]-gingerol significantly decreased the number of cells in the G1 phase as opposed to the G2 phase of the cell cycle at 72 h post-treatment and had no effect on the G2 or G1 phases at 48 or 72 h post-treatment.

In 4T1 cell cultures (Figure 4.5B), 50, 100, and 200 μM of [8]-gingerol significantly increased the number of cells in the S phase at 48 (i) and 72 h (ii) post-treatment. An additional significant decrease in the percentage of cells in the G1 phase was observed with all concentrations of [8]-gingerol after 48 h and with 50 and 200 μM after 72 h. [10]-Gingerol induced a significant increase of cells in the S phase and a significant decrease in the G1 and G2 phases with 50 μM at 48 h. At 48 h, there was also a significant increase in the percentage of cells in the G2 phase and S phase with 100 and 200 μM, respectively. At 72 h, [10]-gingerol significantly decreased the percentage of cells in the G1 phase. No significant change in the cell cycle of MDA-MB-231 (Figure 4.5A) or 4T1 (Figure 4.5B) cell cultures was viewed upon [6]-gingerol treatment in comparison to the vehicle control.

This data indicates that [8]- and [10]-gingerol both inhibited the proliferation of mouse 4T1 cell cultures and human MDA-MB-231 cell cultures by causing the cells to arrest in the S phase.

4.8 [8]-Gingerol and [10]-Gingerol, But Not [6]-Gingerol, Induce Cell Death in Mammary Carcinoma and Non-Cancerous Cell Cultures

The percentage of cells undergoing apoptosis (present in the sub G1 peak) at 48 and 72 h was also measured during cell cycle analysis by PI staining. In MDA-MB-231 cells, a significant increase in apoptosis compared to the vehicle control was seen with

200 μM of [8]- and [10]-gingerol after 48 and 72 h (Figure 4.6A). Additionally, 100 μM of [10]-gingerol induced significant apoptosis at 72 h post-treatment. In comparison to Figure 4.6 the vehicle control, no significant change in apoptosis was viewed upon gingerol treatment after 48 h in 4T1 cells cultures (Figure 4.6B). However, [8]-gingerol induced significant apoptosis at 200 μM and [10]-gingerol induced significant apoptosis at 100 μM 72 h post-treatment.

Further exploration of the possible cytotoxic effects of gingerol at 24 h post-treatment was provided by Annexin-V-FLUOS and PI staining of gingerol-treated human and mouse mammary carcinoma and non-cancerous cell cultures. This assay detects phosphatidylserine membrane translocation and a loss in membrane integrity, respectively. In MDA-MB-231 (Figure 4.7A), MDA-MB-468 (Figure 4.7B), 4T1 (Figure 4.7C), and E0771 (Figure 4.7D) cell cultures, a significant increase in the percentage of cells undergoing late apoptosis/necrosis and the percent of total cell death was viewed with 200 μM of [8]- and [10]-gingerol. Moreover, there was a significant increase in the percentage of cells undergoing early apoptosis with 200 μM of [8]-gingerol in MDA-MB-231 and with 200 μM of [10]-gingerol in MDA-MB-468 cell cultures. [10]-Gingerol (200 μM) significantly increased the percentage of 4T1 cells undergoing early apoptosis. Additionally, a significant increase in the percentage of cells undergoing late apoptosis/necrosis and the percent of total cell death was viewed with 100 μM of [8]-gingerol in E0771 cell cultures.

In human dermal fibroblast cultures, [8]-gingerol (200 μM) significantly increased the percentage of cells undergoing late apoptosis/necrosis and the percent of total cell death (Figure 4.8). In addition, [10]-gingerol (100 and 200 μM) significantly

Figure 4.6. [8]-Gingerol and [10]-Gingerol, But Not [6]-Gingerol, Induce Significant Apoptosis After 48 and 72 h. MDA-MB-231 (A) and 4T1 (B) cells were seeded and allowed to adhere overnight. The next day, cells were treated with vehicle and [6]-, [8]-, or [10]-gingerol for 48 or 72 h, fixed and permeabilized in ethanol, then stored at -20 °C for a minimum of 24 h. Samples were then stained with PI and the fluorescence was analyzed by flow cytometry and the percent apoptosis was determined from the sub G1 peak following cell cycle analysis. Data shown are the averages of $\geq$ 3 independent experiments $\pm$ SEM; * $p < 0.05$ compared to the respective vehicle at the corresponding time point by a one-way ANOVA with a Tukey-Kramer multiple parameters post-test.

A. MDA-MB-231 Human Breast Carcinoma

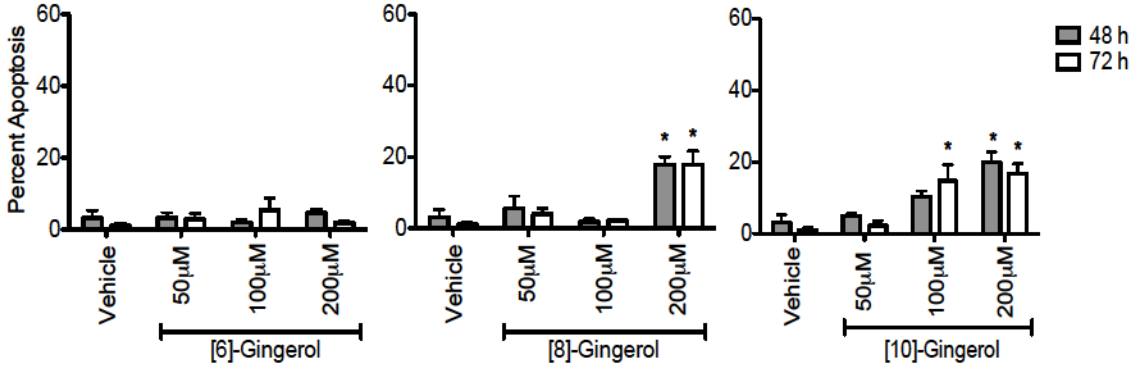

B. 4T1 Mouse Mammary Carcinoma

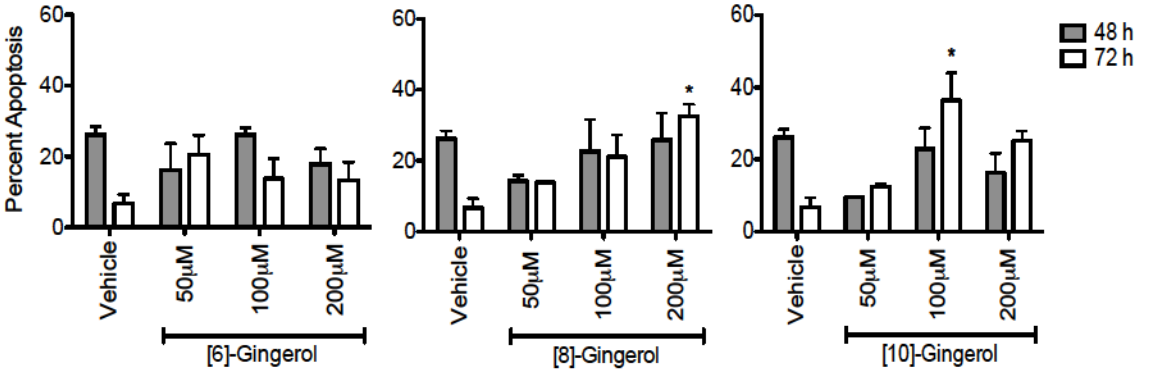

Figure 4.6

Figure 4.7. High Concentrations of [8]-Gingerol and [10]-Gingerol, But Not [6]-Gingerol, are Cytotoxic to Human and Mouse Mammary Carcinoma Cell Cultures. MDA-MB-231 (A), MDA-MB-468 (B), 4T1 (C), and E0771 (D) cells were seeded, allowed to adhere overnight, then treated with vehicle or [6]-, [8]- or [10]-gingerol for 24 h. Following treatment, cells were stained with Annexin-V-FLUOS and PI and the fluorescence was analyzed by flow cytometry. Data shown are the mean percentages of cells in early apoptosis, of cells in late apoptosis/necrosis, or of total cell death of $\geq$ 3 independent experiments $\pm$ SEM; * $p < 0.05$ when compared to the vehicle at the corresponding time point by one-way ANOVA with a Tukey-Kramer multiple parameters post-test.

A. MDA-MB-231 Human Breast Carcinoma

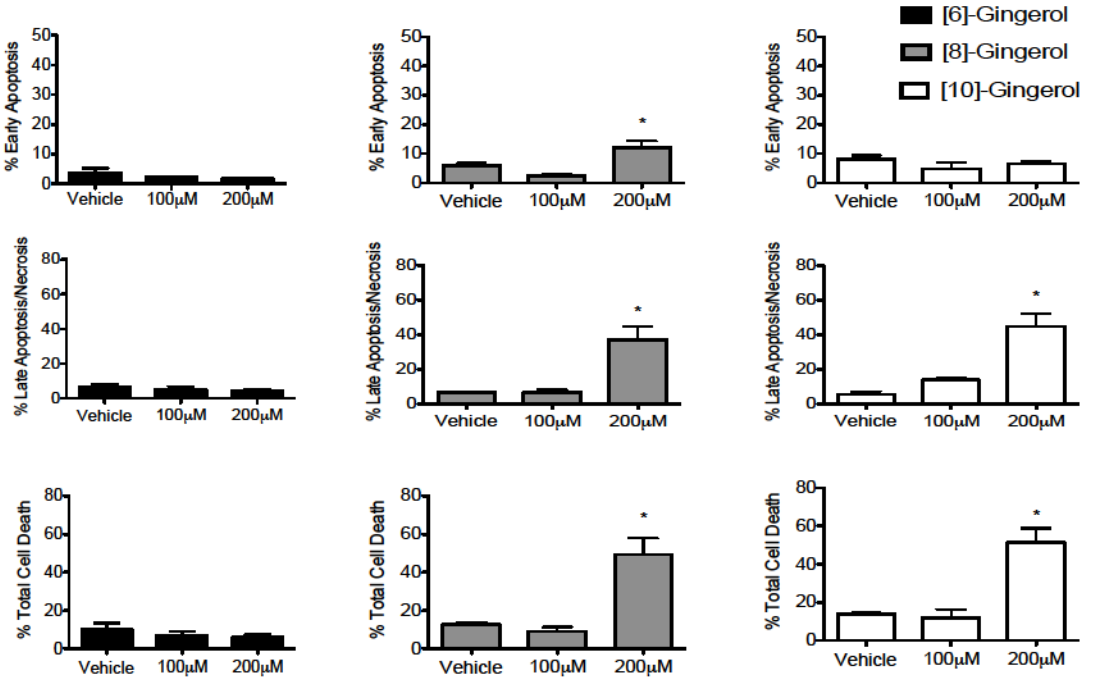

B. MDA-MB-468 Human Breast Carcinoma

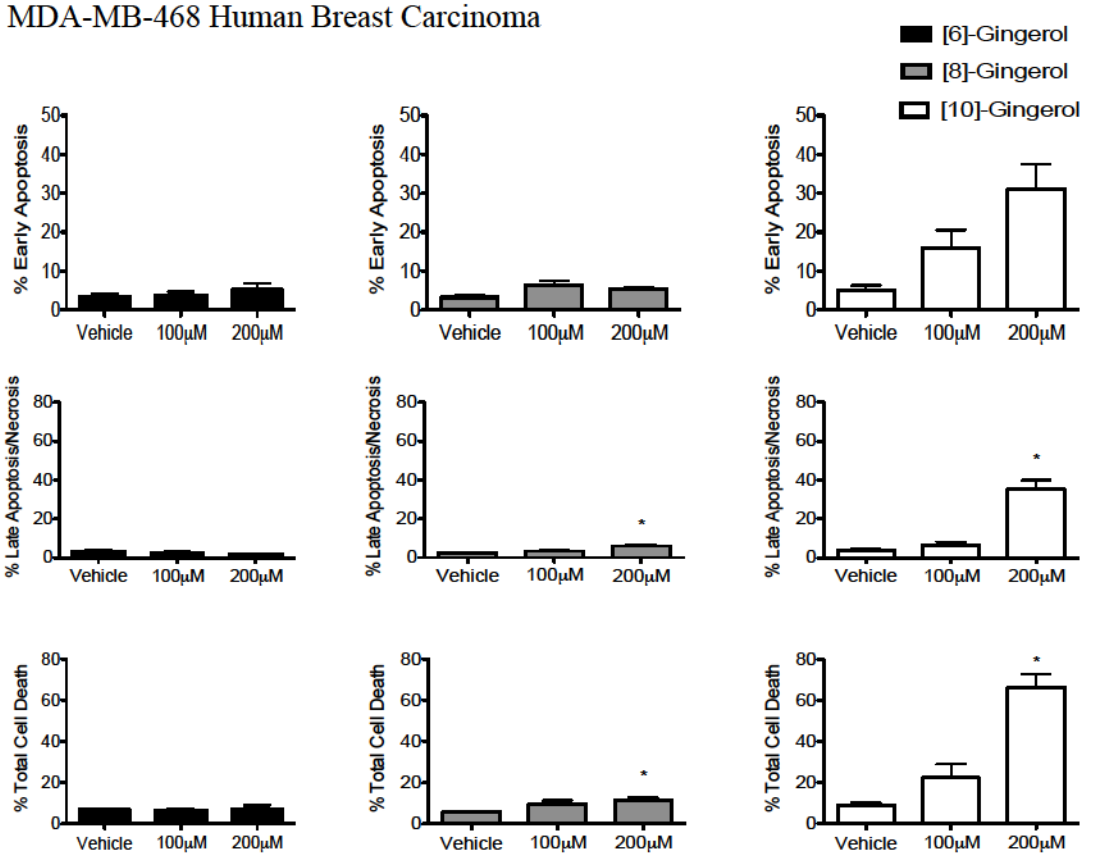

C. 4T1 Mouse Mammary Carcinoma

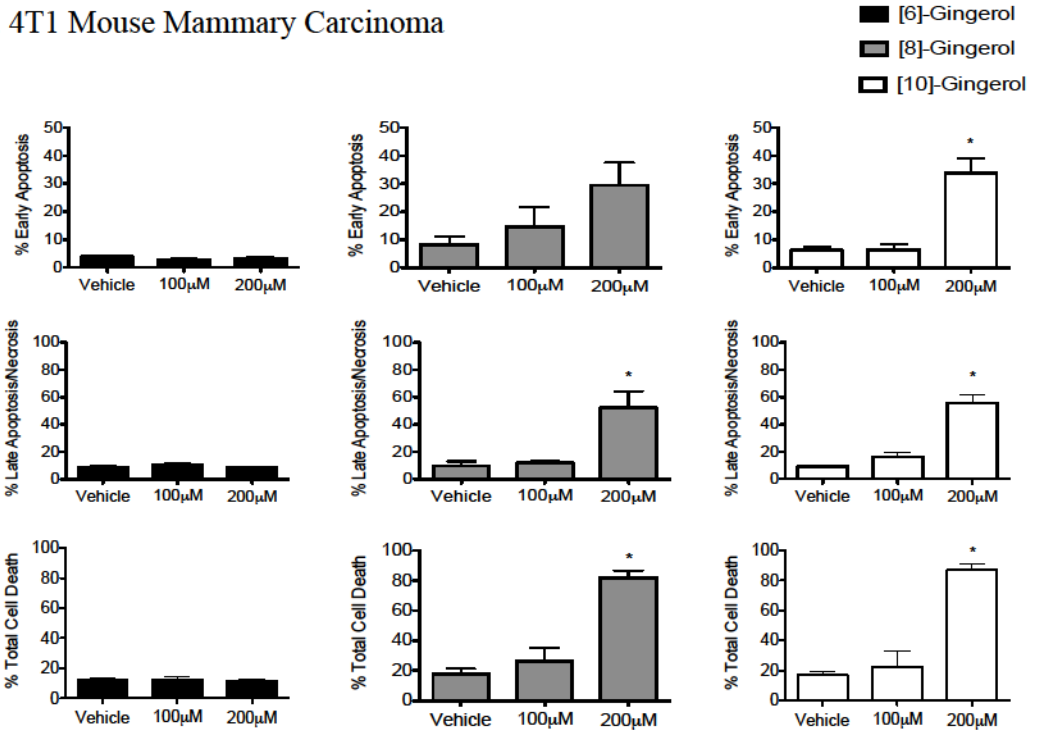

D. E0771 Mouse Mammary Carcinoma

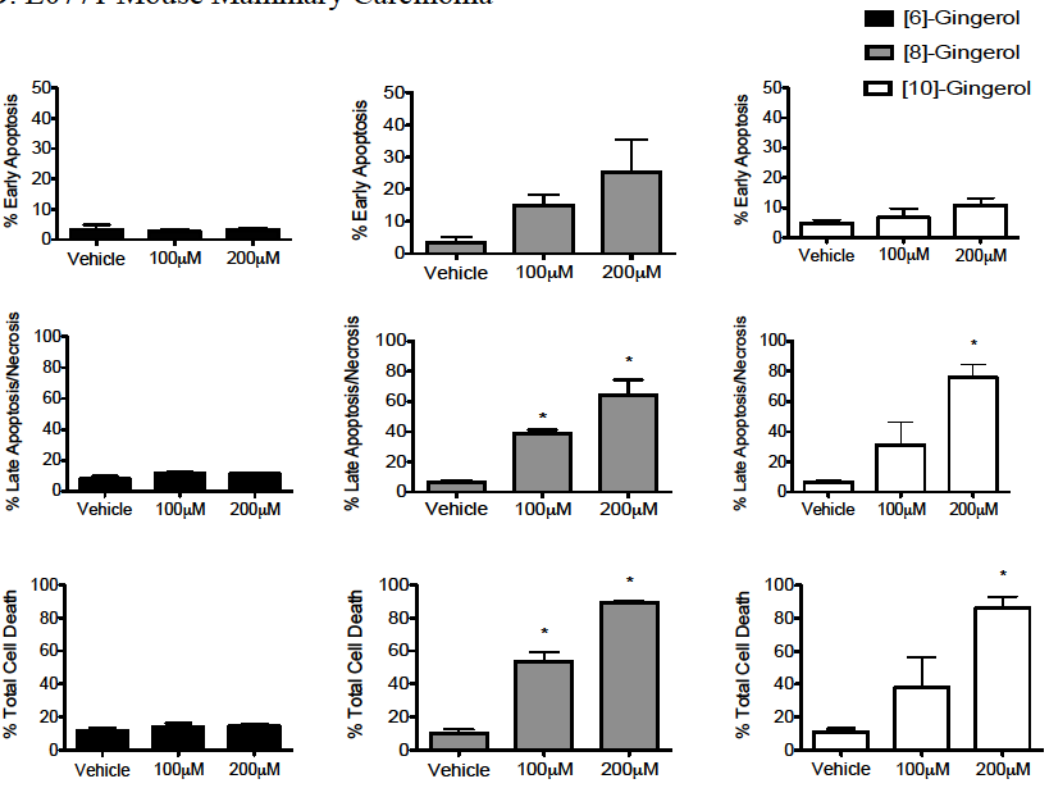

Figure 4.8. [8]-Gingerol and [10]-Gingerol, But Not [6]-Gingerol, are Cytotoxic to Human Dermal Fibroblast Cultures. Human dermal fibroblasts were seeded, allowed to adhere overnight, then treated with vehicle or [6]-, [8]- or [10]-gingerol for 24 h. Following treatment, cells were stained with Annexin-V-FLUOS and PI and the fluorescence was analyzed by flow cytometry. Data shown are the mean percentages of cells in early apoptosis, of cells in late apoptosis/necrosis, or of total cell death of ≥ 3 independent experiments $\pm$ SEM; * $p < 0.05$ when compared to the vehicle at the corresponding time point by one-way ANOVA with a Tukey-Kramer multiple parameters post-test.

Human Dermal Fibroblasts

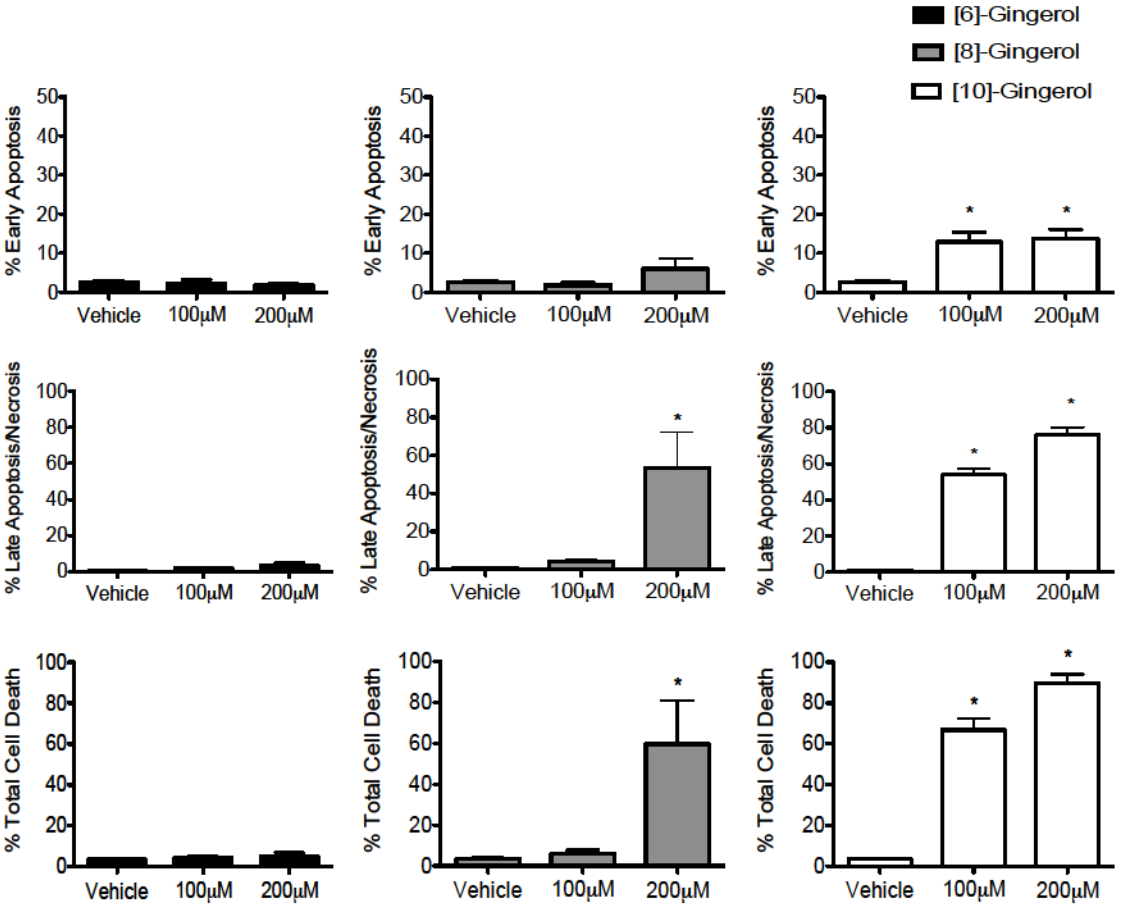

Figure 4.8

increased the percentage of cells undergoing early apoptosis and late apoptosis/necrosis and the percent of total cell death.

Generally, [8]- and [10]-gingerol exhibited similar cytotoxic effects at the same concentrations. However, there were a few exceptions. For example, [10]-gingerol caused a much higher degree of cytotoxicity in MDA-MB-468 cells than did [8]-gingerol. Additionally, [10]-gingerol at 100 and 200 μM significantly increased the percentage of human dermal fibroblast cells undergoing early apoptosis, although [8]-gingerol had no effect on the percentage of human fibroblasts in early apoptosis. Also, 100 and 200 μM of [10]-gingerol significantly increased the number of cells undergoing late apoptosis/necrosis and the total cell death, whereas only 200 μM of [8]-gingerol showed statistical significance in human fibroblasts. In all cell cultures investigated, [6]-gingerol did not appear to induce any form of cell death when compared to the vehicle control (Figures 4.7 and 4.8).

4.9 [8]-Gingerol and [10]-Gingerol-Induced Cell Death Does Not Require Reactive Oxygen Species Production or Caspase Activation

Previous studies have shown that phytochemicals can induce cancer cell death through the production of ROS[100] and/or the activation of caspases[134]. Annexin-V-FLUOS and PI staining of 4T1 mouse mammary carcinoma cultures treated with [8]-gingerol in the presence or absence of a ROS scavenger (N-acetyl-cysteine [NAC]) and a pan-caspase inhibitor (ZVAD-FMK) were performed to investigate the mechanism behind [8]-gingerol-induced cytotoxicity.

There was no change in the percentage of 4T1 cells undergoing late apoptosis/necrosis or the percent of total cell death (Figure 4.9) when treated with vehicle

Figure 4.9. [8]-Gingerol-Induced Cell Death Does Not Require Caspase Activation and Reactive Oxygen Species Production. 4T1 cells were seeded, allowed to adhere overnight, then treated with vehicle or [8]-gingerol in the absence or presence of 50 μM ZVAD-FMK or 10 mM NAC. Samples were stained with Annexin-V-FLUOS and PI and the fluorescence was analyzed by flow cytometry at 24 h post-treatment. Data shown are the mean percentages of cells in early apoptosis, of cells in late apoptosis/ necrosis, or of total cell death of $\geq$ 3 independent experiments $\pm$ SEM; *$p < 0.05$ compared to the respective vehicle and ZVAD-FMK or NAC treatment by a one-way ANOVA and Tukey-Kramer multiple parameters post-test. Dot plots depict a representative experiment (ii).

4T1 Mouse Mammary Carcinoma

i.

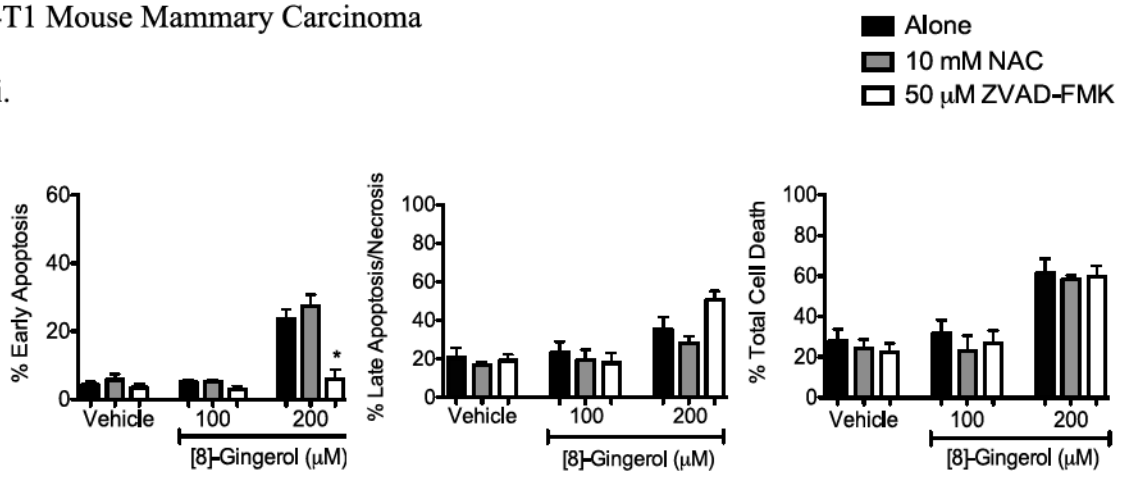

ii.

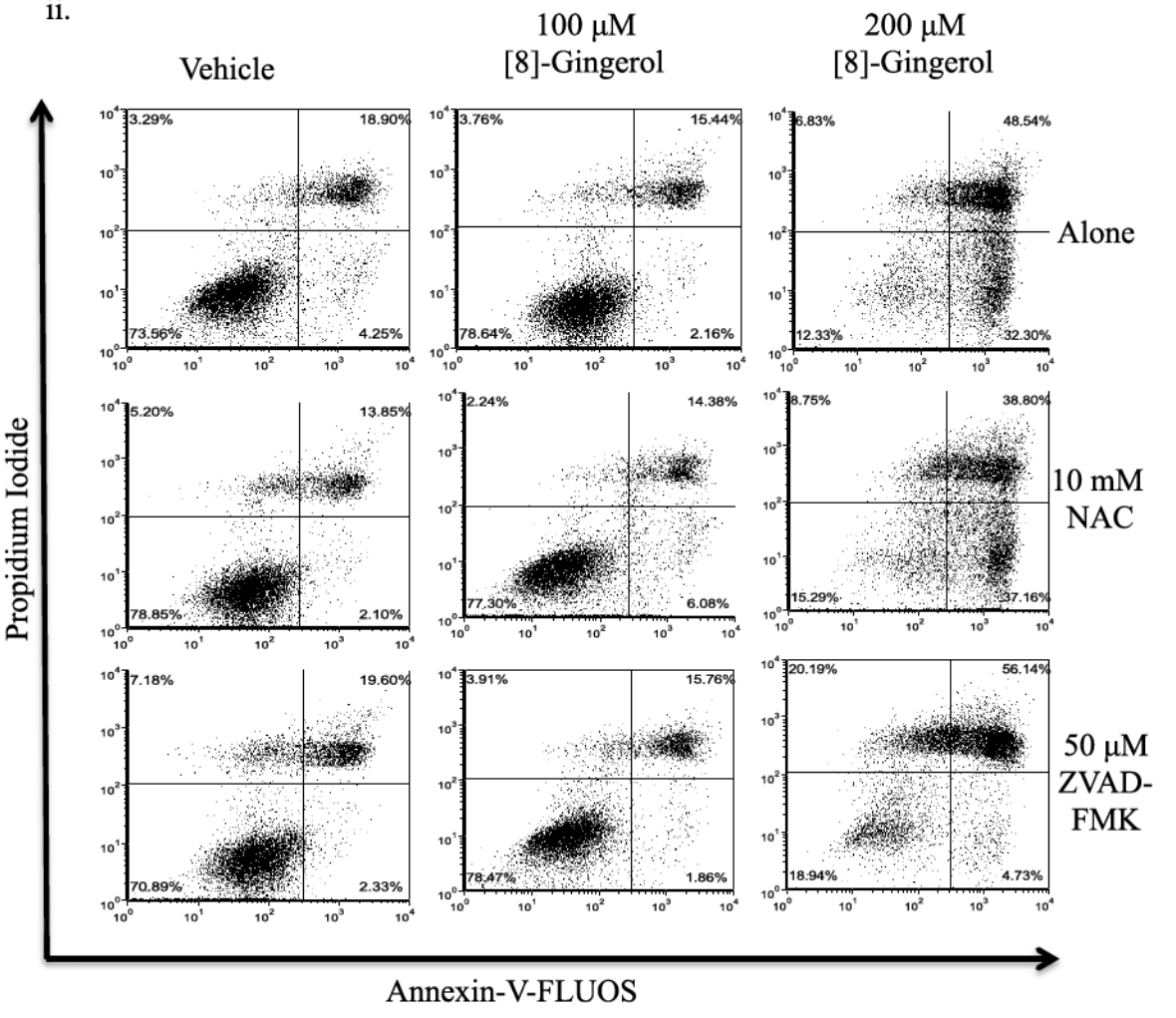

Figure 4.9

or [8]-gingerol compared to those treated with vehicle or [8]-gingerol in the presence of NAC or ZVAD-FMK. Additionally, there was no change in the percentage of 4T1 cells in early apoptosis when treated with vehicle or [8]-gingerol compared to those treated with vehicle or [8]-gingerol in the presence of NAC. Interestingly, there was a significant decrease in the number of 4T1 cells undergoing early apoptosis in the presence of ZVAD-FMK treated with 200 μM of [8]-gingerol compared to only 200 μM of [8]-gingerol; however, as there was no change in the total cell death, this data suggests that [8]-gingerol-induced cell death is not dependent upon the production of ROS or the activation of caspases.

Additionally, Annexin-V-FLUOS and PI staining of MDA-MB-231 and 4T1 carcinoma cultures treated with [10]-gingerol in the presence or absence of NAC and ZVAD-FMK were performed to investigate the mechanism behind the [10]-gingerol-induced cytotoxicity. There was no significant decrease in the viability of MDA-MB-231 (Figure 4.10A) or 4T1 (Figure 4.10B) cell cultures treated with vehicle or [10]-gingerol compared to those treated with vehicle or [10]-gingerol in the presence of NAC or ZVAD-FMK. This data suggests that [10]-gingerol-induced cell death depends upon mechanisms independent of ROS production or caspase activation.

To ensure that NAC and ZVAD-FMK were fully functioning, cisplatin was used as a positive control. Cisplatin has previously been described to induce cell death through the induction of ROS[148,149] and the activation of caspases[150]. When 4T1 cell cultures were treated with cisplatin and cultured in the presence of NAC or ZVAD-FMK, there was a decrease in cell death compared to cisplatin-treated 4T1 cell cultures in the absence of NAC or ZVAD-FMK at 24 h post-treatment (Appendix Figure 1), indicating that the

Figure 4.10. [10]-Gingerol-Induced Cell Death Does Not Require Caspase Activation and Reactive Oxygen Species Production. MDA-MB-231 (A) and 4T1 (B) cells were seeded, allowed to adhere overnight, then treated with vehicle or [10]-gingerol in the absence or presence of 50 μM ZVAD-FMK or 10 mM NAC. Samples were stained with Annexin-V-FLUOS and PI and the fluorescence was analyzed by flow cytometry at 24 h post-treatment. Data shown are the mean percentages of cells in early apoptosis, of cells in late apoptosis/necrosis, or of total cell death of ≥ 3 independent experiments $\pm$ SEM; *$p < 0.05$ compared to the respective vehicle and ZVAD-FMK or NAC treatment by a one-way ANOVA and Tukey-Kramer multiple parameters post-test. Dot plots depict a representative experiment (ii).

A. MDA-MB-231 Human Breast Carcinoma

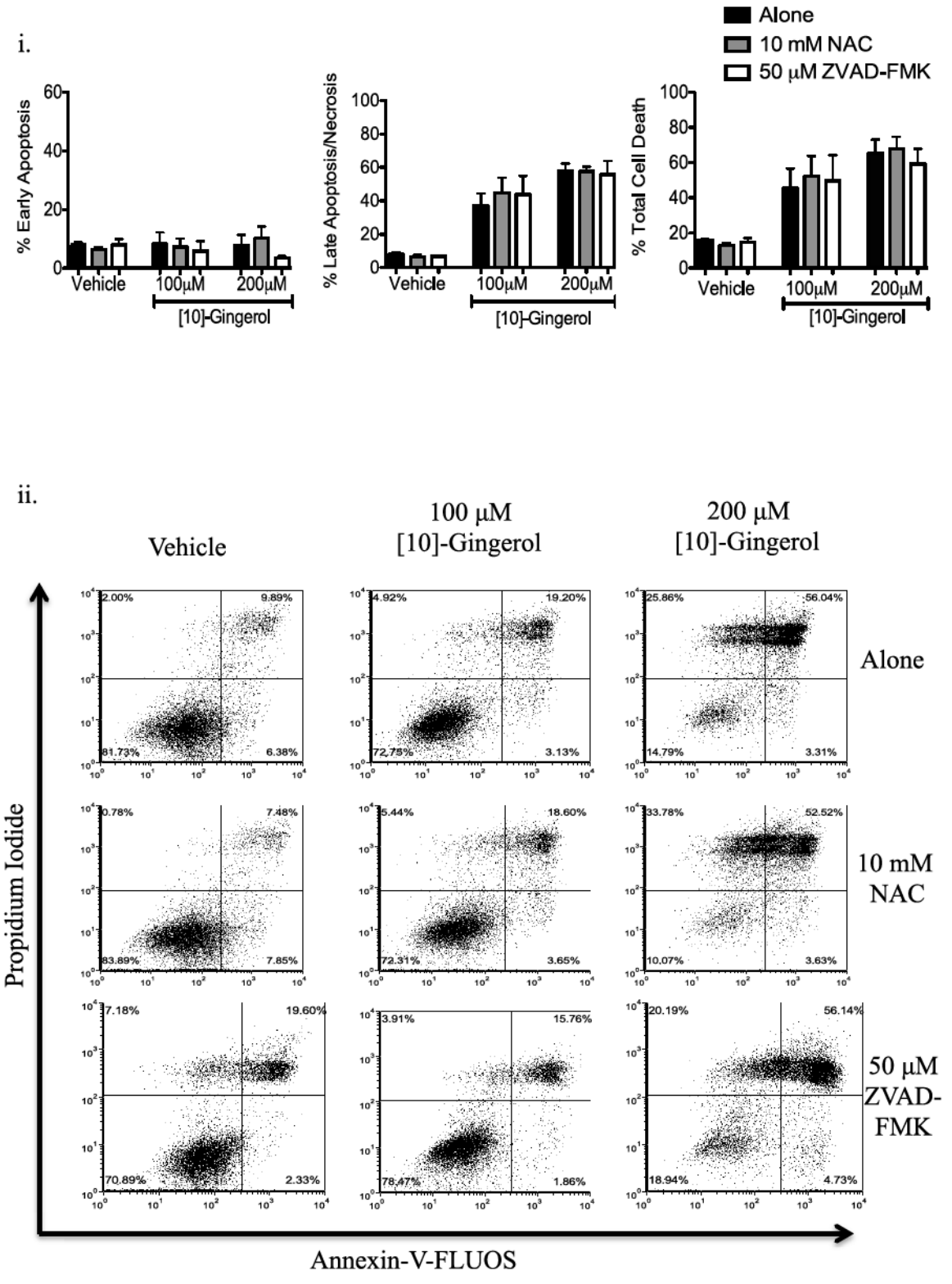

Figure 4.10

B. 4T1 Mouse Mammary Carcinoma

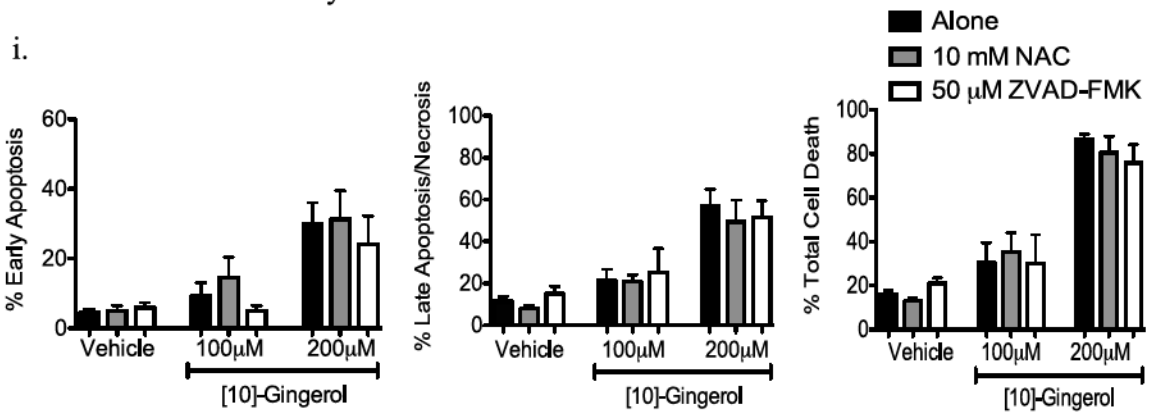

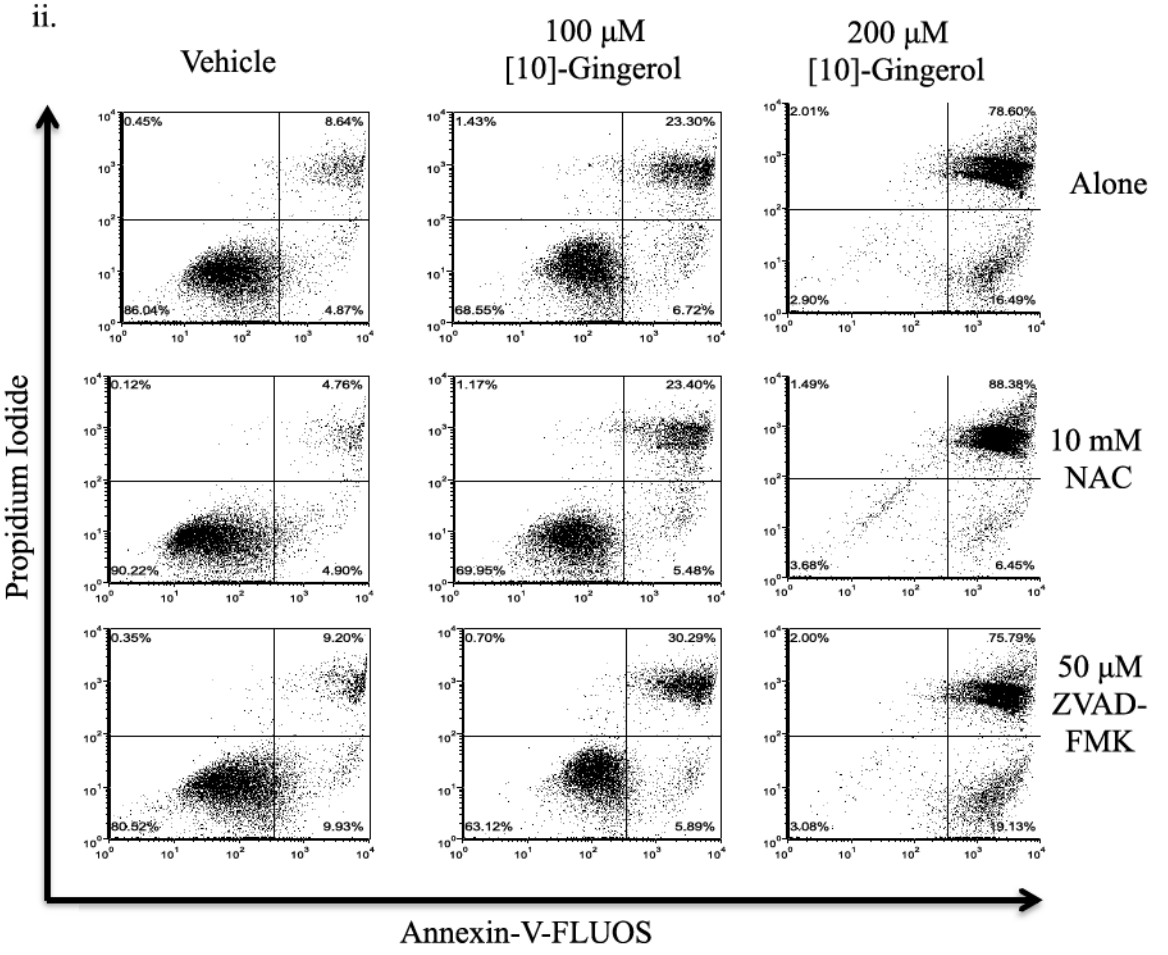

Figure 4.10 (continued)

NAC and ZVAD-FMK are functioning to scavenge ROS and inhibit pan caspase activation, respectively, as was expected.

A recent publication has shown that two olive polyphenols use sodium bicarbonate as the primary source for their production of hydrogen peroxide[151]. The hydrogen peroxide produced from this reaction has been shown to decrease the number of breast cancer and normal cell cultures[151]. The Amplex Red assay was used to investigate if gingerol could initiate a reaction with sodium bicarbonate in the medium to produce hydrogen peroxide in a cell-free environment. Although [8]- and [10]-gingerol-induced cell death was determined to be independent of ROS-production and caspase-activation, the Amplex Red assay was used for further evidence. No significant increase in absorbance readings of the gingerol treatments compared to the medium (Med) or vehicle (Veh) controls were identified at 90 min or 24 h post-treatment (Appendix Figure 2). Myricetin at 50 μM was used as a positive control and demonstrated a significant increase in absorbance readings compared to the medium, vehicle, and gingerol treatments at 90 min and 24 h post-treatment. Myricetin has previously demonstrated the ability to produce hydrogen peroxide in a cell-free environment in our laboratory (Allison Knickle, personal communication).

CHAPTER 5

DISCUSSION

5.1 A Summary of the Major Findings and a Comparison to the Literature

5.1.1 The Effects of [6]-, [8]-, and [10]-Gingerol on T Cell Proliferation and Death

In the present study, [6]-, [8]-, and [10]-gingerol caused a significant dose-dependent decrease in isolated T cell proliferation, whether induced by antibody-coated beads or by co-culture with DCs and α-TCR antibody. This is in agreement with other studies regarding the immunomodulatory properties of ginger[113,116]. Particularly, it is in agreement with a recent study demonstrating [8]-gingerol-induced inhibition of splenocyte proliferation[128]. In the study by Lu et al., *in vivo* intraperitoneal administration of 50 and 100 mg/kg of [8]-gingerol were found to inhibit the proliferation of ConA-, LPS-, and OVA-induced splenocytes, and decrease the percentage of $CD19^+$ B cells and $CD3^+$ T cells. Additionally, IgG, IgG1, IgG2b levels were reduced in OVA-immunized mice. Although no investigation into the effects of gingerol on B cells or any *in vivo* experiments were performed in the current study, as in the study by Lu et al., [8]-gingerol, as well as [6]- and [10]-gingerol, inhibited the proliferation of T cells *in vitro*, as seen using [^{3}H]TdR incorporation. Further investigation by Oregon Green 488 staining of isolated T cells confirmed that [8]- and [10]-gingerol significantly reduced the rounds of T cell division and the proportion of proliferating T cells, whereas [6]-gingerol did not have any effect on T cell division. Furthermore, gingerol treatment of CTLL-2 cell cultures caused a decrease in proliferation with 100 μM of [8]-gingerol and [10]-gingerol, but not [6]-gingerol. It is interesting to note that, although [6]-gingerol appears to inhibit the proliferation of isolated T cells using [^{3}H]TdR incorporation, no effects on

proliferation were viewed using Oregon Green 488-stained T cells. One possible explanation is that [6]-gingerol may be inducing the cells to produce additional cold thymidine which will compete with radiolabeled thymidine during DNA synthesis, leading to a decrease in radiolabeled DNA.

In the study by Lu et al.[100], the proliferation of LPS-stimulated splenocytes was inhibited by [8]-gingerol treatment at approximately 124 and 248 μM, but not 62 and 31.5 μM, while the proliferation of ConA-stimulated splenocytes was only inhibited by 248 μM [8]-gingerol. In my study, the proliferation of isolated T cells was inhibited by [8]- and [10]-gingerol by as low as 50 μM when investigated by [^{3}H]TdR incorporation and Oregon Green 488 staining. CTLL-2 proliferation was inhibited by 100 μM of [8]-gingerol and [10]-gingerol, a much lower concentration than seen in the previous study by Lu et al. The different effects seen between the two studies could be because T cells are more responsive to the anti-proliferative effects of gingerol than whole splenocyte isolates. More likely, it is possible that the *in vitro* and *in vivo* results do not correspond due to additional interactions that occurred in the *in vivo* environment, and/or that the differences in gingerol concentrations, mechanisms of stimulation, and experimental time differences accounted for the variances between my study and the study by Lu et al.

[8]-Gingerol and [10]-gingerol inhibited CTLL-2 proliferation with 100 μM, indicating that they may inhibit IL-2 cell signaling. Interestingly, CTLL-2 proliferation was not inhibited by [6]-gingerol, potentially indicating that [6]-gingerol acts through a different pathway than does [8]-gingerol and [10]-gingerol. It is also possible that [6]-gingerol is not potent enough to have an effect on CTLL-2 cell cultures. Interestingly, the results of the current study suggest that DCs do not appear to play a direct role in

gingerol-mediated suppression of T cell activation, as the degree of suppression by gingerol was similar in the antibody-coated bead-stimulated model and in co-culture with DCs and α-TCR antibody. As a control, DCs were pulsed with α-TCR in the absence of T cells and background cpm levels were detected. To confirm this evidence, fluorescence analysis of Oregon Green 488 stained-T cells co-cultured with DCs and pulsed with α-TCR could be performed to compare to antibody-coated bead-stimulated Oregon Green 488-stained T cells.

In the study by Lu et al., [8]-gingerol did not induce cytotoxicity in unstimulated splenocytes at concentrations up to approximately 310 μM – more than three times the highest concentration applied to T cells in the current study. In contrast, in my study [8]-gingerol induced cell death in antibody-coated bead stimulated and unstimulated isolated T cell cultures at 100 μM, although it did not induce cell death in CTLL-2 cell cultures at concentrations up to 100 μM. The differences in cytotoxicity between T cells and CTLL-2 cells within my study could be due to the alterations within the CTLL-2 cells to make them immortal, which could leave them less vulnerable than isolated primary T cells. It is possible that T cells may be more vulnerable to the cytotoxic effects of [8]-gingerol than whole splenocyte isolates used in the study by Lu et al. More likely, it is possible that the mechanisms of stimulation and experimental time differences accounted for the variances between my study and the study by Lu et al. Additionally, in the previous study, the cytotoxicity of [8]-gingerol on splenocytes was only investigated at 24 h post-treatment using the MTT assay, whereas the proliferation assay (another MTT assay) was performed at 48 h post-treatment. Notably, the MTT assay measures the number of metabolically active cells and does not differentiate between cytostatic and cytotoxic

effects[136]. Due to these discrepancies, it cannot be ascertained if the decrease in proliferation seen at 48 h was due to a decrease in cell number due to inhibited proliferation or reduced cell viability.

5.1.2 The Effects of [6]-, [8]-, and [10]-Gingerol on Surface Molecule Expression and Cytokine Production by T cells

Although [8]- and [10]-gingerol did induce significant cell death at high concentrations, no significant change in cell death in stimulated T cells occurred with concentrations up to 50 μM of gingerol. Therefore, T cell or DC death did not account for reduced T cell proliferation, cytokine production, and cell surface antibody expression with application of 50 μM or lower of gingerol.

While the proportion of activated T cells expressing CD25 and CD69 were unchanged following gingerol treatment, the surface expression of these receptors on individual cells was significantly decreased with [8]- and [10]-gingerol treatment. Early activation markers CD25 and CD69 are not constitutively expressed on unstimulated T cells but are expressed on the surface of T cells upon activation to function as a transmitting receptor of proliferation signals[32]. Therefore, it can be determined that gingerol is inhibiting the transmission of proliferation signals (and therefore T cell proliferation) at least in part by decreasing the expression of these cell surface molecules. No changes in the expression of CD25 by CTLL-2 cells or the proliferation of CTLL-2 cells were seen with 50 μM of gingerol treatment. However, CTLL-2 cell proliferation was inhibited with 100 μM of [8]- and [10]-gingerol treatment. Further investigation needs to be performed to determine whether 100 μM of [8]-gingerol and [10]-gingerol affect IL-2 receptor signaling.

Reduction of CD25 expression negatively regulates the production of IL-2, an important cytokine for promoting T cell proliferation[31]. Therefore, the production of IL-2 by gingerol-treated T cells was investigated, determining that 50 μM of [8]-gingerol and [10]-gingerol significantly decreased the production of IL-2. This suggests that [8]-gingerol and [10]-gingerol suppress the transmission of T cell proliferation signals at least in part by suppressing the production of IL-2 and the expression of CD25. This is in agreement with the properties of the well-studied phytochemical, curcumin, which decreases the production of IL-2, the expression of CD25, and subsequently the proliferation of mouse T cells *in vitro*[152].

Although there was a significant decrease in the production of IFN-γ by T cells with [6]-, [8]-, and [10]-gingerol treatment, no change in the expression of CD119 (IFN-γR1) was evident. This suggests that [6]-, [8]- and [10]-gingerol can decrease T cell production of IFN-γ, but does not affect the ability of T cells to react to IFN-γ through IFN-γR1, although gingerol may exhibit an effect on IFN-γR2 or IFN-γ signaling and thereby affect the ability of T cells to react to IFN-γ. Moreover, [8]-gingerol and [10]-gingerol reduced the production of both IL-2 and IFN-γ, both of which are important cytokines produced by Th1 cells[4]. This data suggests that [8]-gingerol and [10]-gingerol may inhibit the Th1 response, either by decreasing Th1 cell differentiation or effector function. No effect by gingerol was seen on the synthesis of the Th2 cytokine, IL-4.

5.1.3 The Anti-Proliferative Effects of [6]-, [8]-, and [10]-Gingerol on Mammary Carcinoma Cells

This study also examined the effects of [6]-, [8]-, and [10]-gingerol on mammary carcinoma cell proliferation. I observed that [8]-gingerol and [10]-gingerol, but not [6]-

gingerol, significantly decreased the rounds of cell division in cultures of mouse and human mammary carcinoma cells by causing an arrest in the S phase of the cell cycle. A previous study has shown that [6]-gingerol at concentrations ranging from 12.5 – 50 μM inhibits the growth of colon cancer cells by causing an arrest at the G2/M phase of the cell cycle[133]. It is interesting that [6]-gingerol is able to induce an S phase arrest in one cell line and not another. However, cancers of distinct origins can exhibit an arrest at different cell cycle phases following phytochemical treatment. For example, one study discovered a curcumin-induced G2/M arrest in human pancreatic cells[153] while another showed an arrest in the G1 phase of the cell cycle of human breast carcinoma cells[154]. In accordance with the current study, Chang et al. showed that capsaicin, a structural relative to gingerol, also induces an arrest in the S phase of the cell cycle of MCF-7 and BT-20 human breast cancer cell cultures[101]. A search of the literature did not return any studies on the effects of [8]-gingerol and [10]-gingerol on the cell cycle of cancer cell cultures.

The data from the MTT and acid phosphatase assays in the current study suggested that [6]-gingerol had a cytostatic effect on mammary carcinoma cells. Although Oregon Green 488 staining did not indicate a decrease in MDA-MB-231 or 4T1 cell proliferation following treatment with [6]-gingerol, it is possible that the decrease in cancer cell growth seen using the MTT and acid phosphatase assays were too slight to be detected by Oregon Green 488 staining. Another possibility is that [6]-gingerol is inhibiting the enzymatic activities of the mitochondrial succinate dehydrogenase and cytosolic phosphatases, causing an apparent reduction in cell number.

This could be investigated further using [^{3}H]TdR incorporation as another readout for cell proliferation in mammary carcinoma cell cultures.

5.1.4 The Cytotoxic Effects of [8]- and [10]-Gingerol on Mammary Carcinoma Cells

While [8]-gingerol and [10]-gingerol demonstrated cytostatic activity in mammary carcinoma cell cultures, a population of dead cells observed in flow cytometric analyses also suggested a cytotoxic mode of action. A previous report found that concentrations of approximately 170 – 615 μM of [6]-gingerol induced apoptosis in HeLa ovarian carcinoma cells[134], and another study found that capsaicin, a structural relative of gingerol, induced apoptosis of HepG2 liver carcinoma cells[102]. Upon consideration of the above evidence, I concluded that gingerol was inducing cytotoxicity in addition to inhibiting the proliferation of cancer cell cultures. Exposure to [8]- and [10]-gingerol induced a significant proportion of human and mouse mammary carcinoma cells to enter the sub G1 phase of the cell cycle, as determined by PI staining for cell cycle analysis. The cytotoxic activity of [8]-gingerol and [10]-gingerol was confirmed by Annexin-V-FLUOS and PI staining and showed that [8]- and [10]-gingerol induced late apoptosis/necrosis in mouse and human mammary carcinoma cells as early as 24 h post-treatment. However, unlike the previous study on HeLa cells[134], [6]-gingerol did not induce cytotoxicity in the mammary carcinoma cells at the concentrations tested in the current study. These discrepancies imply a cell-type-specific sensitivity to the cytotoxic effects of [6]-gingerol, or, that higher concentrations of [6]-gingerol are required to induce cytotoxicity in mammary carcinoma cell cultures.

Parallel Annexin-V-FLUOS/PI staining of human dermal fibroblasts indicated that [6]-gingerol did not cause any cytotoxicity while 100 and 200 μM concentrations of

[8]- and [10]-gingerol were quite toxic. This suggests that gingerol-induced cytotoxicity is not selective for cancer cells and a targeted delivery system is required to avoid gingerol-induced damage to surrounding healthy cells.

As studies investigating the mechanisms by which [8]- and [10]-gingerol kill cancer cells were sparse, I aimed to investigate the cytotoxic mechanism of actions of these phytochemicals on mammary carcinoma cells. [6]-Gingerol at 24 h post-treatment induced apoptosis in HeLa ovarian carcinoma cells through down-regulating the overexpression of NF-κB, Akt, and Bcl2 genes, and by triggering caspase-3 activation[134]. Additionally, piperine has been shown to induce ROS-dependent apoptosis of rectal carcinoma cells[107]. Therefore, the pan-caspase inhibitor ZVAD-FMK, as well as the ROS scavenger NAC were incubated with mammary carcinoma cell cultures treated with gingerol to investigate whether gingerol induced cell death by activating caspases or producing ROS. Incubation of human and mouse mammary carcinoma cells with ZVAD-FMK or NAC did not reduce [8]-gingerol or [10]-gingerol-induced total cell death, suggesting that the activation of caspases or ROS production were not necessary to induce cell death. This was in contrast to the findings regarding caspase-3-dependent [6]-gingerol-induced cell death of HeLa cells[134]. The differences in modes of cell death could be due to a cell-type-specific sensitivity of gingerol. In addition, the described study applied much higher concentrations of [6]-gingerol to the HeLa cells. These findings were also in contrast to the studies regarding ROS-induced apoptosis by piperine; however, as previously mentioned, different phytochemicals (although structurally related) may exhibit different pharmacological properties, and again the mechanism of cell death may be cell-type-specific.

[8]-Gingerol and [10]-gingerol exhibit similar cytostatic and cytotoxic effects on mammary carcinoma cell cultures, with [10]-gingerol being slightly more potent. [10]-Gingerol was also found to be the most potent gingerol in another study that compared the anti-inflammatory effects of [6]-, [8]-, and [10]-gingerol and [6]-shogaol[118]. Furthermore, all gingerols appear to exhibit stronger anti-proliferative and cytotoxic effects on mouse mammary carcinoma cells in comparison to human mammary carcinoma cells, but are less cytotoxic to the non-cancerous mouse HC11 cells compared to the non-cancerous human HMECs and dermal fibroblasts. Although slightly stronger cytostatic and cytotoxic effects on mouse mammary carcinoma cells compared to human mammary carcinoma cells were seen following gingerol treatment, the mode of action appeared to be the same. This is important for possible future *in vivo* experiments in mouse model systems, as well as for clinical studies.

5.2 Study Limitations

One of the major limitations in this study was the use of mammary carcinoma cell cultures in place of primary cell isolates. Additionally, the complex interactions that occur within the extracellular environment *in vivo* are lacking *in vitro*, and therefore it is well known that the *in vitro* effects do not always correlate with *in vivo* experiments. The same limitation applies to the use of antibody-coated beads and DCs pulsed with α-TCR to stimulate T cells. This method is commonly accepted for *in vitro* experimentation; however, it represents only a small part of the many complex interactions that occur *in vivo*. *In vitro* activation of T cells with a polyclonal stimulus results in a greater number of responding T cells compared to antigen-specific activation of T cells *in vivo* and does not account for antigenic-specific effects. Furthermore, *in vivo* stimulation allows for the

interaction of T cells with multiple co-stimulatory molecules (in addition to α-CD28 on antibody-coated beads) on the surfaces of APCs and a more robust activation than would be seen *in vitro*. Nevertheless, anti-proliferative effects of gingerol on α-TCR antibody-pulsed DC stimulation of T cell cultures is physiologically relevant to *in vivo* stimulation and lends strength to the inhibitory impact of gingerol on T cell proliferation.

In this study, gingerol was applied at concentrations that, according to the pharmacokinetics of ginger, are not achievable from the consumption of whole ginger. In effect, the concentration of gingerol needed for bioactivity is much higher than can be achieved from eating whole ginger or taking a ginger pill. Therefore, an obstacle to therapeutic use of gingerol is finding a proper method for its administration at effective doses. Additionally, from the current study it is difficult to determine whether it is gingerol or gingerol metabolites that are ultimately responsible for the effects that were seen. According to the NMR and HPLC data described in the introduction[129–132], other metabolites of gingerol, such as the gingerdiols, glucuronides, and sulfates, are in greater abundance than gingerol after either ginger or gingerol metabolism; therefore, it is possible that these metabolites may be responsible for the anti-proliferative and cytotoxic effects on T cells and mammary carcinoma cells seen in this study, as well as the overall health-benefits of ginger consumption.

The use of phytochemicals as adjuvant therapies with current chemotherapeutics to decrease dosages and harm to healthy cells is a common goal for much of the current research on phytochemicals. However, as [6]-gingerol has been shown to exhibit ROS scavenging properties, and as many chemotherapeutics rely on the production of ROS to induce cell death, using gingerol as an adjuvant therapy may negatively influence the

anti-cancer effects of chemotherapeutics. Future studies should therefore be performed to confirm the ROS-scavenging activities of [6]-gingerol and to investigate the potential ROS-scavenging activities of [8]- and [10]-gingerol. Gingerols, especially [8]- and [10]-gingerol, may also inhibit T cell-mediated destruction of cancer cells given the inhibitory effect on mouse T cell activation.

Although gingerol did not dissolve readily in cell culture medium, this problem was rectified by warming the media to 37 °C in a water bath before adding the gingerol and by applying aggressive vortexing. However, the solution containing gingerol required immediate application, as it tended to precipitate at concentrations greater than 200 μM. Gingerol did not appear to precipitate in culture as the gingerol solution was diluted to 200 μM or less.

5.3 Future Directions

Currently, the effect of gingerol on IL-2 receptor signaling is unknown. Further staining for CD25 expression on CTLL-2 cells with 100 μM of gingerol may provide insight into whether [8]- and [10]-gingerol inhibit T cell and CTLL-2 cell proliferation by disrupting IL-2 receptor signaling. JAK1 and JAK3 phosphorylate STAT5 and are of central importance in the JAK/STAT pathway in IL-2 receptor signal transduction[155]. Additionally, PI3K and MAPK are both involved in IL-2 receptor signaling pathways. Investigating the expression of these molecules in gingerol-treated CTLL-2 cells would provide further information on the involvement of gingerol in IL-2 receptor signaling. Additional exploration into the expression and phosphorylation of specific molecules in gingerol-treated T cells, such as ZAP-70, Akt, and NF-κB, would provide a basic

understanding of the effects of gingerol on T cell signaling, from which future studies could be expanded.

Additionally, as gingerol was shown to reduce the production of IL-2 and IFN-γ, which are two cytokines that are produced by Th1 cells, the effects of gingerol on the differentiation and function of Th1 cells should be investigated. Investigating a possible change in the expression of STAT4 and T-bet (both important for inducing $CD4^+$ cells to differentiate into Th1 cells[4,19]) in gingerol-treated T cells would provide insight into the effects of gingerol on Th1 differentiation. Polarizing $CD4^+$ T cells into Th1 cells and measuring their production of IL-2, IFN-γ, and TNF-β and the expression of STAT4 and T-bet in the absence or presence of gingerol would determine the effects of gingerol on Th1 function. These cytokines and proteins are indicative of functioning Th1 cells[4].

Interestingly, [6]-gingerol did not decrease the rounds of division of T cells or mammary carcinoma cells or induce cytotoxicity, unlike what was reported in previous studies. It is possible that the [6]-gingerol I used was less potent than the [6]-gingerol used in previous studies, or, that the effects of [6]-gingerol are cell-type specific. The potency of [6]-gingerol could be tested by using concentrations similar to those in other studies and/or increasing the concentration of [6]-gingerol until an effect is demonstrated. The potential cell-type specificity of [6]-gingerol could be tested by repeating previously documented [6]-gingerol experiments using the [6]-gingerol isolate that I used. Additionally, replicating experiments that have already been performed with [6]-gingerol (such as the study by Chakraborty et al. performed using HeLa cells) would provide insight into the similarity or differences between the [6]-gingerol used in this study and other studies.

Investigating the mechanisms by which gingerol induces mammary carcinoma cell death and inhibits the proliferation of T cells and mammary carcinoma cells are the next objectives of this research. Calcium influx in excess or overstimulation of the calcium receptor have been noted to induce cell death in various tissues in the body[156]. Based on previous studies, [6]-, [8]-, and [10]-gingerol have shown involvement in calcium modulation in numerous cell culture systems[123,125,157–159]. In a previous study, [10]-gingerol demonstrated the ability to cause calcium to become elevated in a concentration-dependent manner in human colon carcinoma cells, leading the authors to speculate that this may account for [10]-gingerol-induced cell death[125]; however, this study did not correlate calcium levels with treatment of 50-100 μM of gingerol - concentrations that induced significant cell death. Another promising study demonstrated the ability of a steam-distilled extract of ginger to inhibit the proliferation of and induce apoptosis in endometrial cells by increasing intracellular calcium levels, as well as a deficiency in mitochondrial function[159]. To explore the mechanism of [8]-gingerol and [10]-gingerol-induced mammary carcinoma cell death, one should perform $DiOC_6$ staining to examine effects of gingerol on the mitochondrial membrane potential, and measuring the Indo-1 fluorescence would provide an indication of any changes in intracellular calcium. Furthermore, it is possible that gingerol induces necroptosis, a form of necrosis that is independent of caspases and only occurs in cells that express the kinase, RIPK3[160]. An initial step to investigate whether gingerol causes cell death by necroptosis would be to determine whether the mammary carcinoma cells used in this study express RIPK3, as it has already been determined that [8]- and [10]-gingerol induce death that is caspase-independent. There are also various necroptosis pathway inhibitors,

such as necrostatin, that could be applied to gingerol-treated mammary carcinoma cell cultures.

The expression and/or phosphorylation status of cyclins and cyclin-dependent kinases (CDKs; cell cycle regulator molecules) may provide insight into how gingerol causes an arrest in the S phase of the cell cycle in mammary carcinoma cell cultures. Molecules of particular interest for examining gingerol-treated 4T1 cell cultures are cyclin-E, cyclin-A, and CDK-2, which are important regulators of the S phase, and cyclin-D and CDK-4, which are important regulators of the G1 phase[161]. In gingerol-treated MDA-MB-231 cell cultures, regulators of the G2/M phase, such as cyclin-B and CDK-1[161], would be important to consider in addition to the above-mentioned cyclins and CDKs.

Unfortunately, although clinical studies have shown that the consumption of ginger tablets has very few side effects[162], *in vitro* exposure to [8]- and [10]-gingerol in the current study were found to be toxic to non-cancerous cells. With this in mind, a safe and targeted gingerol delivery system to cancerous cells or sites of inflammation would be required to administer the drug without damage to the surrounding environment. Another future objective would be to develop this delivery system. Delivery systems that have previously been used in the delivery of phytochemicals are liposomes, micelles, implants, and nanoparticles. Each of these have been shown to enhance the delivery of several chemotherapeutics to target sites, as well as their bioavailability[163].

Lastly, application of [6]-, [8]-, and [10]-gingerol metabolites to cancer cell cultures would help determine whether it is the gingerol or its metabolites that induce the anti-inflammatory and cytotoxic effects seen in the current study. Also, combining [6]-,

[8]- and [10]-gingerol together in proportions that would be similar to those found in ginger would provide an interesting view on how these homologs may interact in comparison to the effects seen with individual gingerols. In addition, using gingerol in combination with current chemotherapeutic and anti-inflammatory medications may be more efficacious than monotherapy with chemotherapeutics or anti-inflammatory drugs.

5.4 Conclusions

The results from this study show that [8]-gingerol and [10]-gingerol, but not the more frequently studied [6]-gingerol, induce cell death in human and mouse mammary carcinoma cell cultures that appears to be independent of ROS production and caspase activation. Unfortunately, [8]-gingerol and [10]-gingerol, but not [6]-gingerol, are also cytotoxic to non-cancerous cells. [8]-Gingerol and [10]-gingerol, but not [6]-gingerol, inhibit the proliferation of human and mouse mammary carcinoma cell cultures by causing an arrest in the S phase of the cell cycle. [8]-Gingerol and [10]-gingerol, but not [6]-gingerol, inhibit the proliferation of isolated mouse T cells, seemingly by decreasing the amount of CD25 and CD69 expressed on T cell surfaces and the production of IFN-γ and IL-2. [8]-Gingerol and [10]-gingerol also inhibit the proliferation of CTLL-2 cells at high concentrations. [6]-Gingerol is the least effective, followed by [8]-gingerol, leaving [10]-gingerol as the most effective for inducing anti-breast cancer and anti-inflammatory properties. Overall, [8]- and [10]-gingerol exhibit anti-breast cancer and anti-inflammatory properties that warrant further investigation for their potential use as preventative and/or adjuvant therapies for breast cancer and inflammatory diseases.

REFERENCES

1. Parkin, J. & Cohen, B. An overview of the immune system. *The Lancet* **357,** 1777–1789 (2001).
2. Nathan, C. Points of control in inflammation. *Nature* **420,** 846–852 (2002).
3. Barton, G. M. A calculated response: control of inflammation by the innate immune system. *J. Clin. Invest.* **118,** 413–420 (2008).
4. Bonilla, F. A. & Oettgen, H. C. Adaptive immunity. *J. Allergy Clin. Immunol.* **125,** S33–S40 (2010).
5. Rock, K. L., Latz, E., Ontiveros, F. & Kono, H. The Sterile Inflammatory Response. *Annu. Rev. Immunol.* **28,** 321–342 (2010).
6. Rock, K. L., Lai, J.-J. & Kono, H. Innate and adaptive immune responses to cell death. *Immunol. Rev.* **243,** 191–205 (2011).
7. Vyas, J. M., Van der Veen, A. G. & Ploegh, H. L. The known unknowns of antigen processing and presentation. *Nat. Rev. Immunol.* **8,** 607–618 (2008).
8. Smith-Garvin, J. E., Koretzky, G. A. & Jordan, M. S. T Cell Activation. *Annu. Rev. Immunol.* **27,** 591–619 (2009).
9. Bousso, P. T-cell activation by dendritic cells in the lymph node: lessons from the movies. *Nat. Rev. Immunol.* **8,** 675–684 (2008).
10. Vantourout, P. & Hayday, A. Six-of-the-best: unique contributions of γδ T cells to immunology. *Nat. Rev. Immunol.* **13,** 88–100 (2013).
11. Call, M. E. & Wucherpfennig, K. W. Molecular mechanisms for the assembly of the T cell receptor–CD3 complex. *Mol. Immunol.* **40,** 1295–1305 (2004).
12. Chen, L. & Flies, D. B. Molecular mechanisms of T cell co-stimulation and co-inhibition. *Nat. Rev. Immunol.* **13,** 227–242 (2013).
13. Lenschow, D. J., Walunas, T. L. & Bluestone, J. A. CD28/B7 System of T Cell Costimulation. *Annu. Rev. Immunol.* **14,** 233–258 (1996).
14. Linsley, P. S. & Ledbetter, J. A. The Role of the CD28 Receptor During T Cell Responses to Antigen. *Annu. Rev. Immunol.* **11,** 191–212 (1993).
15. Watts, T. H. Staying Alive: T Cell Costimulation, CD28, and Bcl-xL. *J. Immunol.* **185,** 3785–3787 (2010).
16. Elgueta, R. *et al.* Molecular mechanism and function of CD40/CD40L engagement in the immune system. *Immunol. Rev.* **229,** 152–172 (2009).
17. Jensen, S. M. *et al.* Signaling Through OX40 Enhances Antitumor Immunity. *Semin. Oncol.* **37,** 524–532 (2010).
18. Hutloff, A. *et al.* ICOS is an inducible T-cell co-stimulator structurally and functionally related to CD28. *Nature* **402,** 21–24 (1999).
19. Szabo, S. J. *et al.* A Novel Transcription Factor, T-bet, Directs Th1 Lineage Commitment. *Cell* **100,** 655–669 (2000).
20. Veldhoen, M. *et al.* Transforming growth factor-β 'reprograms' the differentiation of T helper 2 cells and promotes an interleukin 9–producing subset. *Nat. Immunol.* **9,** 1341–1346 (2008).
21. Korn, T., Bettelli, E., Oukka, M. & Kuchroo, V. K. IL-17 and Th17 Cells. *Annu. Rev. Immunol.* **27,** 485–517 (2009).
22. Schmidt, A. Molecular mechanisms of Treg-mediated T cell suppression. *Front. T Cell Biol.* **3,** 51 (2012).

23. Curotto de Lafaille, M. A. & Lafaille, J. J. Natural and Adaptive Foxp3+ Regulatory T Cells: More of the Same or a Division of Labor? *Immunity* **30,** 626–635 (2009).
24. Ohkura, N., Kitagawa, Y. & Sakaguchi, S. Development and Maintenance of Regulatory T cells. *Immunity* **38,** 414–423 (2013).
25. Williams, M. A. & Bevan, M. J. Effector and Memory CTL Differentiation. *Annu. Rev. Immunol.* **25,** 171–192 (2007).
26. Gillis, S., Ferm, M. M., Ou, W. & Smith, K. A. T cell growth factor: parameters of production and a quantitative microassay for activity. *J. Immunol. Baltim. Md 1950* **120,** 2027–2032 (1978).
27. Setoguchi, R., Hori, S., Takahashi, T. & Sakaguchi, S. Homeostatic maintenance of natural Foxp3(+) CD25(+) CD4(+) regulatory T cells by interleukin (IL)-2 and induction of autoimmune disease by IL-2 neutralization. *J. Exp. Med.* **201,** 723–735 (2005).
28. Boyman, O., Surh, C. D. & Sprent, J. Potential use of IL-2/anti-IL-2 antibody immune complexes for the treatment of cancer and autoimmune disease. *Expert Opin. Biol. Ther.* **6,** 1323–1331 (2006).
29. Paul, W. E. & Seder, R. A. Lymphocyte responses and cytokines. *Cell* **76,** 241–251 (1994).
30. Minami, Y., Kono, T., Miyazaki, T. & Taniguchi, T. The IL-2 Receptor Complex: Its Structure, Function, and Target Genes. *Annu. Rev. Immunol.* **11,** 245–268 (1993).
31. Smith, K. A. Interleukin-2: inception, impact, and implications. *Science* **240,** 1169–1176 (1988).
32. Marzio, R., Mauël, J. & Betz-Corradin, S. CD69 and Regulation of the Immune Function. *Immunopharmacol. Immunotoxicol.* **21,** 565–582 (1999).
33. Shiow, L. R. *et al.* CD69 acts downstream of interferon-α/β to inhibit S1P1 and lymphocyte egress from lymphoid organs. *Nature* **440,** 540–544 (2006).
34. Bach, E. A., Aguet, M. & Schreiber, R. D. THE IFNγ RECEPTOR:A Paradigm for Cytokine Receptor Signaling. *Annu. Rev. Immunol.* **15,** 563–591 (1997).
35. Edeer Karaca, N. *et al.* Granulomatous skin lesions, severe scrotal and lower limb edema due to mycobacterial infections in a child with complete IFN-γ receptor-1 deficiency. *Immunotherapy* **4,** 1121–1127 (2012).
36. Scalapino, K. J. & Daikh, D. I. CTLA-4: a key regulatory point in the control of autoimmune disease. *Immunol. Rev.* **223,** 143–155 (2008).
37. Qian, L., Wu, Z. & Shen, J. Advances in the treatment of acute graft-versus-host disease. *J. Cell. Mol. Med.* n/a–n/a (2013). doi:10.1111/jcmm.12093
38. Benichou, G., Valujskikh, A. & Heeger, P. S. Contributions of Direct and Indirect T Cell Alloreactivity During Allograft Rejection in Mice. *J. Immunol.* **162,** 352–358 (1999).
39. Colotta, F., Allavena, P., Sica, A., Garlanda, C. & Mantovani, A. Cancer-related inflammation, the seventh hallmark of cancer: links to genetic instability. *Carcinogenesis* **30,** 1073–1081 (2009).
40. Alberts, B. *et al.* The Preventable Causes of Cancer. (2002). at <http://www.ncbi.nlm.nih.gov/books/NBK26897/>

41. Schreiber, R. D., Old, L. J. & Smyth, M. J. Cancer Immunoediting: Integrating Immunity's Roles in Cancer Suppression and Promotion. *Science* **331,** 1565–1570 (2011).
42. Hanahan, D. & Weinberg, R. A. Hallmarks of Cancer: The Next Generation. *Cell* **144,** 646–674 (2011).
43. Hanahan, D. & Weinberg, R. A. The Hallmarks of Cancer. *Cell* **100,** 57–70 (2000).
44. Oyagbemi, A. A., Saba, A. B. & Azeez, O. I. Molecular targets of [6]-gingerol: its potential roles in cancer chemoprevention. *BioFactors* **36,** 169–178 (2010).
45. Kumar, A., Takada, Y., Boriek, A. M. & Aggarwal, B. B. Nuclear factor-κB: its role in health and disease. *J. Mol. Med.* **82,** 434–448 (2004).
46. Porta, C. *et al.* Cellular and molecular pathways linking inflammation and cancer. *Immunobiology* **214,** 761–777 (2009).
47. Borrello, M. G. *et al.* Induction of a proinflammatory program in normal human thyrocytes by the RET/PTC1 oncogene. *Proc. Natl. Acad. Sci. U. S. A.* **102,** 14825–14830 (2005).
48. Terzić, J., Grivennikov, S., Karin, E. & Karin, M. Inflammation and Colon Cancer. *Gastroenterology* **138,** 2101–2114.e5 (2010).
49. Zosin, I., Golu, I., Cornianu, M., Vlad, M. & Balasa, M. Some Clinical Aspects in Chronic Autoimmune Thyroiditis Associated with Thyroid Differentiated Cancer. *Mædica* **7,** 277 (2012).
50. Larson, S. D. *et al.* Increased Incidence of Well-Differentiated Thyroid Cancer Associated with Hashimoto Thyroiditis and the Role of the PI3k/Akt Pathway. *J. Am. Coll. Surg.* **204,** 764–773 (2007).
51. Faridi, R., Zahra, A., Khan, K. & Idrees, M. Oncogenic potential of Human Papillomavirus (HPV) and its relation with cervical cancer. **8,** (2011).
52. Wroblewski, L. E., Peek, R. M. & Wilson, K. T. Helicobacter pylori and Gastric Cancer: Factors That Modulate Disease Risk. *Clin. Microbiol. Rev.* **23,** 713–739 (2010).
53. Gruber, I. *et al.* Relationship Between Circulating Tumor Cells and Peripheral T-Cells in Patients with Primary Breast Cancer. *Anticancer Res.* **33,** 2233–2238 (2013).
54. Dudley, M. E. *et al.* Adoptive cell transfer therapy following non-myeloablative but lymphodepleting chemotherapy for the treatment of patients with refractory metastatic melanoma. *J. Clin. Oncol. Off. J. Am. Soc. Clin. Oncol.* **23,** 2346–2357 (2005).
55. Rosenberg, S. A., Restifo, N. P., Yang, J. C., Morgan, R. A. & Dudley, M. E. Adoptive cell transfer: a clinical path to effective cancer immunotherapy. *Nat. Rev. Cancer* **8,** 299–308 (2008).
56. Kennedy, R. & Celis, E. Multiple roles for CD4+ T cells in anti-tumor immune responses. *Immunol. Rev.* **222,** 129–144 (2008).
57. Dranoff, G. *et al.* Vaccination with irradiated tumor cells engineered to secrete murine granulocyte-macrophage colony-stimulating factor stimulates potent, specific, and long-lasting anti-tumor immunity. *Proc. Natl. Acad. Sci. U. S. A.* **90,** 3539–3543 (1993).

58. Levitsky, H. I., Lazenby, A., Hayashi, R. J. & Pardoll, D. M. In vivo priming of two distinct antitumor effector populations: the role of MHC class I expression. *J. Exp. Med.* **179,** 1215–1224 (1994).
59. Hung, K. *et al.* The Central Role of CD4+ T Cells in the Antitumor Immune Response. *J. Exp. Med.* **188,** 2357–2368 (1998).
60. Knutson, K. L. & Disis, M. L. Augmenting T helper cell immunity in cancer. *Curr. Drug Targets Immune Endocr. Metab. Disord.* **5,** 365–371 (2005).
61. Thomas, W. D. & Hersey, P. TNF-related apoptosis-inducing ligand (TRAIL) induces apoptosis in Fas ligand-resistant melanoma cells and mediates CD4 T cell killing of target cells. *J. Immunol. Baltim. Md 1950* **161,** 2195–2200 (1998).
62. Association between NSAIDs use and breast cancer risk: a systematic review and meta-analysis - Springer. at <http://link.springer.com.ezproxy.library.dal.ca/article/10.1007/s10549-008-0228-6/fulltext.html>
63. Tang, X. Tumor-associated macrophages as potential diagnostic and prognostic biomarkers in breast cancer. *Cancer Lett.* **332,** 3–10 (2013).
64. Oluwole, S. F., Ali, A. O., Shafaee, Z. & DePaz, H. A. Breast cancer in women with HIV/AIDS: report of five cases with a review of the literature. *J. Surg. Oncol.* **89,** 23–27 (2005).
65. Stewart, T., Tsai, S.-C., Grayson, H., Henderson, R. & Opelz, G. Incidence of de-novo breast cancer in women chronically immunosuppressed after organ transplantation. *The Lancet* **346,** 796–798 (1995).
66. Pierce, B. L. *et al.* Elevated Biomarkers of Inflammation Are Associated With Reduced Survival Among Breast Cancer Patients. *J. Clin. Oncol.* **27,** 3437–3444 (2009).
67. Wu, W.-M., Lin, B.-F., Su, Y.-C., Suen, J.-L. & Chiang, B.-L. Tamoxifen Decreases Renal Inflammation and Alleviates Disease Severity in Autoimmune NZB/W F1 Mice. *Scand. J. Immunol.* **52,** 393–400 (2000).
68. Salman, S. *et al.* Role of adrenal gland hormones in the anti-inflammatory effect mechanism of tamoxifen, a partial antagonist for oestrogen receptors, and relation with COX levels. *Gynecol. Endocrinol.* **27,** 241–247 (2011).
69. Cushman, M. *et al.* Tamoxifen and Cardiac Risk Factors in Healthy Women Suggestion of an Anti-inflammatory Effect. *Arterioscler. Thromb. Vasc. Biol.* **21,** 255–261 (2001).
70. *Breast Cancer in Canada, 2013*. (Canadian Breast Cancer Foundation). at <http://www.cbcf.org/central/AboutBreastCancerMain/AboutBreastCancer/Pages/BreastCancerinCanada.aspx>
71. *Breast Cancer*. (National Cancer Institute). at <http://www.cancer.gov/cancertopics/types/breast>
72. *Male Breast Cancer*. (The Breast Cancer Society of Canada). at <http://www.bcsc.ca/p/322/l/355/t/Male-Breast-Cancer>
73. American Cancer Society. *Breast Cancer Overview*. (American Cancer Society, 2013). at <http://www.cancer.org/cancer/breastcancer/overviewguide/breast-cancer-overview-what-is-breast-cancer>

74. Kumar, V., Abbas, A. & Fausto, N. *Robbins and Cotran Pathologic Basis of Disease*. (Elsevier, 2005).
75. Viale, G. The current state of breast cancer classification. *Ann. Oncol.* **23,** x207–x210 (2012).
76. Weigelt, B. & Reis-Filho, J. S. Histological and molecular types of breast cancer: is there a unifying taxonomy? *Nat. Rev. Clin. Oncol.* **6,** 718–730 (2009).
77. Maughan, K. L., Lutterbie, M. A. & Ham, P. S. Treatment of breast cancer. *Am. Fam. Physician* **81,** 1339–1346 (2010).
78. *Inflammatory Breast Cancer*. (American Cancer Society). at <http://www.cancer.org/cancer/breastcancer/moreinformation/inflammatorybreastcancer/inflammatory-breast-cancer-what-is-inflammatory-br-ca>
79. Nadji, M., Gomez-Fernandez, C., Ganjei-Azar, P. & Morales, A. R. Immunohistochemistry of Estrogen and Progesterone Receptors Reconsidered Experience With 5,993 Breast Cancers. *Am. J. Clin. Pathol.* **123,** 21–27 (2005).
80. Emde, A., Köstler, W. J. & Yarden, Y. Therapeutic strategies and mechanisms of tumorigenesis of HER2-overexpressing breast cancer. *Crit. Rev. Oncol. Hematol.* **84, Supplement 1,** e49–e57 (2012).
81. Arteaga, C. L. *et al.* Treatment of HER2-positive breast cancer: current status and future perspectives. *Nat. Rev. Clin. Oncol.* **9,** 16–32 (2012).
82. Liberato, N. L., Marchetti, M. & Barosi, G. Cost Effectiveness of Adjuvant Trastuzumab in Human Epidermal Growth Factor Receptor 2–Positive Breast Cancer. *J. Clin. Oncol.* **25,** 625–633 (2007).
83. Seidman, A. *et al.* Cardiac Dysfunction in the Trastuzumab Clinical Trials Experience. *J. Clin. Oncol.* **20,** 1215–1221 (2002).
84. Krishnan, A. V., Swami, S. & Feldman, D. The potential therapeutic benefits of vitamin D in the treatment of estrogen receptor positive breast cancer. *Steroids* **77,** 1107–1112 (2012).
85. Dent, S. F., Gaspo, R., Kissner, M. & Pritchard, K. I. Aromatase inhibitor therapy: toxicities and management strategies in the treatment of postmenopausal women with hormone-sensitive early breast cancer. *Breast Cancer Res. Treat.* **126,** 295–310 (2011).
86. Collins, K. K. *et al.* Effects of breast cancer surgery and surgical side effects on body image over time. *Breast Cancer Res. Treat.* **126,** 167–176 (2011).
87. Montgomery, G. H., Schnur, J. B., Erblich, J., Diefenbach, M. A. & Bovbjerg, D. H. Presurgery Psychological Factors Predict Pain, Nausea, and Fatigue One Week After Breast Cancer Surgery. *J. Pain Symptom Manage.* **39,** 1043–1052 (2010).
88. Partridge, A. H., Burstein, H. J. & Winer, E. P. Side Effects of Chemotherapy and Combined Chemohormonal Therapy in Women With Early-Stage Breast Cancer. *JNCI Monogr.* **2001,** 135–142 (2001).
89. Liu, R. H. Potential Synergy of Phytochemicals in Cancer Prevention: Mechanism of Action. *J. Nutr.* **134,** 3479S–3485S (2004).
90. Singh, R. P., Dhanalakshmi, S. & Agarwal, R. Phytochemicals as cell cycle modulators--a less toxic approach in halting human cancers. *Cell Cycle Georget. Tex* **1,** 156–161 (2002).
91. World Health Organization. Diet, nutrition and the prevention of chronic disease: report of a joint WHO/FAO expert consultation. (2002).

92. Lee, K. W., Bode, A. M. & Dong, Z. Molecular targets of phytochemicals for cancer prevention. *Nat. Rev. Cancer* **11,** 211–218 (2011).
93. Szallasi, A. & Blumberg, P. M. Vanilloid (Capsaicin) Receptors and Mechanisms. *Pharmacol. Rev.* **51,** 159–212 (1999).
94. Derry, S., Sven-Rice, A., Cole, P., Tan, T. & Moore, R. A. Topical capsaicin (high concentration) for chronic neuropathic pain in adults. *Cochrane Database Syst. Rev. Online* **2,** CD007393 (2013).
95. Treede, R.-D. *et al.* Mechanism- and experience-based strategies to optimize treatment response to the capsaicin 8% cutaneous patch in patients with localized neuropathic pain. *Curr. Med. Res. Opin.* **29,** 527–538 (2013).
96. Shin, Y.-H. *et al.* Capsaicin Regulates the NF-κB Pathway in Salivary Gland Inflammation. *J. Dent. Res.* **92,** 547–552 (2013).
97. Iancu, A. D., Petcu, I., Radu, B. M. & Radu, M. Capsaicin short term administration effect on different immune parameters. *Roum. Arch. Microbiol. Immunol.* **71,** 221–254 (2012).
98. Ghosh, A. K. & Basu, S. Tumor macrophages as a target for Capsaicin mediated immunotherapy. *Cancer Lett.* **324,** 91–97 (2012).
99. Bhutani, M. *et al.* Capsaicin Is a Novel Blocker of Constitutive and Interleukin-6–Inducible STAT3 Activation. *Clin. Cancer Res.* **13,** 3024–3032 (2007).
100. Yang, K. M. *et al.* Capsaicin induces apoptosis by generating reactive oxygen species and disrupting mitochondrial transmembrane potential in human colon cancer cell lines. *Cell. Mol. Biol. Lett.* **14,** 497–510 (2009).
101. Chang, H. C. *et al.* Capsaicin may induce breast cancer cell death through apoptosis-inducing factor involving mitochondrial dysfunction. *Hum. Exp. Toxicol.* **30,** 1657–1665 (2011).
102. Huang, S.-P. *et al.* Capsaicin-induced Apoptosis in Human Hepatoma HepG2 Cells. *Anticancer Res.* **29,** 165–174 (2009).
103. Sánchez, A. M., Sánchez, M. G., Malagarie-Cazenave, S., Olea, N. & Díaz-Laviada, I. Induction of apoptosis in prostate tumor PC-3 cells and inhibition of xenograft prostate tumor growth by the vanilloid capsaicin. *Apoptosis* **11,** 89–99 (2006).
104. Srinivasan, K. Black Pepper and its Pungent Principle-Piperine: A Review of Diverse Physiological Effects. *Crit. Rev. Food Sci. Nutr.* **47,** 735–748 (2007).
105. Vaibhav, K. *et al.* Piperine suppresses cerebral ischemia–reperfusion-induced inflammation through the repression of COX-2, NOS-2, and NF-κB in middle cerebral artery occlusion rat model. *Mol. Cell. Biochem.* **367,** 73–84 (2012).
106. Bae, G.-S. *et al.* Piperine Inhibits Lipopolysaccharide-induced Maturation of Bone-marrow-derived Dendritic Cells Through Inhibition of ERK and JNK Activation. *Phytother. Res.* **26,** 1893–1897 (2012).
107. Yaffe, P. B., Doucette, C. D., Walsh, M. & Hoskin, D. W. Piperine impairs cell cycle progression and causes reactive oxygen species-dependent apoptosis in rectal cancer cells. *Exp. Mol. Pathol.* **94,** 109–114 (2013).
108. Doucette, C. D., Hilchie, A. L., Liwski, R. & Hoskin, D. W. Piperine, a dietary phytochemical, inhibits angiogenesis. *J. Nutr. Biochem.* **24,** 231–239 (2013).
109. Singh, A., Duggal, S., Singh, J. & Katekhaye, S. Experimental advances in pharmacology of gingerol and analogues. *Int. J. Compr. Pharm.* **1,** 1–5 (2010).

110. Kundu, J. K., Na, H.-K. & Surh, Y.-J. in *Forum Nutr.* (Yoshikawa, T.) **61,** 182–192 (KARGER, 2009).
111. Kubra, I. R. & Rao, L. J. M. An Impression on Current Developments in the Technology, Chemistry, and Biological Activities of Ginger (Zingiber officinale Roscoe). *Crit. Rev. Food Sci. Nutr.* **52,** 651–688 (2012).
112. Shukla, Y. & Singh, M. Cancer preventive properties of ginger: A brief review. *Food Chem. Toxicol.* **45,** 683–690 (2007).
113. Ali, B. H., Blunden, G., Tanira, M. O. & Nemmar, A. Some phytochemical, pharmacological and toxicological properties of ginger (Zingiber officinale Roscoe): A review of recent research. *Food Chem. Toxicol.* **46,** 409–420 (2008).
114. Shao, X. *et al.* Quantitative Analysis of Ginger Components in Commercial Products Using Liquid Chromatography with Electrochemical Array Detection. *J. Agric. Food Chem.* **58,** 12608–12614 (2010).
115. Rafi, M., Lim, L. W., Takeuchi, T. & Darusman, L. K. Simultaneous determination of gingerols and shogaol using capillary liquid chromatography and its application in discrimination of three ginger varieties from Indonesia. *Talanta* **103,** 28–32 (2013).
116. Afzal, M., Al-Hadidi, D., Menon, M., Pesek, J. & Dhami, M. Ginger: an ethnomedial, chemical and pharmacological review. *Metab. Interactions* **18,** 159–190 (2001).
117. Surh, Y. J. *et al.* Anti-tumor-promoting activities of selected pungent phenolic substances present in ginger. *J. Environ. Pathol. Toxicol. Oncol. Off. Organ Int. Soc. Environ. Toxicol. Cancer* **18,** 131–139 (1999).
118. Dugasani, S. *et al.* Comparative antioxidant and anti-inflammatory effects of [6]-gingerol, [8]-gingerol, [10]-gingerol and [6]-shogaol. *J. Ethnopharmacol.* **127,** 515–520 (2010).
119. Kim, S. O., Chun, K.-S., Kundu, J. K. & Surh, Y.-J. Inhibitory effects of [6]-gingerol on PMA-induced COX-2 expression and activation of NF-kappaB and p38 MAPK in mouse skin. *BioFactors Oxf. Engl.* **21,** 27–31 (2004).
120. Lee, H. S., Seo, E. Y., Kang, N. E. & Kim, W. K. [6]-Gingerol inhibits metastasis of MDA-MB-231 human breast cancer cells. *J. Nutr. Biochem.* **19,** 313–319 (2008).
121. Bode, A. M., Ma, W.-Y., Surh, Y.-J. & Dong, Z. Inhibition of Epidermal Growth Factor-induced Cell Transformation and Activator Protein 1 Activation by [6]-Gingerol. *Cancer Res.* **61,** 850–853 (2001).
122. Kim, E.-C. *et al.* [6]-Gingerol, a pungent ingredient of ginger, inhibits angiogenesis in vitro and in vivo. *Biochem. Biophys. Res. Commun.* **335,** 300–308 (2005).
123. Kobayashi, M., Ishida, Y., Shoji, N. & Ohizumi, Y. Cardiotonic action of [8]-gingerol, an activator of the Ca++-pumping adenosine triphosphatase of sarcoplasmic reticulum, in guinea pig atrial muscle. *J. Pharmacol. Exp. Ther.* **246,** 667–673 (1988).
124. Ohizumi, Y., Sasaki, S., Shibusawa, K., Ishikawa, K. & Ikemoto, F. Stimulation of sarcoplasmic reticulum Ca(2+)-ATPase by gingerol analogues. *Biol. Pharm. Bull.* **19,** 1377–1379 (1996).
125. Chen, C.-Y., Li, Y.-W. & Kuo, S.-Y. Effect of [10]-Gingerol on [Ca2+]i and Cell Death in Human Colorectal Cancer Cells. *Molecules* **14,** 959–969 (2009).

126. Abdel-Aziz, H., Windeck, T., Ploch, M. & Verspohl, E. J. Mode of action of gingerols and shogaols on 5-HT3 receptors: Binding studies, cation uptake by the receptor channel and contraction of isolated guinea-pig ileum. *Eur. J. Pharmacol.* **530,** 136–143 (2006).
127. Li, M. *et al.* Pungent ginger components modulates human cytochrome P450 enzymes in vitro. *Acta Pharmacol. Sin.* doi:10.1038/aps.2013.49
128. Lu, J. *et al.* Immunosuppressive Activity of 8-Gingerol on Immune Responses in Mice. *Molecules* **16,** 2636–2645 (2011).
129. Yu, Y. *et al.* Examination of the Pharmacokinetics of Active Ingredients of Ginger in Humans. *AAPS J.* **13,** 417–426 (2011).
130. Zick, S. M. *et al.* Pharmacokinetics of 6-Gingerol, 8-Gingerol, 10-Gingerol, and 6-Shogaol and Conjugate Metabolites in Healthy Human Subjects. *Cancer Epidemiol. Biomarkers Prev.* **17,** 1930–1936 (2008).
131. Lv, L. *et al.* 6-Gingerdiols as the Major Metabolites of 6-Gingerol in Cancer Cells and in Mice and Their Cytotoxic Effects on Human Cancer Cells. *J. Agric. Food Chem.* **60,** 11372–11377 (2012).
132. Chen, H. *et al.* [10]-Gingerdiols as the Major Metabolites of [10]-Gingerol in Zebrafish Embryos and in Humans and Their Hematopoietic Effects in Zebrafish Embryos. *J. Agric. Food Chem.* **61,** 5353–5360 (2013).
133. Lin, C.-B., Lin, C.-C. & Tsay, G. J. 6-Gingerol Inhibits Growth of Colon Cancer Cell LoVo via Induction of G2/M Arrest. *Evid. Based Complement. Alternat. Med.* **2012,** (2012).
134. Chakraborty, D. *et al.* [6]-Gingerol induces caspase 3 dependent apoptosis and autophagy in cancer cells: drug-DNA interaction and expression of certain signal genes in HeLa cells. *Eur. J. Pharmacol.* **694,** 20–29 (2012).
135. Lee, T.-Y., Lee, K.-C., Chen, S.-Y. & Chang, H.-H. 6-Gingerol inhibits ROS and iNOS through the suppression of PKC-α and NF-κB pathways in lipopolysaccharide-stimulated mouse macrophages. *Biochem. Biophys. Res. Commun.* **382,** 134–139 (2009).
136. Twentyman, P. R. & Luscombe, M. A study of some variables in a tetrazolium dye (MTT) based assay for cell growth and chemosensitivity. *Br. J. Cancer* **56,** 279–285 (1987).
137. Yang, T.-T., Sinai, P. & Kain, S. R. An Acid Phosphatase Assay for Quantifying the Growth of Adherent and Nonadherent Cells. *Anal. Biochem.* **241,** 103–108 (1996).
138. Borrelli, F. *et al.* Phytochemical compounds involved in the anti-inflammatory effect of propolis extract. *Fitoterapia* **73, Supplement 1,** S53–S63 (2002).
139. Proksch, P. *et al.* Rocaglamide Derivatives Are Immunosuppressive Phytochemicals That Target NF-AT Activity in T Cells. *J. Immunol.* **174,** 7075–7084 (2005).
140. Hara, T., Jung, L., Bjorndahl, J. & Fu, S. Human T cell activation. III. Rapid induction of a phosphorylated 28 kD/32 kD disulfide-linked early activation antigen (EA 1) by 12-o- tetradecanoyl phorbol-13-acetate, mitogens, and antigens. *J. Exp. Med.* **164,** 1988–2005 (1986).
141. Zhu, J., Yamane, H. & Paul, W. E. Differentiation of Effector CD4 T Cell Populations. *Annu. Rev. Immunol.* **28,** 445–489 (2010).

142. Rhode, J. *et al.* Ginger inhibits cell growth and modulates angiogenic factors in ovarian cancer cells. *BMC Complement. Altern. Med.* **7,** 44 (2007).
143. Wang, D. & DuBois, R. N. Eicosanoids and cancer. *Nat. Rev. Cancer* **10,** 181–193 (2010).
144. Brahmbhatt, M., Gundala, S. R., Asif, G., Shamsi, S. A. & Aneja, R. Ginger Phytochemicals Exhibit Synergy to Inhibit Prostate Cancer Cell Proliferation. *Nutr. Cancer* **65,** 263–272 (2013).
145. Talorete, T. P. N., Bouaziz, M., Sayadi, S. & Isoda, H. Influence of medium type and serum on MTT reduction by flavonoids in the absence of cells. *Cytotechnology* **52,** 189–198 (2007).
146. Gul, M. Z., Ahmad, F., Kondapi, A. K., Qureshi, I. A. & Ghazi, I. A. Antioxidant and antiproliferative activities of Abrus precatorius leaf extracts - an in vitro study. *BMC Complement. Altern. Med.* **13,** 53 (2013).
147. Dilshad, A., Abulkhair, O., Nemenqani, D. & Tamimi, W. Antiproliferative properties of methanolic extract of Nigella sativa against the MDA-MB-231 cancer cell line. *Asian Pac. J. Cancer Prev. APJCP* **13,** 5839–5842 (2012).
148. Berndtsson, M. *et al.* Acute apoptosis by cisplatin requires induction of reactive oxygen species but is not associated with damage to nuclear DNA. *Int. J. Cancer J. Int. Cancer* **120,** 175–180 (2007).
149. Casares, C. *et al.* Reactive oxygen species in apoptosis induced by cisplatin: review of physiopathological mechanisms in animal models. *Eur. Arch. Oto-Rhino-Laryngol. Off. J. Eur. Fed. Oto-Rhino-Laryngol. Soc. EUFOS Affil. Ger. Soc. Oto-Rhino-Laryngol. - Head Neck Surg.* **269,** 2455–2459 (2012).
150. Cepeda, V. *et al.* Biochemical mechanisms of cisplatin cytotoxicity. *Anticancer Agents Med. Chem.* **7,** 3–18 (2007).
151. Odiatou, E. M., Skaltsounis, A. L. & Constantinou, A. I. Identification of the factors responsible for the in vitro pro-oxidant and cytotoxic activities of the olive polyphenols oleuropein and hydroxytyrosol. *Cancer Lett.* **330,** 113–121 (2013).
152. Forward, N. A. *et al.* Curcumin blocks interleukin (IL)-2 signaling in T-lymphocytes by inhibiting IL-2 synthesis, CD25 expression, and IL-2 receptor signaling. *Biochem. Biophys. Res. Commun.* **407,** 801–806 (2011).
153. Sahu, R. P., Batra, S. & Srivastava, S. K. Activation of ATM/Chk1 by curcumin causes cell cycle arrest and apoptosis in human pancreatic cancer cells. *Br. J. Cancer* **100,** 1425–1433 (2009).
154. Li, H. *et al.* Effect of curcumin on proliferation, cell cycle, and caspases and MCF-7 cells. *Afr. J. Pharm. Pharmacol.* **6,** 864–870 (2012).
155. Gaffen, S. L. SIGNALING DOMAINS OF THE INTERLEUKIN 2 RECEPTOR. *Cytokine* **14,** 63–77 (2001).
156. De Smedt, H., Verkhratsky, A. & Muallem, S. Ca2+ signaling mechanisms of cell survival and cell death: An introduction. *Cell Calcium* **50,** 207–210 (2011).
157. Chen, C.-Y., Chen, C.-H., Kung, C.-H., Kuo, S.-H. & Kuo, S.-Y. [6]-gingerol induces Ca2+ mobilization in Madin-Darby canine kidney cells. *J. Nat. Prod.* **71,** 137–140 (2008).

158. Ohizumi, Y., Sasaki, S., Shibusawa, K., Ishikawa, K. & Ikemoto, F. Stimulation of sarcoplasmic reticulum Ca(2+)-ATPase by gingerol analogues. *Biol. Pharm. Bull.* **19,** 1377–1379 (1996).
159. Liu, Y. *et al.* Terpenoids from Zingiber officinale (Ginger) Induce Apoptosis in Endometrial Cancer Cells through the Activation of p53. *PLoS ONE* **7,** e53178 (2012).
160. Martin, S. J. & Henry, C. M. Distinguishing between apoptosis, necrosis, necroptosis and other cell death modalities. *Methods* **61,** 87–89 (2013).
161. Pestell, R. G. *et al.* The Cyclins and Cyclin-Dependent Kinase Inhibitors in Hormonal Regulation of Proliferation and Differentiation. *Endocr. Rev.* **20,** 501–534 (1999).
162. Marx, W. M. *et al.* Ginger (Zingiber officinale) and chemotherapy-induced nausea and vomiting: a systematic literature review. *Nutr. Rev.* **71,** 245–254 (2013).
163. Aqil, F., Munagala, R., Jeyabalan, J. & Vadhanam, M. V. Bioavailability of phytochemicals and its enhancement by drug delivery systems. *Cancer Lett.* **334,** 133–141 (2013).

APPENDIX

Table 1. List of Products and Reagents.

Category	Reagent	Distributor/Manufacturer	Location of Manufacturer
Antibodies	α-CD119-FITC	BD Biosciences	Mississauga, ON, Canada
	α-CD25-PE	BD Biosciences	Mississauga, ON, Canada
	α-CD69-FITC	BD Biosciences	Mississauga, ON, Canada
	Horse-radish peroxidase (HRP)-conjugated secondary antibody	Invitrogen Canada	Oakville, ON, Canada
Cell Culture/ Growth Factors/ Stimulation	Anti-mouse TCR-β (Functional Grade Purified)	eBioscience Inc	San Diego, CA, USA
	Dulbecco's Modified Eagle's Medium	Sigma-Aldrich Canada	Oakville, ON, Canada
	Dynabeads Mouse T-Activator CD3/CD28	Life Technologies	Carlsbad, CA, USA
	Fetal bovine serum	Invitrogen Canada	Oakville, ON, Canada
	Fibroblast Basal Medium	Lonza Inc.	Walkersville, MD, USA
	Fibroblast Growth Medium Bullet Kit	Lonza Inc.	Walkersville, MD, USA
	L-glutamine (200 mM)	Invitrogen Canada	Oakville, ON, Canada
	IL-2	PeproTech	Rocky Hill, NJ, USA
	4-(2-hydroxyethyl)-1-piperazineethanesulfonic acid (HEPES) buffer solution (1M)	Invitrogen Canada	Oakville, ON, Canada
	Lipopolysaccharide (LPS)	PeproTech	Rocky Hill, NJ, USA
	Mammary Epithelial Basal Medium	Lonza Inc.	Walkersville, MD, USA
	Mammary Epithelial Growth Medium Bullet Kit	Lonza Inc.	Walkersville, MD, USA
	10 000 U/mL Penicillin/10 000 µg/mL streptomycin solution	Invitrogen Canada	Oakville, ON, Canada
	Phenol red-free Dulbecco's Modified Eagle's Medium	Sigma-Aldrich Canada	Oakville, ON, Canada
	Recombinant mouse granulocyte/macrophage-colony stimulating factor	PeproTech	Rocky Hill, NJ, USA
	Roswell Park Memorial Institute 1640	Sigma-Aldrich Canada	Oakville, ON, Canada
	TrypLE™ Express	Invitrogen Canada	Oakville, ON, Canada
	0.25% trypsin-EDTA	Invitrogen Canada	Oakville, ON, Canada
Chemicals/ Solutions/ Reagents	Amplex Red	Invitrogen Canada	Oakville, ON, Canada
	β-mercaptoethanol	Sigma-Aldrich Canada	Oakville, ON, Canada
	Bovine serum albumin	Sigma-Aldrich Canada	Oakville, ON, Canada
	Calcium chloride	Sigma-Aldrich Canada	Oakville, ON, Canada
	Dimethyl sulfoxide	Sigma-Aldrich Canada	Oakville, ON, Canada
	3-(4,5-Dimethylthiazol-2-yl)-2,5-diphenyltetrazolium bromide (MTT solution)	Sigma-Aldrich Canada	Oakville, ON, Canada
	Ethylene diaminete traacetic acid	EM Industries Inc.	Hawthorne, NY, USA
	Hydrochloric acid	Fisher Scientific	Ottawa, ON, Canada
	Paraformaldehyde	Bio-Shop Canada Inc	Burlington, ON, Canada
	Phosphatase substrate tablet	Sigma-Aldrich Canada	Oakville, ON, Canada
	Phosphate buffered saline	Sigma-Aldrich Canada	Oakville, ON, Canada
	RNase A	Qiagen Inc.	Mississauga, ON, Canada
	Sodium azide	Sigma-Aldrich Canada	Oakville, ON, Canada
	Sodium chloride	Bio-Shop Canada Inc	Burlington, ON, Canada
	Sodium hydroxide	Fisher Scientific	Ottawa, ON, Canada
	Tris base	Bio-Shop Canada Inc	Burlington, ON, Canada
	Triton-X-100	Sigma-Aldrich Canada	Oakville, ON, Canada
	TrypLE EXPRESS	Life Technologies	Carlsbad, CA, USA
	Tween-20	Bio-Shop Canada Inc	Burlington, ON, Canada

Category	Reagent	Distributor/Manufacturer	Location of Manufacturer
Dyes/Labels	Annexin-V-FLUOS	Roche Diagnostics	Laval, PQ, Canada
	Bio-Rad Protein Assay Dye Reagent	Bio-Rad Laboratories Inc.	Mississauga, ON, Canada
	Cell Trace™ Oregon Green®488 carboxylic acid diacetate	Invitrogen Canada	Oakville, ON, Canada
	Propidium iodide (PI)	Invitrogen Canada	Oakville, ON, Canada
	Tritiated-thymidine ([3H]-TdR)	MP Biomedicals	Santa Ana, CA, USA
	0.4% Trypan Blue dye solution	Invitrogen Canada	Oakville, ON, Canada
Pre-Manufactured Kits	FMB supplemental bullet kit*	Lonza Inc.	Walkersville, MD, USA
	MEBM supplemental bullet kit**	Lonza Inc.	Walkersville, MD, USA
	OptEIA™ Mouse IL-2 Set (ELISA kit)	BD Biosciences	Mississauga, ON, Canada
	OptEIA™ Mouse IFN-γ Set (ELISA kit)	BD Biosciences	Mississauga, ON, Canada
	Pan T Cell Isolation MACS® Kit II	Miltenyi Biotec	Auburn, CA, USA
	Ready-Set-Go! IL-4 (ELISA kit)	eBioscience Inc	San Diego, CA, USA
Other	Amersham™ ECL™ prime western blotting reagents	GE Healthcare	Baie d'Urfe, PQ, Canada
	Cisplatin	Sigma-Aldrich Canada	Oakville, ON, Canada
	[6]-Gingerol	Dalton Pharma Services	Toronto, ON, Canada
	[8]-Gingerol	Chengdu Biopurify	Chengdu, China
	[10]-Gingerol	Chengdu Biopurify	Chengdu, China
	Myricetin	Sigma-Aldrich Canada	Oakville, ON, Canada
	Plastic culture products	Sarstedt Inc.	Montreal, PQ, Canada

*recombinant human insulin, recombinant human growth factor, gentamicin sulphate, and fetal bovine serum

**recombinant human insulin, recombinant human epidermal growth factor, hydrocortisone, gentamicin sulphate, amphotericin, and bovine pituitary extract

Table 2. Composition of the Different Media.

Medium	Composition	Application
Bone Marrow Derived Dendritic Cell (BMDC) Medium	Roswell Park Memorial Institute 1640	Dendritic Cells
	10 % heat-inactivated fetal bovine serum	
	100 U/mL penicillin	
	100 µg/mL streptomycin	
	2 mM L-glutamine	
	5 mM HEPES buffer (pH 7.4)	
	50 µM β-mercaptoethanol	
CTLL-2 Medium	Roswell Park Memorial Institute 1640	CTLL-2 Cells
	10 % heat-inactivated fetal bovine serum	
	100 U/mL penicillin	
	100 µg/mL streptomycin	
	2 mM L-glutamine	
Complete Dulbecco's Modified Eagle's Medium (cDMEM)	Dulbecco's Modified Eagle Medium (DMEM)	MDA-MB-231, MDA-MB-468, 4T1, E0771
	10 % heat-inactivated fetal bovine serum	
	100 U/mL penicillin	
	100 µg/mL streptomycin	
	2 mM L-glutamine	
	5 mM HEPES buffer (pH 7.4)	
Fibroblast Growth Medium (FGM)	FBM	Human Dermal Fibroblasts
	FGM bullet kit	
Mammary Epithelial Growth Medium (MEGM)	MEBM	Human Mammary Epithelial Cells (HMEC)
	MEGM bullet kit	
HC11 Medium	Dulbecco's Modified Eagle Medium (DMEM)	HC11 Cells
	10 % heat-inactivated fetal bovine serum	
	100 U/mL penicillin	
	100 µg/mL streptomycin	
	2 mM L-glutamine	
Complete Roswell Park Memorial Institute 1640 Medium (cRPMI)	Roswell Park Memorial Institute 1640	T cells
	5 % heat-inactivated fetal bovine serum	
	100 U/mL penicillin	
	100 µg/mL streptomycin	
	2 mM L-glutamine	
	5 mM HEPES buffer (pH 7.4)	
Phenol Red-Free Complete Dulbecco's Modified Eagle's Medium (phenol red-free cDMEM)	Phenol Red-Free DMEM	Amplex Red Assay
	10 % heat-inactivated fetal bovine serum	
	100 U/mL penicillin	
	100 µg/mL streptomycin	
	2 mM L-glutamine	
	5 mM HEPES buffer (pH 7.4)	

Table 3. Cell Culture Origin and Receptor Expression.

Cells	Origin	ER Expression	PR Expression	HER2 Overexpressed?
MDA-MB-231	Human	Negative	Negative	No
MDA-MB-468	Human	Negative	Negative	No
4T1	Mouse	Not known	Not known	Not known
E0771	Mouse	Not known	Not known	Not known

Figure 1. NAC And ZVAD-FMK Reduce Cisplatin-Induced Cell Death. 4T1 cells were seeded and allowed to adhere overnight before being treated with saline vehicle or 1.0 µg/mL cisplatin (Cis) in the presence or absence of 10 mM NAC or 50 µM ZVAD-FMK. At 24 h post-treatment, cells were harvested and stained with Annexin-V-FLUOS and PI and the fluorescence was analyzed by flow cytometry. n = 1.

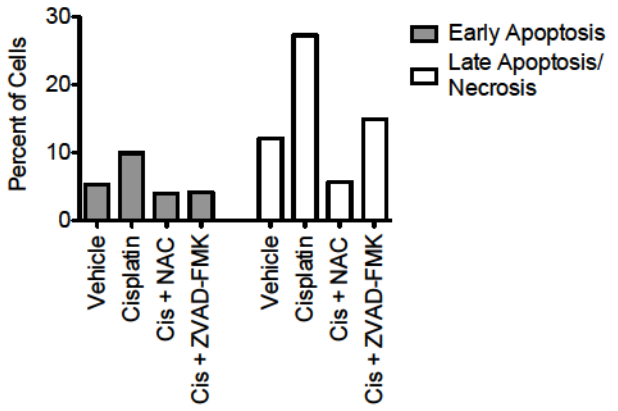

Appendix Figure 1

Figure 2. Gingerol Does Not React With Sodium Bicarbonate in the Medium to Produce Hydrogen Peroxide. Medium, vehicle, and 200 μM of [6]-, [8]-, and [10]-gingerol and 50 μM of myricetin (positive control) were plated in triplicate into 96-well plates. In the dark, master mix (25 μM Amplex Red and 0.005 U/mL HRP in phenol red-free cDMEM) was added to the treatments. The absorbance was read at 570 nm at 90 min and 24 h post-treatment. Data shown are averages of 3 independent experiments $\pm$ SEM; * $p < 0.05$ compared to the vehicle control at the corresponding time points and # $p < 0.05$ for myricetin compared to medium, vehicle, or gingerol treatments at the corresponding time points.

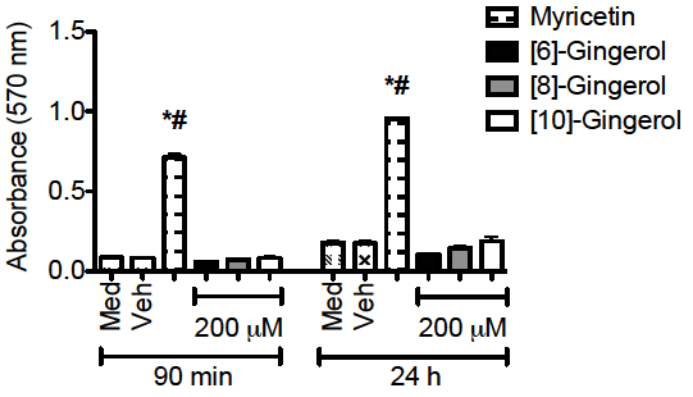

Appendix Figure 2